The Antibacterial Properties and Biocompatibility of Silver and Hydroxyapatite Nanoparticles Coating on Dental Implants

By

Sanna Dara Hadi

A thesis submitted to the University of Plymouth
in partial fulfilment for the degree of

RESEARCH MASTERS

School of Biological Sciences,
Faculty of Science and Environment.

May 2014

Copyright Statement

Sanna Dara Hadi

The Antibacterial Properties and Biocompatibility of Silver and Hydroxyapatite Nanoparticles Coating on Dental Implants.

Abstract

Introduction

Infection associated with dental implants is the most common cause of their failure. The aim of this study was to discover a new coating for dental implants that has a good antibacterial and antibiofilm activity against an early colonizer on implant surfaces: *Streptococcus sanguinis.* Furthermore, the coating should have a good biocompatibility with bone.

Methods

Different coatings were prepared on the surface of titanium alloy (Ti4Al6V) discs. Silver, titanium dioxide, and hydroxyapatite nanoparticles, as well as hydroxyapatite microparticles were used to coat titanium discs. Three techniques were used to coat the titanium discs; (i) Solution deposition and heating for hydroxyapatite micro and nanoparticles, (ii) silver plating, and (iii) anodization to coat the discs with titanium dioxide. The antibacterial effect of these coating was investigated against the clinically relevant microbe, *Streptococcus sanguinis*. End point assays such as lactate production and a live/dead staining kit were used to check for bacterial growth inhibition. The bacterial growth was also qualitatively assessed by scanning electron microscopy. The total concentration of silver, calcium and phosphorus in the media was measured to check the stability of the coatings. Then the biocompatibility

of the coatings with good antibacterial activity was evaluated using primary human osteoblast cells; toxicity assays such as lactate dehydrogenase leak and cell protein concentration were used for this purpose. The total concentration of silver and electrolytes (K^+ and Na^+) were measured in the media and in the cell homogenates. Uncoated titanium discs were used as a control group in both experiments.

Results

This study revealed that silver plus hydroxyapatite nanoparticles (Ag+nHA) and silver plus hydroxyapatite microparticles (Ag+mHA) coatings have an excellent antibacterial activity against *S. sanguinis* compared to uncoated titanium discs. , This observation was also confirmed by SEM images. Furthermore, the stability of the coating was confirmed by ICP-MS measurement, as the silver release from these two coatings was low (<0.5 mg/l). However, the biocompatibility test showed that these coatings reduced the viability of osteoblast cells, as measured by less LDH activity and alkaline phosphatase activity in the cell homogenates compared to the control. The activity of these enzymes in the cell homogenates was about 75 % lower than the control. In addition, the silver ion release from these coatings into the cell culture media (DMEM) was 30-fold higher compared to the silver release in the bacterial test.

Conclusion

The antibacterial activity of Ag+nHA and Ag+mHA coatings was confirmed against *Streptococcus sanguinis*. These coatings could be of great use clinically to prevent the bacterial infection of dental implant. However, this study raise concerns regarding the biosafety of silver-releasing implantable materials, because they may compromise the biocompatibility of the bone cells in certain conditions. Hence, more

investigations are needed to ensure the biocompatibility of these two coatings before their clinical application.

Table of contents

List of Tables

List of Figures

This thesis is dedicated to my parents

For their endless love, support and encouragement.

Acknowledgment

I would like to thank Professor Richard Handy for his supervision and support. Special thanks to technicians: William Vevers, Andrew Atfield, Andrew Fisher, Sarah Jamieson and Matthew Emery for their help. Also, I would like to thank Professor Christopher Tredwin, Dr. Huirong Le, Professor Waleed Al-Murrani and Alexander Besinis for their support. Last, but not least, I would like to thank my sisters and brothers for their love and support.

Author's Declaration

At no time during the registration for the degree of research master has the author been registered for any other University award.

I declare that the work submitted in this thesis is the results of my own investigations except where reference is made to published literature and where assistance has been acknowledged.

This study was sponsored by the Human Capacity Development Program (HCDP)

Candidate

Director of Studies

Skills and development courses attended

Modules

1- Cellular Basis of Immunity Biol3408

2- Research Skill and Methodology Biol5124

Skills

1- Implant symposium session in peninsula dental school.

2- Scientific Writing Skills for Environmental Scientists.

3- The Nobel Journal Club.

Conferences attended

1- World Congress of Implant Aesthetics on the 17th and 18th of October 2012. A total of 14 hours of CPD at The University of Warwick.

2- Joint annual Meeting of the Ecotoxicology Research and Innovation Centre Plymouth University, and the Society of Environmental Toxicology and Chemistry UK Branch.

Chapter 1

Introduction and Literature review

1.1

Recently, the use of dental implants for replacing missing teeth has increased. Dental implants are biocompatible materials that are surgically inserted into the jaw bone underneath the gingiva in order to support artificial crowns (Oshida et al., 2010). Titanium and its alloy (Ti6Al4V) are the most common bulk materials that are used in dental implants, because of their good biocompatibility, mechanical strength, and corrosion resistance (Williams, 1977; Zhao et al., 2009; Norowski, 2009). The first uses of titanium and titanium alloy as medical implants date back to 1971; based on the results of research showing that titanium can attach to the bone firmly (Pye et al., 2009). Despite clinical success, dental implants have a number of problems in their use. Common problems are infections associated with the implants (peri-implantitis) and inadequate osseointegration (i.e., difficulty in obtaining good bone-implant contact) (Tomsia et al., 2011). Several attempts have been made to solve the current implant issues, such as modification of the implant surfaces, or coating the surfaces with different bioactive materials (Wan et al., 2007; Svanborg et al., 2011; Kazemzadeh-Narbat et al., 2013).

Nanotechnology has been used to improve the success rate of dental implants. This may be achieved by producing nano-sized structures that could improve the osteointegration and decrease infection associated with dental implants (Meirelles *et al*., 2008; Tomsia *et al.*, 2011). Nanotechnology can be defined as a science that deals with manufacturing of the nanomaterials. Nanomaterials can be defined as "Any form of a material that is composed of discrete functional parts, many of which have one or more dimensions of the order of 100 nm or less" (Lövestam *et al*., 2010). Nanomaterials have unique physical, chemical and biological properties. This

is partly because of two factors; an increase in the surface area/volume of the material, and unusual physico-chemical properties such as quantum effect that may appear at the nano scale (Kanaparthy *et al*., 2011). Nanomaterials are widely applied in medical and dental fields in areas such as drug and gene delivery, diagnostics (Sahoo *et al*., 2007; Howes, 2014; Goenka, 2014); as well as their use in medical implants (Liu, 2007).

1.2 Infections associated with dental implants (peri-implantitis)

Biomaterials have been used widely in medicine to restore the functions of body parts such as heart valves, orthopedic and dental implants (Langer et al., 2004). However, the infections associated with biomaterials might cause serious complications for some patients (Harris *et al*., 2006; De Giglio, 2013). For example, infections can lead to the surgical removal of the dental implant (Subbiahdoss *et al*., 2009; Sivolella *et al*., 2012). The rate of the infectious complication of implants that requires surgical removal is approximately 5-10 % of patients (Maathuisa, 2007). In addition to the effect of bacteria on the tissues, bacteria have an effect on the biomaterials as well. Bacteria can reduce the durability of the titanium alloy used in implants, because of the production of pitting corrosion on the exposed surface of titanium in physiological conditions (Gil *et al*., 2012).

Peri-implantitis is a condition that can be identified as an inflammation of the tissues surrounding the implant and causes bone resorption (Albrektsson *et al*., 1994). Dental implants are partially exposed to the oral environment because of their transgingival abutment. Hence the gingival part of implants has a pivotal role in bacterial entry and infections (Juan *et al.,* 2010). There are two main causes of peri-

implantitis, biofilm formation on the surface of implant and decrease of the immune response at the implant-tissue interface (Zhao *et al.*, 2009).

The biocompatibility of titanium is dependent on the formation of a protein layer on the surface of the titanium. However, this protein layer on the titanium surface enhances bacterial colonization and biofilm formation (Harris et al., 2006). Biofilms are complex communities of host cells and microbes attached to a substratum, and consists of cells irreversibly attached to the surface, with the cells embedding in extracellular polymeric substances that are produced by the cells as the biofilm develops (Donlan *et al*., 2002). The biofilm protects the microbes from environmental conditions such as dehydration, biocides, and also enhances bacterial growth (Dunne *et al*., 2002). Bacteria in the biofilm may become more resistant to host defenses and need almost 1000-times the antibiotic dose that inhibits the same bacteria in suspension (Vasilev et al., 2009). Thus, it is difficult to treat peri-implantitis with common systemic antibiotics (Zhao *et al.*, 2009). The micro-organisms that cause peri-implantitis are very similar to those that cause chronic periodontitis; the predominant strains are; *Porphyromonas gingivalis*, *Prevotella intermedia*, *Veillonella* species and *Treponema denticola. Candida* species such as *Candida albicans* are also isolated from peri-implant lesion which is uncommon in periodontitis (Leonhardt *et al.,* 1999). One of the early colonizers on the surface of implants is *Streptococcus sanguinuis*. This species provides a favorable condition for the more pathogenic species to grow in the biofilm (Größner-Schreiber *et al*., 2001).

The other cause of peri-implantitis is the impaired immunological response at the site of the implant, as surgical trauma compromises the local immune defense at the implant site, especially at the early stage of implantation. Hence patients will be more prone to infection at this stage of implantation. Even after the healing phase, the

immune response remains impaired at the implant-tissue interface on account of the small number of blood vessel in the surgical zone (Zhao *et al.*, 2009).

In addition to peri-implantitis, there is another type of infection that is associated with dental implants which is peri-implant mucositis. The latter condition can be defined as the infection of the soft tissues overlying dental implants, which is considered as one of the causes of peri-implantitis; and consequently bone loss (Jovanovic, 1993). One of the common causes of peri-implant mucositis is an accumulation of debris around the suture during the healing period, which provides a favorable environment for bacteria. Mucositis is a reversible inflammation (Mombelli *et al*., 1998) and its prognosis is better than peri-implantitis (Meffert, 1994).

Many therapeutic methods are used to treat peri-implantitis such as, conventional mechanical debridement, using local antibiotic and antimicrobial agents (chlorhexidine, tetracycline fiber), using systemic antibiotics, open flap debridement (surgical procedures) and other treatments (Pye *et al*., 2009; Zhao *et al.,* 2009). The success rate of these treatments is very poor and usually ends with implant removal (Esposito *et al.,* 1998; Pye *et al*., 2009). Therefore the production of implants with antibacterial coatings is suggested to be a successful strategy to prevent the initial bacterial colonization. Many surface coatings are used for this purpose. One important requirement for these antibacterial coatings is not to impede the tissueintegration, but to enhance tissue integration instead (Zhao *et al.*, 2009).

Coating the surface of the implant with broad spectrum antibiotics is one of the attempts to prevent bacterial colonization on the surface of implants. For example, antibiotic-hydroxyapatite coatings were used to improve the antibacterial properties of the implants (Alt *et al*., 2006). However, this method fails to incorporate the antibiotic into the hydroxyapatite during the formation of the mineral, because of the

high temperatures that are usually used to make hydroxyapatite coatings, as in the plasma spray method. In addition, the amount of material loaded, and its release characteristics, also might be affected due to the physical absorption of the antibiotics. For example, in dipping methods 80-90% of antibiotic can be released from the calcium phosphate within the first 60 minutes (Radin *et al*., 1997). Furthermore, there are several issues that need to be considered before applying these coatings clinically, such as; the long term activity of the antibiotic, whether the antibiotics are harmful to human cells or not, and finally ensuring that the dose of antibiotics used are effective to inhibit bacterial growth (Zhao *et al.*, 2009).

The other types of coatings used to prevent peri-implantitis include antimicrobial coatings such as chlorhexidine. Chlorhexidine is a broad spectrum antibacterial agent with less risk of drug resistance than antibiotics. It is widely used in dentistry, for instance, in mouthwash, and in gelatin to treat periodontal diseases (Heasman *et al.,* 2001). Chlorhexidine can be absorbed by the surface of implant and released for several days (Kozlovsky *et al*., 2006). Despite its good antimicrobial efficacy, many studies reported that chlorhexidine may cause cell damage (Harris *et al*., 2006). For example, an *in vitro* study showed that chlorhexidine has toxic effects on human fibroblast cells; it suppressed cell divisions, decrease the protein synthesis by the cells and other cell activities (Pucher *et al*., 1992).

Another approach to prevent the biofilm formation on dental implants is to coat the implant surface with inorganic antimicrobial agents such as silver. Silver is well known for its antibacterial effects on a broad spectrum of bacteria including antibiotic resistant species (Lansdown *et al*., 2002). The mechanism of the antibacterial action of silver is still not fully understood. However, there are several possible mechanisms by which silver can kill bacteria. Some studies suggest that the interaction between

the silver ions and membrane contents of bacteria might be the cause of its antibacterial action (Berger *et al*., 1976; Jung *et al*., 2008). Klasen *et al*. (2000) linked antibacterial action of silver to its reaction with thiol group in bacterial respiratory enzymes which lead to inhibition of respiration, and consequently mortality of the bacteria. In spite of its good antibacterial activity, silver has adverse effects on human cells; this depends on many factors such as the speciation chemistry of silver in the biological fluids, the distance between the silver and the cells, as well as the exposure time. Moreover, the biocompatibility of silver coating will decrease with time, inducing changes in the osteoblasts perhaps due to Ag^{+} toxicity (Cortizo *et al*., 2004). The ingestion of colloidal silver solutions by humans may cause argyrosis, which is a blue-black discoloration of the skin that may be local or extend to other parts of the body, including mucosa and the conjunctiva of the eye (Lansdown *et al*., 2002). Likewise, any soluble silver may cause other toxic effects in other organs in humans such as, the liver, kidney, and changes in the blood cells (Panyala *et al*., 2008).

The alternative to dissolved silver could be silver nanoparticles (Ag NPs) as they have a good antibacterial activity. Like metallic silver the exact mechanism of action for Ag NPs is not well known. Shrivastava *et al*. (2007) showed that Ag NPs manifested their antibacterial properties through their effect on the bacterial cell wall (penetrating the cell wall), and by modulating cellular signaling by dephosphorylating putative key peptide substrates on tyrosine residues. Shrivastava *et al*. (2007) used four different concentrations of AgNPs (5, 10, 25, 35 µg ml^{-1}), all the concentrations and especially 25 µg ml^{-1} were found to be inhibitory to Gram negative bacterial growth. In addition, AgNPs may retain their antimicrobial effect for a long period of time, possible due to a steady slow release rate of the silver ions from the AgNPs

(Cabal *et al.*, 2012). Hence AgNPs would be a good alternative to be used as a coating for dental implants. Various methods have been used to prepare AgNPs on titanium dioxide such as the sol-gel method, photochemical reduction, and chemical reduction in aqueous and non-aqueous solvents (Sharma *et al*., 2009). Anodization has also been used to prepare AgNPs on titanium surfaces (Wan *et al*., 2007).

Despite the fact that AgNPs are now being used in the medical field, there is still insufficient information about their biological effects on human cells. Hence, further studies are needed to clarify their antibacterial properties and cytotoxicity before their clinical application (Zhao *et al.*, 2009). Furthermore, there are concerns that AgNPs may be toxic to mammalian cells (Foldbjerg *et al*., 2009; Ahamed *et al*., 2010). The cytotoxicity of AgNPs was found to be concentration-dependent in human cells. it has been shown that AgNPs become cytotoxic to human mesenchymal cells at 5 mg/l, while no toxicity was observed at lower concentration 2.5 mg/l; instead, cell growth was induced at the latter concentration (Greulich *et al*., 2009). Moreover, Bosetti *et al*. (2002) stated that silver-coated material was not toxic to osteoblast-like cells compared to stainless steel. In contrast, Albers *et al*. (2013) found that the AgNPs were more toxic to the human osteoblast and osteoclast cells than silver microparticles.

1.3 Biocompatibility of implant materials

The biocompatibility of the implant is essential to make the prosthesis work properly in the oral cavity (Chaturvedi *et al*., 2009). Biocompatibility can be defined as the ‘‘ability of a material to perform with an appropriate host response in a specific application” (Williams, 1987). It largely depends on the mechanical properties of the metal such as, corrosion resistance, surface topography, chemical composition of

the surface of implants and the type of relation with the host tissues; either it will be in direct contact with bone (i.e., osteointegration), or have indirect contact via fibrous tissue (fibrous encapsulation) (Chaturvedi *et al*., 2009). The materials that are used for implants should neither cause adverse reaction nor endanger the life of patients. It is well known that titanium and its alloy are cytocompatible, but coating the surface of titanium with other material at the micrometer-scale to improve one of the issues of implant might adversely affect the cytocompatibility of implants. Silver for example may be toxic to human cells as described above (Foldbjerg *et al*., 2009; Ahamed *et al*., 2010).

Corrosion is one of the problems that decreases the biocompatibility of the implants and leads to implant failure. It can arise from the degradation of the metal surfaces due to electrochemical attack (Anusavice *et al*., 2003). Corrosion can be subcategorised into two types: (i) chemical (dry) corrosion by which metallic and non-metallic elements interact and produce chemical compounds, for example by oxidation, halogenation or sulphating reactions; and (ii) electrochemical (wet) corrosion which mainly depends on the presence of liquids such as water or other electrolyte fluids (Chaturvedi *et al*., 2009). The most common types of corrosion that occur in dental implants are fretting corrosion and microbial corrosion (pitting corrosion) which are types of wet corrosion (Chaturvedi *et al*., 2009). Fretting corrosion can be defined as process of degradation of the materials that is caused by the combined action of a corrosive environment and small movement (fretting wear). It mainly occurs between the dental implant and bone during the insertion of implant and also due to the cyclic loads of chewing (Gilbert *et al.,* 2009), whereas microbial corrosion is caused by the microbial adherence to the surface of the titanium. In physiological conditions, bacteria and their metabolites may disturb the

passivity of inert metal and lead to production of pitting corrosion on the exposed surface of the metal (Chaturvedi *et al*., 2009).

Titanium and its alloy have a good corrosion resistance, which is mainly because of the presence of an oxide layer on their surfaces, but this will change with time and leads to the breakdown of the outer oxide layer (Tschernitschek *et al.*, 2005). One of the other factors that affect the corrosion resistance of titanium is inflammation; this make the environment around the implant become acidic and enhances the corrosion of the implant (Lassus *et al.*, 1998). Furthermore, modification of the surface of titanium to improve their properties may adversely affect the corrosion resistance of the titanium, because some modifications resulted in micro cracks, hence increasing the corrosion rate. It has been reported that nanomaterials can improve the corrosion resistance of implants. For example hydroxyapatite nanoparticles can improve the corrosion resistance of implants 50-100 times higher than the micrometer thick hydroxyapatite because of their extremely low porosity (Zhang *et al.,* 2002). Hydrophobic coatings of titanium dioxide nanoparticles can also exhibit an excellent corrosion resistance (Shen *et al*., 2005). Venkateswarlu *et al*. (2012) reported that silver-substituted hydroxyapatite titania coatings increase the corrosion resistance of the titanium by acting as a barrier to the transport of electrons and ions between the substrate and the electrolyte.

1.4 Osseointegration

The success rate of dental implants is closely related to the early osseointegration of the implant surface with the bone, and the maintenance of it (Le Guéhennec *et al*., 2007; Lavenus *et al*., 2010; Goyal *et al*., 2012). Osseointegration can be defined as ‘a direct, structural and functional connection between organized vital bone and the

surface of a titanium implant, capable of bearing the functional load' (Brånemark *et al*., 1969). Osseointegration occurs in two steps; the first step is known as primary stability which is mainly mechanical. The second step of osseointegration is biological stability, i.e., cell-implant surface interaction. In the period between these two steps there is an observed decrease in the dental implant stability, and because of that, implant failure mostly occurs at this time (Lavenus *et al*., 2010).

Mechanical stability involves mechanical interlocking between the implant surfaces and the bone; it depends mainly on the design of implants and the structure of the bone. For example micro rough implant surfaces (1-10 mm) increase the bone implant interlocking. Different methods are used to make implants with rough surfaces for instance: plasma spraying, grit blasting, acid etching and anodization (Le Guéhennec *et al.*, 2007). Each method has its advantage and disadvantage. Table 1.1 summarize the advantage and disadvantage of the main methods used to increase the roughness of implant surfaces.

Biological stability on the other hand depends on the interaction between the implant surfaces and tissues. After implant placement a series of biological events occur, which are: blood and implant interaction, inflammatory response and finally initial bone formation (Junker *et al*., 2009). The interactions that occur between the implant surface and blood lead to absorption of many proteins such as, fibronectin and vitronectin that play a pivotal role in enhancing cell adhesion (Balasundaram *et al*., 2006).

The properties of implant surfaces have an important role in osteointegration. For example, the hydrophilicity of an implant may increase the cell attachment to implants by their interaction with biological fluids (Steinemann, 1998). It is also observed that roughening the surface of implants at the micrometer level will

enhance the osteointegration by inhibiting the osteoclastogenesis (Lossdorfer *et al.,* 2003). However, the rough surface has an adverse effect on implants, because it will enhance the bacterial colonization and contribute to subsequent peri-implantitis (Romeo *et al*, 2005). The chemical composition of the implant surface can improve the osteointegration, hence different chemicals are used such as, calcium phosphate, specifically micrometer thick hydroxyapatite, which is commonly used as a coating material because of its high potential to bond to bone (Liljensten *et al.,* 2003). Many physical and chemical techniques are used to prepare micrometer thick hydroxyapatite on the implant surfaces such as sol-gel, plasma spraying, biomimetic deposition and electrochemical deposition and others (Koch *et al*., 2007). The hydroxyapatite coatings that are produced by these techniques have some disadvantages such as poor adhesion to the titanium surfaces, non-uniform thickness and non-stoichiometric composition of the coatings (Hamdi *et al.,* 2000).

Nanotechnology provides new opportunities for improving the osseointegration of titanium implants. For instance, by making the surface of implants mimic the surface topography that is produced by the extracellular matrix components of bone. Since the extracellular matrix components are at a nanometer scale (10-100 nm), so nano-patterend surface implants could be more compatible with human cells (Le Guéhennec *et al.*, 2007). The nanocoatings may improve the initial healing around the implants by selective attachment of bone cells to implant surfaces (Anselme *et al*., 2002). The proliferation of osteoblasts as well as the long term function of the cells was promoted by nanosized grain or fibre of titania, alumina and hydroxyapatite (Webster *et al*., 2000). To improve the osteointegration, electrochemical deposition was also used to coat titanium implants with nanomaterials like hydroxyapatite nanoparticles (Kim *et al.,* 2009)

Table 1.1 Methods used to increase the roughness of titanium implants for better Osseointegration

Method	Description	Advantages	Disadvantages	References
Acid etching	Immersion of titanium implant in strong acid to create micro pits on the surface of an implant [(1)].	Increase the roughness of titanium implant as such improve the mechanical interlocking [(1)] Promote bone formation at bone-implant contact through increase the cell attachment to the surface because of its ability to attach fibrin scaffold [(3)]. The wettability of the surface also play role in the bone promotion [(4)].	Reduce the mechanical properties of titanium because it can lead to hydrogen embrittlement and create micro cracks on the surface [(2)]. Hydrogen embrittlement may also lead to a reduction in the ductility of titanium [(2)].	(Massaro et al., 2002)[(1)] (Yokoyama et al., 2002)[(2)] (Buser et al., 2004) [(3)] (Le Guéhennec *et al.*, 2007) [(4)]
Titanium plasma spraying	Producing titanium projections on the surface of implant with high temperature [(1)].	Increase the tensile strength of the implant / bone interface [(1)]. Increase the surface area of implant surfaces [(1)].	Wear particles may have local and systemic carcinogenic effect [(2)].	(Buser *et al*., 1991) [(1)] (Martini *et al*., 2003) [(2)]
Anodization	Anodizing titanium surface in strong acids such as H_2SO_4, H_3PO_4, HNO_3, or HF at high current density (200 A/m_2) or potential (100 V) [(1)(2)].	Strong reinforcement of the bone response [(2)].	It is a complex process and affected by many parameters such as, density, concentration of acid, and composition and electrolyte temperature [(3).]	(Sul *et al*., 2001) [(1)] (Sul *et al*., 2002) [(2)] (Le Guéhennec *et al.*, 2007) [(3)]
Grit blasting	Blasting the surface of titanium implant with different materials by projecting the material through a nozzle at high velocity with compressed air [(1)]	Increase the biomechanical fixation of titanium implant [(2)]	Cannot enhance the biological fixation of implants [(3)]	(Aparicio *et al*., 2003) [(1)] (Abron *et al*., 2001) [(2)](Le Guéhennec *et al.*, 2007) [(3)]

1.5 Uses of nanomaterials in dental implants

Many *in vitro* studies have shown that nanostructures are more bioreactive (Svanborg *et al*., 2011), because the nanomaterials have a higher surface area to volume ratio, higher number of atoms, and crystal grains at their surfaces; consequently this will change the corresponding surface energy for protein adsorption (Webster *et al*., 2001; Liu *et al.,* 2007). It has been reported that nanomaterials can increase the interaction between the four proteins (fibronectin, vitronectin, laminin, and collagen) which are crucial to osteoblast functioning (Christenson *et al.*, 2006). Various nanomaterials (Table 1.2) have been used to modify the implant surfaces to improve the clinical outcome (Liu *et al.,* 2007; Lavenus *et al*., 2010). This is by improving the antibacterial and osteointegration properties of implants. However the knowledge of the mechanisms by which nanomaterials improve the implants are still limited. Nanomaterials that are mainly used to coat dental implant include: hydroxyapatite nanoparticles, silver nanoparticles and metal oxide nanostructures (See Table 1.2).

Table 1.2 Uses of Nanomaterials in dental implants/medical implant

Nanomaterials	Purpose of experiment	Experimental design	Results	References
Three types of stable nanoparticle suspensions in water of Calcium phosphate have been used, 20 nm thickness. The coatings are: Phosphorous deficient Hydroxyapatite (HA) (A), needle shaped HA (B) and calcium deficient HA (C).	*In vivo* evaluation of the biological effect of calcium phosphate coatings with nanostructures on smooth implant surfaces.	Implants were coated with calcium phosphate nanoparticles by immersion and subsequent heat treatment (550 °C, 5 minutes), the surface morphology examined by scanning electron microscopy, then implants inserted into the tibia of rabbits for six weeks in order to examine the removal torque testing. Uncoated implant was used as control.	Calcium phosphate coatings with nanostructures increase the biomechanical bonding, they show higher removal torque compared to control (RTQ = 24.7, 29, 28.2, 32.9 for control, A, B, C respectively). Increasing the surface area of the dental implants. Chemical composition of CaP nanocoating has an effect on osteointegration.	(Jimbo *et al*., 2012)
Soda-Lime-glass-nAg powder with 20% wt of silver nanoparticles. (The particle size distribution of silver nanoparticles ranging between 20-90 nm).	Evaluation the effect of a Soda-Lime Glass Containing Silver Nanoparticles coating on Titanium Alloy on the streptococcus oralis biofilm, and measure the release rate of silver from the powder.	Titanium substrate coated with Soda-Lime-glass-nAg by simple sedimentation process (argon atmosphere at 980 ◦C for 1 hour) three strains of streptococcus oralis grown on coated titanium substrate, the surface morphology then characterized by scanning electron microscopy and profilometer.	The adherence of *Streptococcus oralis* strains ATCC35037, CI-1 and CI-2 to titanium coated with soda-lime-glass – nAg significantly decreased by 99.7, 99.8, and 99.9% respectively after 24 hours incubation. The release rate of silver was 0.299 mg/ L /h, in which determines in different time intervals for up to 7 days.	(Cabal *et al*.,2012)

Nanomaterials	Purpose of experiment	Experimental design	Results	References
Nanoparticles of silver, cuprous oxide, cupric oxide , zinc oxide, silver+cupric oxide composite, silver+zinc oxide composite their size ranged between 10-50nm	Examine the antibacterial activity of nanoparticulate metals and metal oxides against 4 species of gram negative bacteria that cause peri-implantitis.	Flame spray pyrolysis was used to prepare the nanoparticles. Brain heart (BHI) infusion broth used for bacterial culture and three species of bacteria was used which are: prevotella intermedia, prevotella gingivalis, fusobacterium nucleatum. Minimum inhibitory concentration (MIC) and minimum bactericidal concentration (MBC) determinations were used to test bactericidal and bacteriostatic activity of these nanoparticles. Nanoparticles were suspended in BHI+ hemin, concentrations tested were 100, 250, 500, 1000 and 2500 µg / mL.	Based on bacteriostatic and bactericidal Values (MIC,MBC), the antimicrobial activity of six nanoparticles and two nanoparticle composites are in descending order Ag>Ag+CuO composite>Cu_2O>CuO> Ag+ZnOcomposite>ZnO>$TiO_{2>}WO_3$ The bactericidal effect was shown to be dose- dependent and rapid. For P. gingivalis the effect reached 100% within 2 hour and within 3 hours for F. nucleatum and prevotella intermedia and 99% within 4 hours for A. actinomycetemcomitans.	(Vargas-Reus *et al*., 2012)
Titanium produced by physical vapor deposition of titanium on the HCl-H2SO4. The average size of titanium nanonodules, ranging from 84nm to 925nm in linear correlation with the deposition time nanonodules	Test the hypothesis that titanium nanostructure can improve titanium-bone integration.	The surfaces of prepared substrate were deposited with one of these metals (nickel, titanium, chromium, silicon, silica) by physical vapor deposition. Atomic force microscopy (AFM) was used to measure the diameter and peak to valley of nanonodules. An established biomechanical push-in test in the rat was used to evaluate the osteointegration of nanonodules implants.	Titanium nanonodules increased the surface area of implant by 40% compared to acid etched micro structured surface when deposition time was 8 min 20 sec. The nanonodules of size 560nm that produce when deposition time was 16 min 40 sec were selected to test their osteointegration by push in test in the rat compared to acid etched implant and found that the push in value at week 2 for nanonodules 3.1 times greater than acid etched titanium.	(Ogawa *et al.*, 2008)

Nanomaterials	Purpose of experiment	Experimental design	Results	References
Poly (lactide-co-glycolide)/bioactive glass Hydroxyapatite (PBGHA) nanocomposite coating. Nanoparticle amount of 10, 15, and 20 weight percent (wt %) were tested to prepare uniform nanocomposite coating.	To prepare and *in-vivo* and *in-vitro* evaluate a novel bioactive, biodegradable, antibacterial nanocomposite coating for dental implant application.	Solvent casting process was used to coat the substrate (commercially pure titanium) with nanocomposite. Human adipose- derived stem cells (HASC) were used to test the attachment and viability of the nanocomposite coating. The implants were soaked in phosphate buffer saline (PBS) in order to examine the degradation of nanocomposite coating, and immersed in stimulated body fluid to test the bioactivity.	Using 10 wt% nanoparticles (5 wt% HA and 5 wt% bioactive glass) can produce desirable uniform nanocomposite coating on the titanium. *In-vitro* study of bioactivity showed rapid formation of bone-like apatite on prepared nanocomposite coatings. After 3 days incubation HASC showed a good adherence to nanocomposite coatings. Nanocomposite coating were degraded after 60 days immersion in PBS.	(Mehdikhani *et al.*, 2012)

1.6 Hypothesis

The main hypothesis being tested in this study is that implants coated with AgNPs and hydroxyapatite nanoparticles may improve the antibacterial properties and biocompatibility with osteoblasts respectively. Silver nanoparticles can improve the antibacterial activity of titanium implants without causing toxicity to the human bone cells. The tested AgNPs can achieve the antibacterial activity either through the release of consistent small amount of silver ion or direct contact with the microbes and inhibit their growth in suspension and most importantly in biofilm. Furthermore, the silver ion release from the tested AgNPs will be lower than the concentration that will affect the biocompatibility of the titanium. In addition, hydroxyapatite nanoparticles can improve the osteointegration of the implants because it is similar to the chemical composition of human bone. Hence it can enhance the absorption of many proteins that are important for bone growth on the surface of implants.

1.7 Aim and objectives

The overall aim of the project was to develop a coating on titanium alloy that can prevent biofilm formation by preventing the growth of the early bacterial colonizers. *Streptococcus sanguinis* was used in this study, because it plays an important role in biofilm formation on implant surfaces.

The specific objectives were to:

(1) Characterize and investigate the antibacterial activity or the minimum inhibitory concentration of the nanomaterials (silver, titanium dioxide, and hydroxyapatite) that are commonly used for implant coatings.

(2) Coat the surface of titanium alloy (Ti6Al4V) with different coatings (silver, titanium dioxide, and hydroxyapatite) and characterize them.

(3) Demonstrate the antibacterial activity of these coatings against *Streptococcus sanguinis in vitro*, and select the coatings that have good antibacterial activity for further study.

(4) Investigate the biocompatibility of the coatings using human osteoblast cells, by testing the viability and the cytotoxic response of the cell to the coatings.

Chapter 2

The Antibacterial Effects of Different Nanoparticles and Their Bulk Material or Metal Salt Equivalents on Streptococcus sanguinis

2.1.1 Introduction

The development of antibiotic resistant microbes has led to the search for an alternative,effective, antimicrobial agent (Rai *et al*., 2009). It is established that nanotechnology may improved the properties of the materials that are in use in medical field (Ciobanu *et al*., 2012). Different nanomaterials have been proposed to improve the antibacterial activity and/or biocompatibility of medical implants such as, nanosilver, titanium dioxide nanoparticles (P25), and hydroxyapatite nanoparticles (nHA). Several studies have focused on investigating the antibacterial activity of Ag NPs against different microbes (Shrivastava *et al*., 2007; Sadeghi *et al*., 2013; Lu *et al*., 2013). Nanosilver has good antibacterial activity (Lansdown *et al*., 2006, Gong *et al*., 2007), but many factors might have an effect on the antimicrobial activity of nanosilver such as; the type of microbe, the size of the AgNPs, the media used for growing the bacteria, and the number of microbes used in the expriments. Sadeghi *et al*. (2013) found that 16 mg/l of nanosilver can inhibit the growth of *Streptococcus sanguinis* in Mueller Hinton broth, whereas 4 mg/l was enough to inhibit the growth of *Actinomyces viscosus* in the same media. The size of the silver nanoparticles also has an effect on their antibacterial effect (Hernández-Sierra et al., 2008). The number of the bacterial cells applied in the test has also an effect on the ability of nanosilver to inhibit the bacterial growth (Sondi *et al*., 2004).

Titanium dioxide nanoparticles have also shown some antibacterial activity against *Streptococcus mutans* at high concentration of 100 mg/l (Besinis *et al*., 2014). Li *et al* (2008) stated that titanium dioxide nanoparticles showed a good antibacterial activity through diverse mechanisms, such as production of reactive oxygen species that can damage cell components.

2.1.2 Aims and objectives

The aim of this study was to identify the nanomaterial that has a good antibacterial activity, in order to use in the dental field such as dental implant. Furthermore, to investigate the effect of the physiological saline and NaCl solution on the effectiveness of these nanomaterials. The facultative anaerobic bacteria *Streptococcus sanguinis* was used as a clinically relevant microbe.

The main objectives of the study were to: (i) characterize the nanomaterial dispersions (AgNPs, nHA, and P25) and their bulk or salt solutions; (ii) investigate the antibacterial activity of the nanomaterial dispersions mentioned above, and to compare them with their bulk powder or salts to indicate any particle-size effect on the antibacterial activity of these materials (chlorhexidine (clinical disinfectant) was used as a positive control); (iii) evaluate the minimum inhibitory concentration assay (MIC) and compare this assay with the lactate production assay; (iv) measure the total concentration of silver for AgNO3 and AgNPs in physiological saline after bacterial exposure; and (v) investigate the dissolution of the nanomaterials in MilliQ water and compare with their dissolution in physiological saline. For this reason inductively coupled plasma mass spectrometry (ICP-MS) was used, which is a powerful analytical technique to measure the concentration of trace elements (Jenner *et al*., 1990).

2.2 Methodology

2.2.1 Preparation of stock solution / dispersions

Stock solutions and dispersions of 1 g/l were prepared in ultra-pure water for the nanomaterials and their bulk powders or metal salts, as appropriate. The materials were: (I) silver nanoparticles; (II) (AgNPs) silver nitrate ($AgNO_3$); (III) titanium dioxide nanoparticles (P25); (IV) bulk titanium dioxide powder (TiO_2); (V) hydroxyapatite

nanoparticles (nHA); and (VI) hydroxyapatite microparticles (mHA). The manufacture's information for the materials is listed in Table 2.1. All stocks were sterilized before use. $AgNO_3$ solution and AgNPs dispersion were sterilized by autoclaving (121 °C for 15 min at 15 psi pressure). Gamma radiation (36.42-40.72 KGy for 10 h) was used to sterilize remaining stocks, because of concerns that the high temperature of the autoclave might affect their reactivity or crystal structure (Besinis et al., 2014). Afterwards, all stocks were sonicated (35 kHz frequency, Fisherbrand FB 11010, Germany) for 4 h to disperse the materials. Then, serial dilutions were prepared to achieve 400, 200, 100, 50, 25, 12.5, 6.25, and 3.125 mg/l). The serial dilutions were also sonicated for 4 h before using in the experiments. Two sets of serial dilutions were prepared for each material, one in poor nutrient solution (0.85% NaCl) and the other in physiological saline. The physiological saline used in this experiment was intended to represent the electrolyte composition of blood serum. The physiological saline is a modified kerb's ringer (De Paiva *et al*., 1993), the component of which are shown in Table 2.2. Physiological saline and 0.85% NaCl (without added particles) were used as a negative control in the experiment. One % of chlorhexidine was used as a positive control, which were then subject to a 50 % dilution series (0.5, 0.25, 0.125, 0.06, 0.03 v/v), to compare the results with Besinis et al. (2014) study. Furthermore, antibacterial activity of the milliQ water was also investigated, two sets of dilution series of milliQ were prepared one in physiological saline and the other in 0.85 % saline (100, 50, 25, 12.5, 6.25, and 3.125 %). The physiological saline was filter sterilized (Filter bottle top Steritop vacuum sterile PES membrane 0.22 µm pore size 1L 45mm neck size, Fisher scientific, UK) to prevent potential bacterial contamination in the media. Secondary stock dispersions and solutions of 400, 200 and 100 mg/l were prepared directly from the 1 g/l stock solution for $AgNO_3$ and AgNPs in the NaCl solution or physiological saline as appropriate.

Table 2.1: Manufacturer's informations of the materials were used in the experiment

Material	Supplier	Manufacture's information
Silver nanoparticles	Sigma-Aldrich, Wisconsin, USA, lot number 7721KH)	Purity, 99.5%, <100 nm. Trace elements in this batch of dry powder: Al 7.3, B 5.6, Ba 5.7, Ca 15, Cr 26, Cu 5.5, Fe 229, Mg 1.5, Mn 7.9, Na 8.0, Ni 7.0, Sn 15, Ti 4.9 ppm. Measured BET surface area, 4.8 m^2/ g.
Silver nitrate	Product code s/ 1280/46, Fisher, Loughborough, UK	Purity, 99.9 %, main impurities <10 ppm Ca and <20 ppm Na. BET surface area below detection limit (<1 m^2/g) and salt contains nitrogen.
Titanium dioxide nanoparticles	DeGussa P25 particles, from Lawrence Industries, Tamworth, UK	Diameter, 21 nm; purity, >99%,approximately 25% rutile and 75% anatase, maximum impurity of 1% Si), specific surface area 50 ± 15 m2 /g. Measured BET surface area, 46.7 m^2 /g.
Bulk TiO_2 powder	Acros, New Jersey, USA	Titanium (IV) oxide, purity of 98.0–100.5% TiO2. Measured BET surface area, 8.7 m^2/g
Hydroxyapatite microparticles	Fluidinova, Rua Eng. Frederico Ulrich 2650, 4470-605 Maia, Portugal	Highly pure forms of hydroxyapatite, with no additives, measured BET surface area greater than 120 m^2/g.
Hydroxyapatite nanoparticles	Fluidinova, Rua Eng. Frederico Ulrich 2650, 4470-605 Maia, Portugal	Highly pure nanocrystalline hydroxyapatite, supplied as 15 % wt. paste, with no other additives. Measured BET surface area, greater than 80 m^2/g

Table 2.2: Physiological saline components (modified Kerb's ringer)

Chemicals	**Concentration (mM)**
Sodium chloride (NaCl)	118 mM
Potassium chloride (KCl)	3 mM
Magnesium sulfate pentahydrate ($MgSO_4.5H_20$)	1 mM
Calcium chloride ($CaCl_2$)	2 mM
Bicarbonate buffer ($NaHCO_3$)	25 mM
Potassium dihydrogen phosphate (KH_2PO_4)	1.2 mM
Glucose	10 mM

2.2.2 Characterization of the nanomaterials

In order to investigate the particle size distribution in the media that were used in the experiment, the nanomaterials and their equivalent bulk or metal salts were characterized using nanoparticle tracking analysis (NTA, using a Nanosight LM 10, Nanosight, Salisbury, UK, laser output set at 30 mW at 640 nm). NTA detects the particles moving under Brownian motion, and relates the particle movement to particle size using Stokes-Einstein Eq.I which is as follow (Filipe *et al*., 2010):

$$\overline{(x, y)^2} = \frac{2K_B T}{3r_h \pi \eta}$$

where kB is the Boltzmann constant and $\overline{(x, y)^2}$ is the mean squared speed of a particle at a temperature T, in a medium of viscosity η, with a hydrodynamic radius of r_h (Filipe *et al*., 2010). Briefly, the initial 1 g/l stocks in milliQ water were diluted to 100 mg/l in physiological saline as described previously in (section 2.2.1). Then the samples were continuously sonicated until they were analysed (n = 3).

2.2.1 Experimental design and preparation of microplates

The experimental design involved exposing *Streptococcus sanguinis* to serial dilutions of different nanomaterials and their bulk powder/salt. *S. sanguinis* was used as a clinically-relevant microbe. *S. sanguinis* NCTC 10904 was originally isolated from dental plaque. The vials as supplied from Health Protection Agency Culture Collections were stored at - 80°C in liquid nitrogen until required. Bacterial cells were firstly grown for 36 h on plates of Columbia blood agar (Oxoid), with 5% sheep blood, and then incubated for 24 h in 15 ml of brain heart infusion broth (BHI, product code: OXCM1135B, Fisher scientific, Loughborough, UK) supplemented with 2% sucrose (BHI) incubated at 37 °C under 5 % CO_2 and 95% air. The bacterial culture that used in this experiment was in exponential stage (Appendix A). The cell suspension was adjusted to a final concentration of 10^7 CFU/ml, determined by optical density at 595 nm. After preparing the serial dilutions of the nanomaterials and their bulk, as well as the negative and positive control (section 2.2.2), 250 µl from each serial dilutions and 25 µl of bacterial suspension were added to each well of a 96 well microplate (flat-bottom sterile polystyrene microplates, dis-210-070j, Fisher Scientific, UK). The experiment was carried out in 6 replicates and 96 well microplates was used as the unit of replication. Additional set of plates were prepared (n = 3 plates), to determine the turbidity of the nanomaterials and their bulk. These plates were identical to those in the main experiment, except for adding the broth without added bacteria (time-matched turbidity measurement of the nanomaterials). Then all plates were incubated for 24 h in 37°C and 5% CO_2 and 95% air incubator.

For the purpose of bacterial growth measurement, MIC and lactate production assays were performed. MIC can be defined as the lowest concentration of the material that can inhibit the growth of bacteria (Andrews *et al*., 2001). This assay has been routinely

used by the microbiologists to measure bacterial growth (Besinis *et al*., 2014). The turbidity was measured at an absorbance of 595 nm using a VersaMax plate reader (VersaMax microplate reader with SoftMax Pro 4.0 software, Molecular Devices, Sunnyvale, CA). Furthermore, the silver ion release from silver nanoparticles and silver nitrate in physiological saline was measured. After 24 h exposure, 200 µl from each dilutions of AgNPs and $AgNO_3$ was transferred to V-shaped bottom 96 well plates and centrifuged for 10 min. then 150 ul of the supernatant was diluted in 2% nitric acid and the silver was measured by ICP-MS.

2.2.3 Lactate production assay

The amount of the lactate produced by *S. sanguinuis* was measured using the lactate production assay, as an indicator of the presence of metabolically active bacterial cells (Besinis *et al*., 2014). After 24 h incubation of the plates, 100 µl from each well were transferred to V-shaped bottom 96-well plates (code: 3896, corning, UK). Then the 96-well plate was centrifuged for 20 minutes at 2000 rpm (2040 Rotors microplate centrifuge, Centurion Scientific Ltd, Ford, UK). Ten µl of the supernatant from each well was carefully transferred to flat bottom 96-well plates and mixed with 211 µl of a lactate assay reagent. The lactate assay reagent consists of 200 µl of glycine/hydrazine buffer, 10 µl of 40 mM nicotinamide adenine dinucleotide (NAD+, Melford Laboratories Ltd, Suffolk, UK) and 1 µl of 1000 units/ml lactate dehydrogenase (LDH, Sigma-Aldrich Ltd, Dorset, UK). The glycine/hydrazine buffer was prepared by dissolving 0.4 M hydrazine and 0.5 M glycine in Milli-Q water and the pH adjusted to 9 using a few drops of 6 M potassium hydroxide. Samples were incubated for 2 h at 37 °C incubator, and then absorbances were read with the VersaMax plate reader at 340 nm. Absorbances were converted to molar concentration using a calibration curve of lactic acid standards in triplicate (0, 0.125,

0.25, 0.5, 1.0, 2.0, 4.0, 8.0, and 16 mM). The standards were prepared by adding 480 µl of 30 % lactic acid to 100 ml of MilliQ water to get 16 mM, and then a 50 % serial dilution was made to get 8, 6, 4, 2, 1, 0.5, 0.25, 0.125 mM (Appendix B).

2.2.4 Dialysis experiment

This experiment was performed to investigate whether the materials used in the above experiment will dissolve in physiological conditions. This was determined by measuring the apparent total dissolved metal concentrations that could pass through the dialysis bags into the external media. The dialysis method is based on Handy *et al*., (1989) with modifications for nanomaterials. Briefly, the experiment consists of preparation of 100 mg/l of AgNPs, $AgNO_3$, P25, nHA and mHA solutions, the initial 1 g/l stock dispersions and solutions were used to prepare the 100 mg/l stock solution in physiological saline and milliQ water as described in section 2.2.2. All the tested solutions were sonicated for 4 h before adding to the dialysis bags. All glassware of identical shape and size was acid washed in 5 % nitric acid for 24 h and then rinsed three times with milliQ water. The dialysis bags (18 cm long x 25 mm wide, dialysis tubing product code: D9777, cellulose membrane with a molecular weight cut off at 12,000 Da, Sigma-Aldrich, St. Louis, USA) were filled with 8 ml of the appropriate stock dispersion, solution, or a control (control groups were milliQ water or physiological saline with no added particles). The ends of the bags were secured by making knots in the bottom and putting medi-clips at the top. The beakers were filled with 492 ml of either milliQ water or physiological saline. Then, the bags were immediately placed in the beakers (they were held by thread to maintain the dialysis bags in the middle of the beaker). The beakers were gently stirred on a multipoint magnetic stirrer (RO 15P power, IKa- Werke GmbH & Co. KG, Staufen, Germany) for 24 h at room temperature. Samples (4.5 ml) were taken from the beakers for metal

analysis and pH measurements at 0, 30 min, 1 h, 2 h, 3 h, 4 h, 6 h, 8 h, and 24 h. Five hundred µl of the samples was used to measure the pH and the remaining (4 ml) were analysed by ICP-MS for total metal concentrations. Furthermore, the temperature of the media in the beakers was measured at each time point. The remaining contents of the dialysis bag were also collected at the end of the experiment for metal analysis.

2.2.5 Statistics

All data were presented as mean ± S.E.M, and were analysed using STATGRAPHICS Centurion XVI.I. The differences between the tested samples and the control; and within each group (dilution effect) were evaluated using one-way ANOVA or Kruskal-Wallis. The All statistical analysis used a 95 % confidence limit, curve fitting for dialysis experiment were done using Sigma Plot 12.0 (Systat Software, Inc.).

2.3 Results

2.3.1 Particle size distribution

The particle size distribution of the nanomaterials and their bulk or salt equivalents in physiological saline was measured using NTA (Figure 2.1). The mean value of aggregate size in control physiological saline (mean ± S.E.M, n = 3) was 147 ± 12 nm. Dispersion of 100 mg/l AgNPs in physiological saline resulted in an aggregate size 128 ± 17 nm. While average aggregate sizes of 100 mg/l $AgNO_3$ was 145 ± 13 nm. The average aggregate size for bulk TiO_2 and the P25 material was 130 ± 10 nm and 150 ± 18 nm respectively, and 171 ± 15.64 nm, 99 ± 14.1 nm for mHA and nHA respectively.

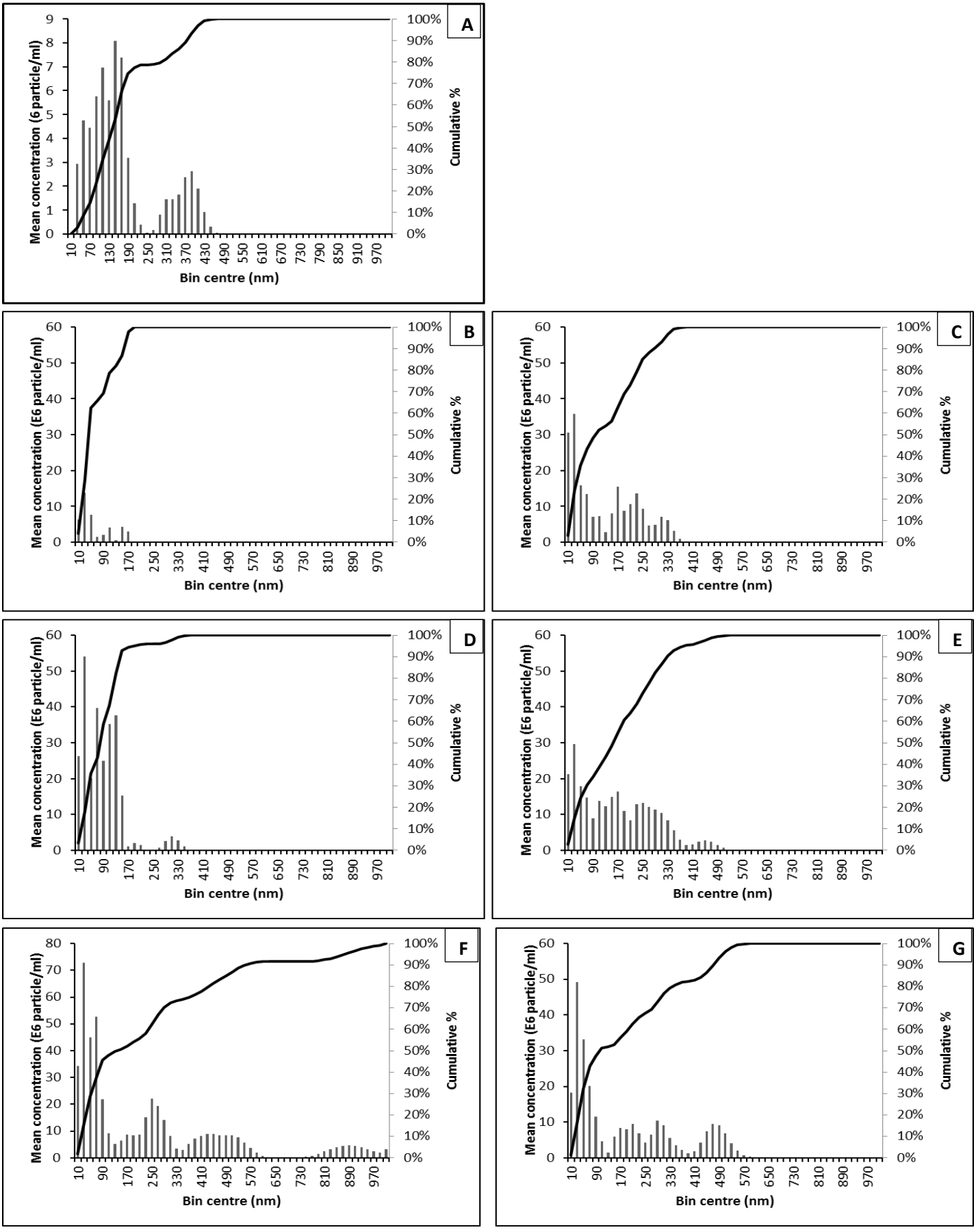

Figure 2.1 Particle size distribution in physiological saline, A) Physiological saline (control), B) silver nitrate, C) silver nanoparticles, D) titanium dioxide (bulk), E) titanium dioxide nanoparticles, F) hydroxyapatite microparticles and G) hydroxyapatite nanoparticles (mean ± S.E.M, *n=3)*.

2.3.2 Minimum inhibitory concentration (MIC) assay

The turbidity of the inoculated solutions after 24 h incubation was measured at 595 nm. Figure 2.2 shows the turbidty of the nanomaterial and their bulk in physiological saline. The reference microplates (the test solutions with no added bacteria) were used to correct the data by subtracting the turbidity caused by the particles alone from the inoculated solution (Figure 2.2). This resulted in negative values for most of the solutions at the high concentrations of these materials, but did adequately correct for particle turbidity at lower concentrations in each dilution series. According to the turbidity measurements, most of the test substances had a concentration-dependent effect on the growth of *S. sanguinius*. All the dilutions of $AgNO_3$ are significantly lower than the control physiological saline, as the turbidity of inoculated physiological saline (mean ± S.E.M) was 0.401 ± 0.012, and the highest concentration of $AgNO_3$ (400 mg/l) was showed a negative value (- 0.168 ± 0.004), whereas the other dilutions of $AgNO_3$ were showed some growth but significantly lower than the control (physiological saline, Figure 2.2). AgNPs also showed a siginficant difference with physiological saline, as 400 mg/l showed a negative values. Whereas 200 and 100 mg/l of AgNPs showed 33.6 % and 37 % growth inhibition compared to control. Other dilutions of the AgNPs showed higher absorbance values compared to the control. The high concentrations of TiO_2 nanoparticles and bulk also showed negative values and the more diluted solutions showed a concentration-effect on bacterial growth. Likewise, mHA and nHA also had a concentration-effect on the bacterial growth. Chlorhexidine caused full growth inhibition at concentrations of 1, 0.5, and 0.25 %. While the lower concentrations of chlorhexidine (0.125, 0.06, and 0.03%) showed no significant difference with the control. The turbidity of milliQ water (without added

physiological saline) was significantly lower than control (physiological saline), as the bacterial grwoth in milliQ water was lower by 78 % compared to physiological saline.

Figure 2.3 shows the results of turbidity of the nanomaterials and their bulk after 24 h exposure in 0.85 % NaCl. The high concentrations of $AgNO_3$ (400, 200, and 100 mg/l) showed high absorbance values compared to the control (0.85 % NaCl alone), even after subtracting the natural turbidity of the particles (Figure 2.3), whereas the turbidity of the more diluted solutions was siginificantly lower than the control. The AgNPs series of dilutions showed growth inhibition down to a concentration of 25 mg/l, whereas the more diluted AgNPs showed no growth inhibition. P25 and TiO_2 showed negative values at high concentrations, whereas the low concetrations of both materials were not significantly different from control.

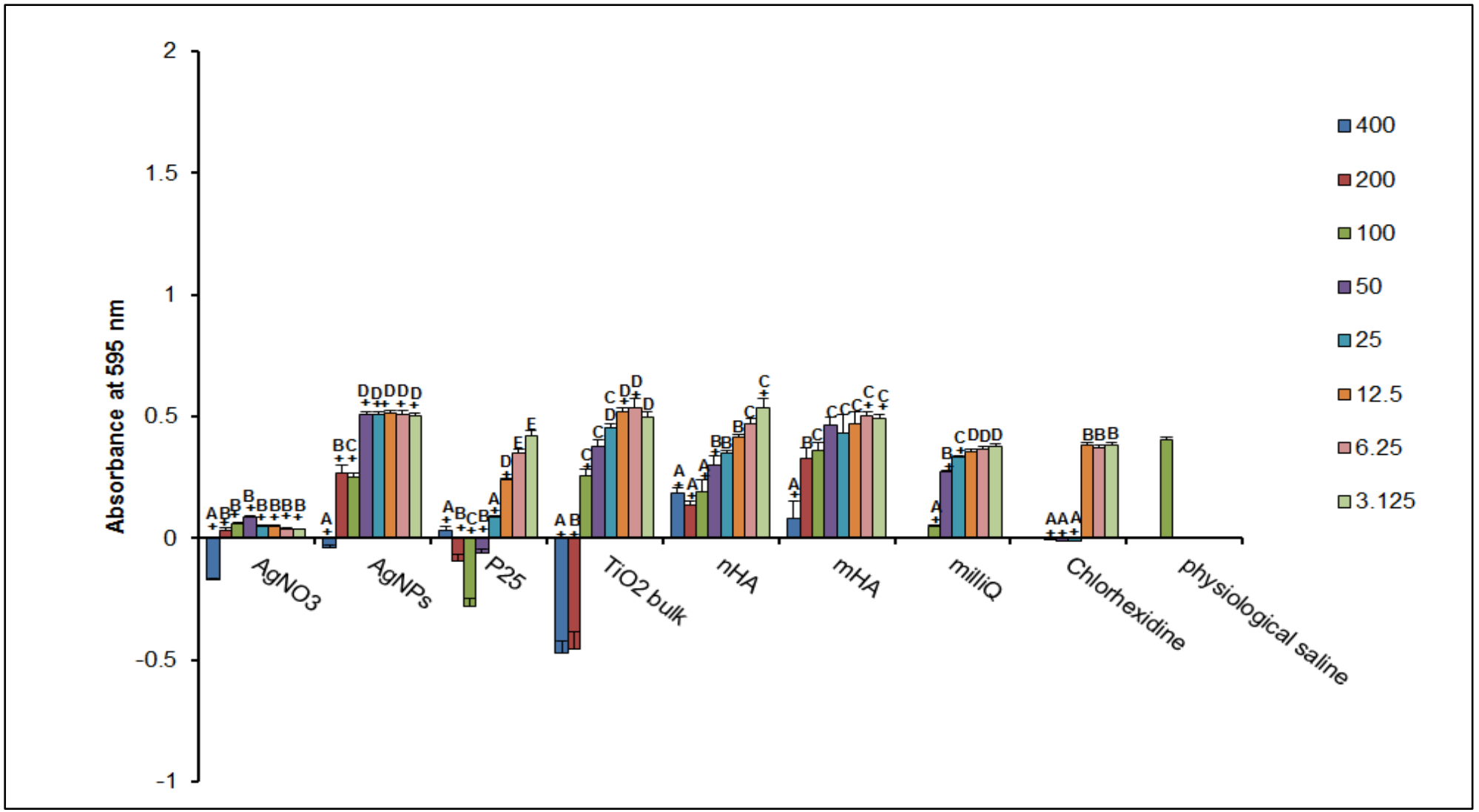

Figure 2.2 the effect of nanomaterials on the growth of *S. sanguinuis* in physiological saline over 24 h in the minimum inhibitory concentration test (MIC). The absorbance values were read at 595 nm. B) Absorbance values after subtracting the natural turbidity of the particles. (+) shows a significant difference from the physiological saline control (Kruskal-Wallis, $p<0.05$). Within each test solution, different letters indicate a statistically significant dilution effect (Kruskal-Wallis, $p<0.001$). The absence of letters indicates no statistical differences between any of the dilutions within the series.

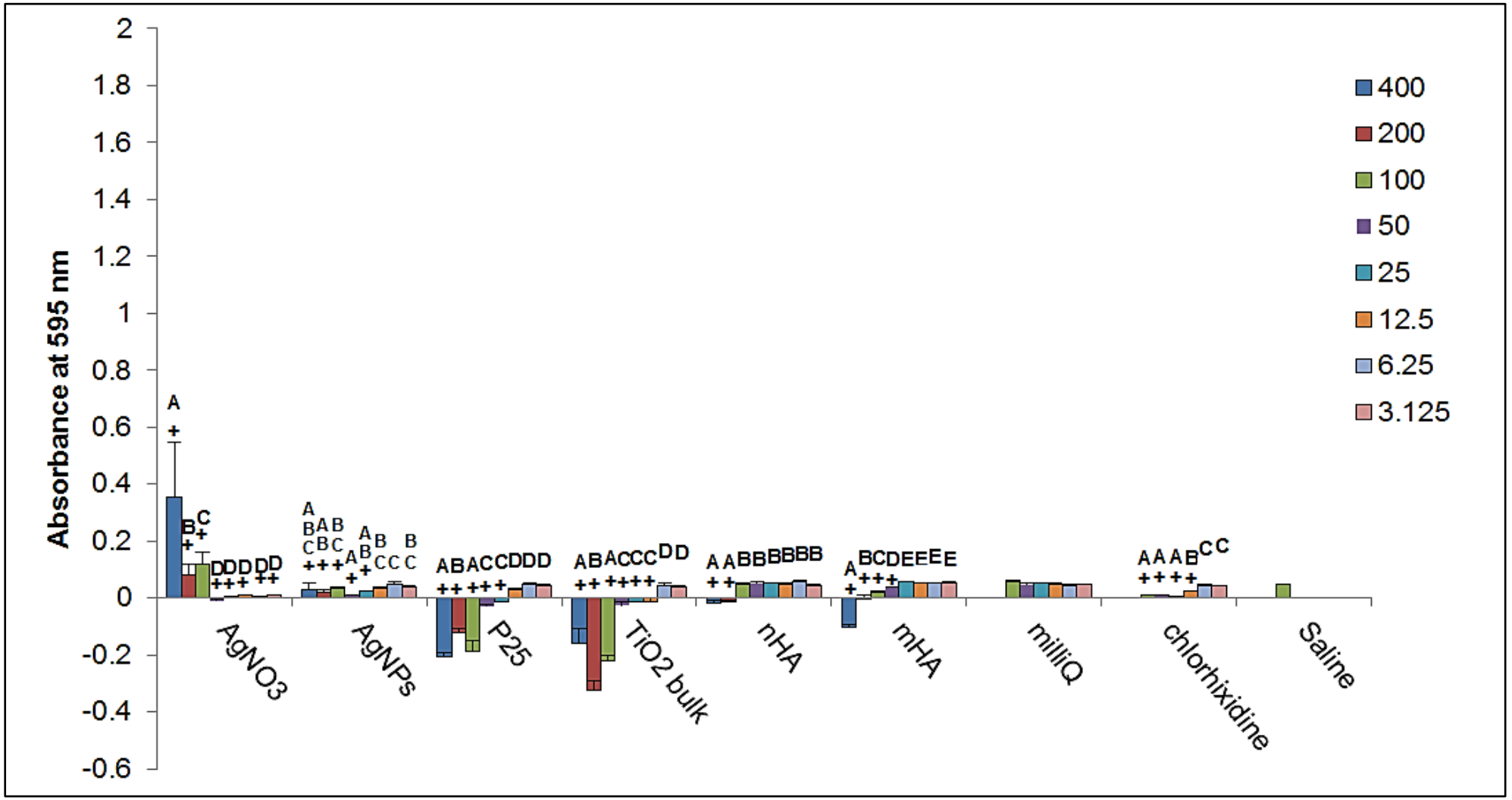

Figure 2.3 the effect of nanomaterials on *S. sanguinuis* in 0.85% NaCl over 24 h in the minimum inhibitory concentration test (MIC). The absorbance values read at 595 nm. B) Absorbance values after subtracting the natural turbidity of the particles. (+) shows the significant difference from the control (Kruskal- Wallis, $p < 0.001$). Within each test solution, different letters indicate a statistically dilution effect (Kruskal-Wallis, $p < 0.001$). The absence of letters indicates no statistical differences between any of the dilutions within the series.

2.3.3 Lactate production

The lactate produced by *S. sanguinis* was measured after 24 h exposure to different nanomaterials and their bulk/metal salts in both 0.85% NaCl and physiological saline (Figure 2.4). In physiological saline (Figure 2.4 A), there was no lactate production in any of the dilutions of $AgNO_3$. Whereas all dilutions of AgNPs showed full lactate production like the control, except 400 mg/l of AgNPs which showed a 99.5 % decrease in lactate production compared to the control. The remaining materials (P25, TiO_2, nHA, and mHA) showed no significant difference with the control; high level of lactate was measured in all dilutions. Chlorhexidine showed a concentration-effect on the lactate production. No lactate was detected in 1 % (v/v) chlorhixidine, whereas the lactate levels in 0.5 % and 0.25 % (v/v) chlorhixidine were lower than the control by 99.5 % and 91.1 % respectively. MilliQ water had a concentration-effect on lactate production; lactate production in 100% milliQ water was 80.3 % lower than the control, whereas further diluted samples showed a negligible decrease in lactate production compared to physiological saline.

Overall, *S. sanguinis* produced lower concentration of lactate in 0.85 % NaCl compared to physiological saline (Figure 2.4 B); the maximum lactate production was 4.355 mM in 0.85 % NaCl whereas in physiological saline was 20.363 mM. Figure 3 B shows that the lactate levels in all $AgNO_3$ dilutions were lower than the control by approximately 90 %. Among the nanoparticles, AgNPs showed antibacterial activity against *S. sanguinis* in the 400, 200, 100, and 50 mg/l dilutions; the lactate production was 91 % lower than the control and lactate levels remained statistically lower than the control in the further dilutions of AgNPs. The lactate production in the P25 and bulk TiO_2 dilutions were statistically lower than the 0.85 % NaCl control, but still were at millimolar levels (> 3.5 mM).

Intrestingly, the high concentrations of mHA (400, 200, 100, and 50 mg/l) showed higher lactate levels compared to the control (0.85 % NaCl); the lactate level was (in mM) 7.052 ± 0.17, 6.180 ± 0.068, 5.17 ± 0.11, 4.936 ± 0.31 for 400, 200, 100, and 50 mg/l of mHA, respectively. While lower concentrations of mHA (25, 12.5, 6.25, and 3.125 mg/l) showed no significant difference with the control. nHA showed no significant difference with the control in all dilutions. Chlorhexidine showed a concentration-dependent antibacterial effect against *S. sanguinis*; the lactate levels in 1%, 0.5 %, and 0.25 % (v/v) dilutions were upto 90 % lower than the control. The lactate production in 0.125 % and 0.06 % (v/v) chlorhixidine was lower than the control by 65 % and 24 % respectively. While the 0.03 % dilution showed no significant difference compared to the control. MilliQ water did not show a negative effect on the lactate production compared to the control. In contrast, 100 % milliQ water (with no added 0.85 % NaCl) showed higher lactate production compared to control.

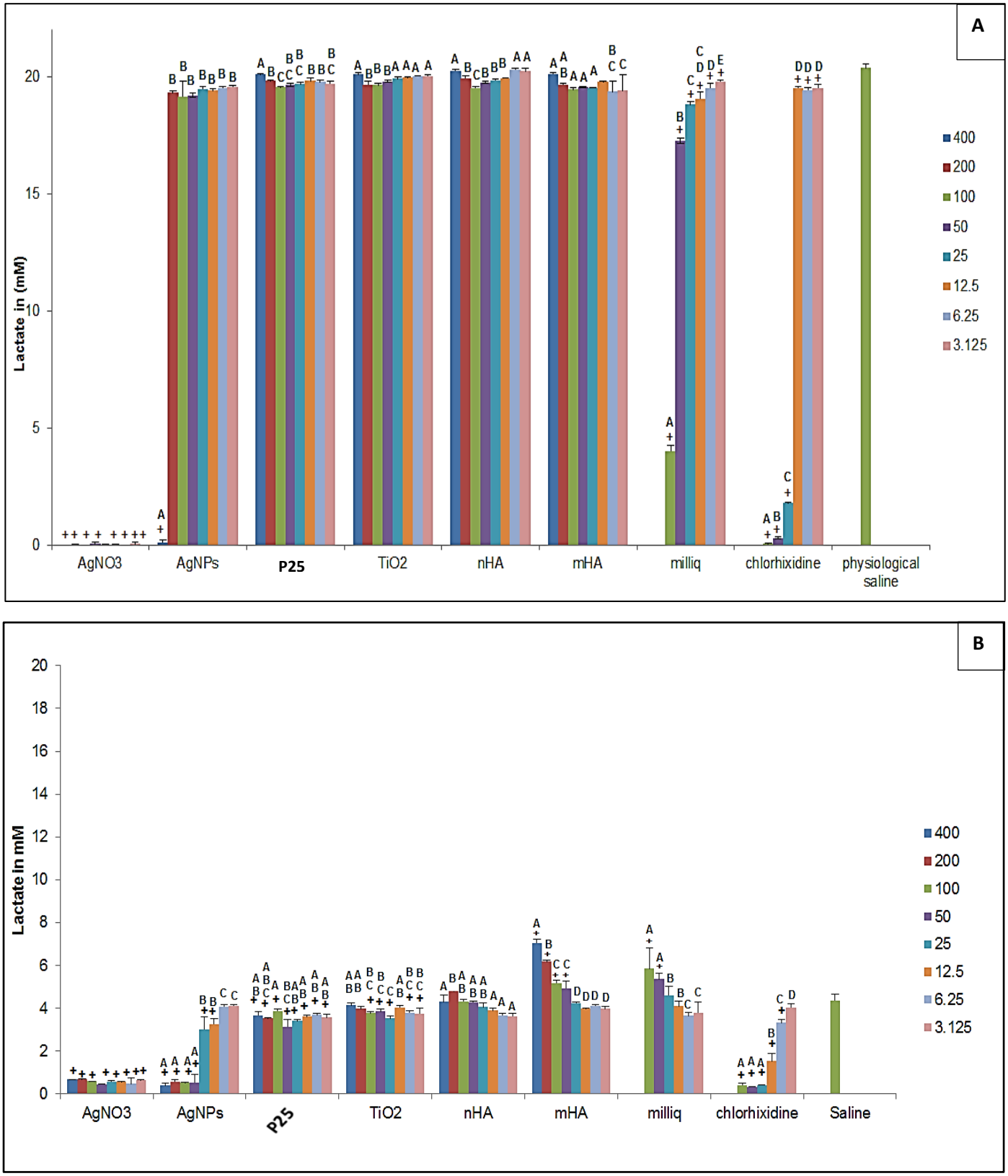

Figure 2.4 the concentration of lactate (mean ± S.E.M in mM) produced by S. sanguinuis exposed to different nanomaterials and their bulk after 24 h. A) Nanomaterials and their bulk in physiological saline. B) Nanomaterials and their bulk in 0.85% NaCl. "+" shows significant difference from the control group (physiological saline and 0.85% NaCl) (Kruskal-Wallis, $p<0.001$), within the test solution, different letters indicate statistically significant dilution effect (Kruskal-Wallis, $p<0.001$) between the dilution series.

2.3.4 Measuring the concentration of dissolved silver

After 24 h incubation, the concentration of the dissolved silver in all serial dilutions of AgNPs and $AgNO_3$ in physiological saline was measured using ICP-MS (Table 2.3). It is apparent that the dissolution of silver was very low for all the dilutions of $AgNO_3$ and AgNPs. In general the silver concentration in $AgNO_3$ serial dilutions was higher compared to the AgNPs. Interestingly, the silver concentration in the nominal 400 mg/l AgNPs was lower than the more diluted dispersions of AgNPs (nominal concentrations, 200, 100, 50, and 25 mg/l).

Table 2.3: The concentration (mg/l) of the dissolved silver in physiological saline at 24h in the MIC assay after centrifugation

Nominal Concentration mg/l	**$AgNO_3$**	**AgNPs**
400	0.469 ± 0.02 ab	0.104 ± 0.00 abc
200	0.437 ± 0.03 ac	0.161 ± 0.01 a
100	0.507 ± 0.01 ab	0.160 ± 0.00 a
50	0.498 ± 0.02 b	0.131 ± 0.01 ab
25	0.387 ± 0.03 cd	0.117 ± 0.01 ab
12.5	0.343 ± 0.02 d	0.078 ± 0.01 bc
6.25	0.288 ± 0.02 e	0.034 ± 0.00 cd
3.125	0.027 ± 0.00 f	0.011 ± 0.00 d

Data are presented as (mean ± S.E.M), data sharing different letters within columns are statistically different (Kruskal-Walis, $p< 0.03$)

2.3.5 Dialysis experiment

The results of the dialysis experiment showed that the total dissolved silver from AgNPs in both milliQ water and physiological saline was lower compared to $AgNO_3$. Figure 2.5A shows the cumulative amount of silver released for AgNPs and $AgNO_3$ in milliQ water. Silver concentration remained in few micrograms per liter for AgNPs over 24 h. In contrast, $AgNO_3$ completely dissolved in milliQ water, as the dissolution of silver from $AgNO_3$ in milliQ water reached 0.5 mg (mean of triplicate, absolute amount released) after 8 h. While in physiological saline, the dissolution of $AgNO_3$ was lower compared to its dissolution in milliQ water; the maximum rate of appearance of cumulative total silver in physiological saline was 0.1 mg over 24 h. The dissolution of AgNPs in physiological saline was only 0.017 mg/l over 24 h (Figure 2.5 B). Figure 2.6 shows the cumulative amount of Ti released for the P25 material, there was no detectable titanium dissolution in milliQ water. While in physiological saline, a few micrograms of Ti rapidly appeared in the external media. The cumulative amount of Ti released over 24 h was 25 µg.

To investigate the dissolution of nHA and mHA, the concentration of of calcium and phosphorus in the external media was measured during dialysis. Figures 2.7A and B shows the cumulative amount of calcium and phosphourus released over 24 h. An increase in the concentration of calcium and phosphorus was observed in milliQ water for both nHA and mHA. In physiological saline, ICP-MS measurements includes the concentration of calcium and phosphorus in physiological saline and nHA and mHA (Figure 2.7 C and D).

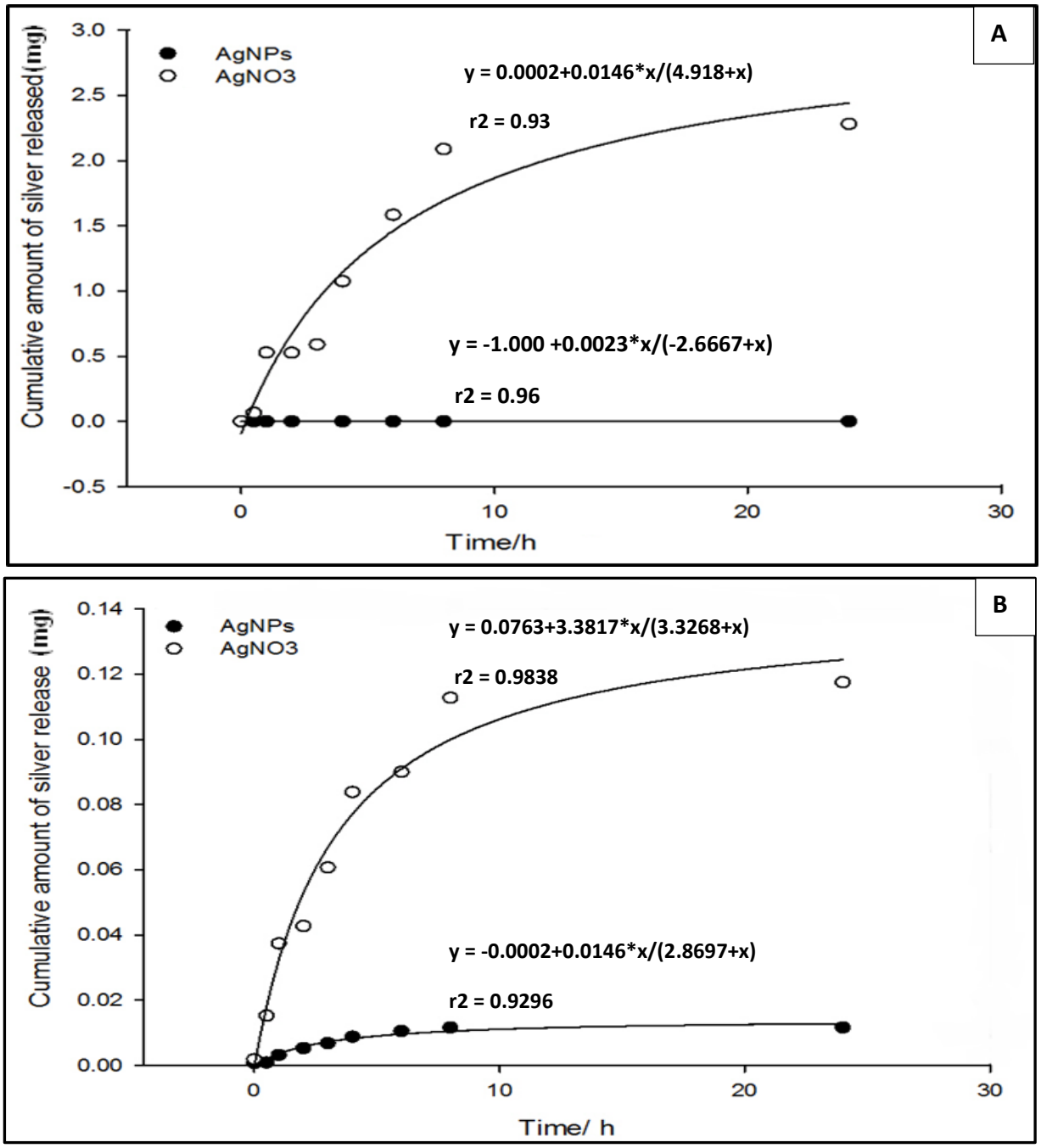

Figure 2.5 The cumulative appearance of total Ag metal (in mg) through dialysis tubing into the external medium of beakers for dialysis bags containing 100 mg/l AgNO3 and AgNPs using either A) milliQ water or B) physiological saline. The data points are mean values derived from triplicate measurements (n = 3 beakers per treatment). Curves are fitted to the mean data points shown using a rectangular hyperbole function (one site, ligand binding to saturation) in Sigma Plot version 12. • refers to silver nanoparticles (AgNPs), and ◦ refers to silver nitrate ($AgNO_3$).

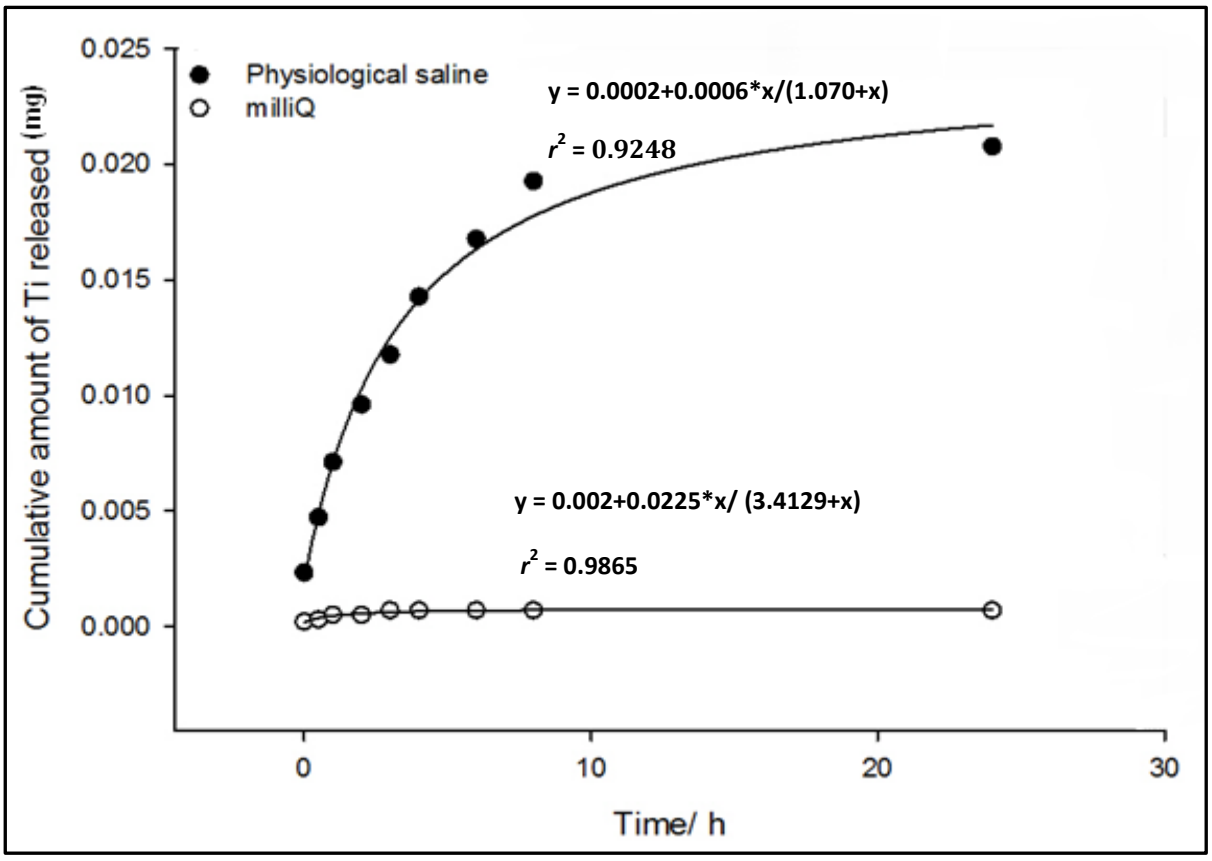

Figure 2.6 The cumulative appearance of total Ti metal (in mg) through dialysis tubing into the external medium of beakers for dialysis bags containing 100 mg/l P25 using either milliQ water or physiological saline. The data points are mean values derived from triplicate measurements (*n* = 3 beakers per treatment). Curves are fitted to the data points shown using a rectangular hyperbole function (one site, ligand binding to saturation) in Sigma Plot version 12.5. • refers to the dissolution of P25 in physiological saline, and ◦ refers to the dissolution of P25 in milliQ water.

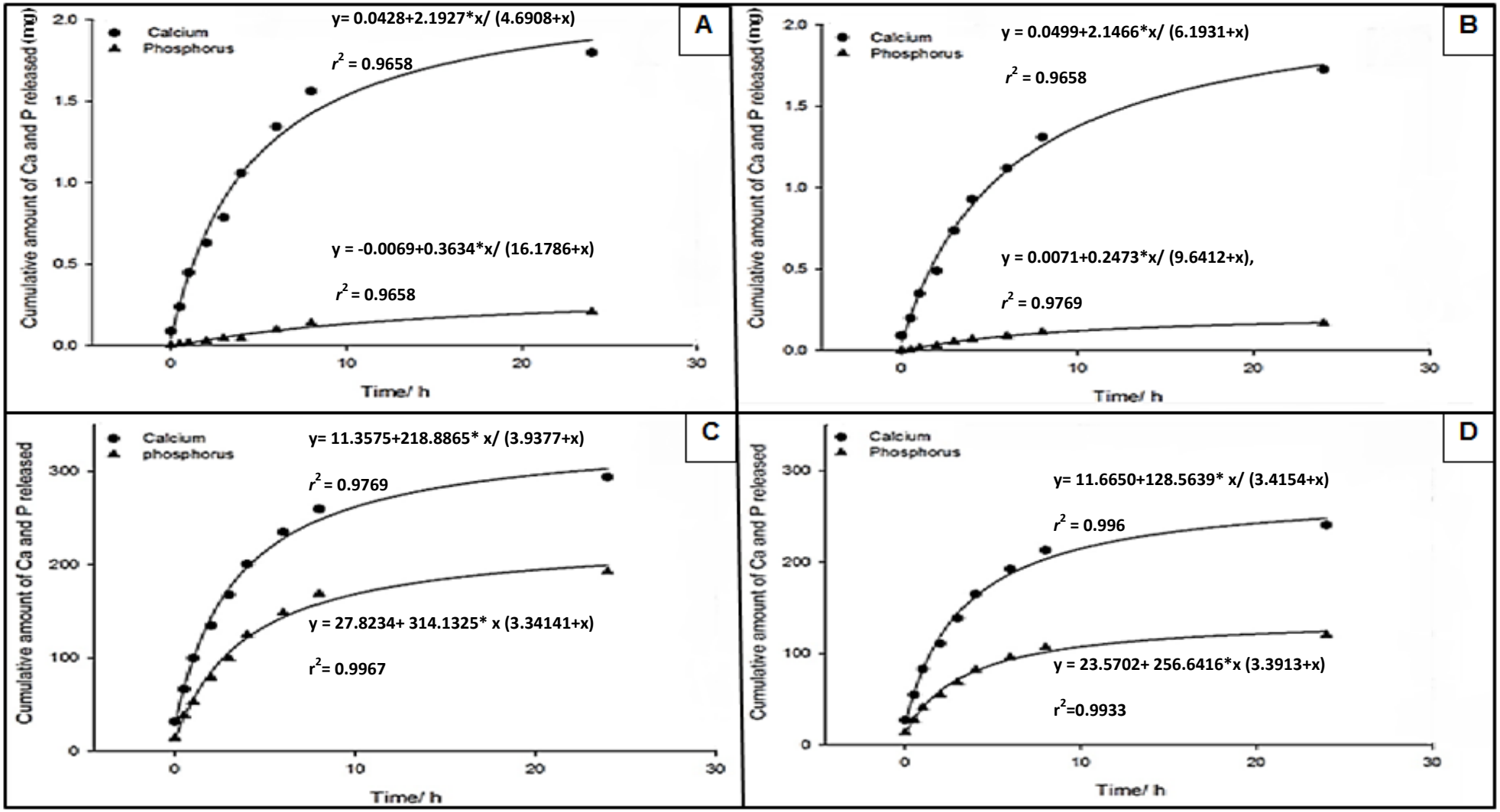

Figure 2.7 The cumulative appearance (in mg) of total calcium and phosphorus through dialysis tubing into the external medium of beakers for dialysis bags containing 100 mg/l nHA and mHA using either milliQ water or physiological saline. The data points are mean values derived from triplicate measurements (*n* = 3 beakers per treatment). Curves are fitted to the data points shown using Hyperbola, Single Rectangular I, 3 Parameter in Sigma Plot version 12.5. A) nHA in milliQ. B) mHA in milliQ. C) nHA in physiological saline. D) mHA in physiological saline.

2.4 Discussion

This study reports the antibacterial activity of different nanomaterial dispersions and their bulk powder or metal salt against the clinically-relevant microbe, *S. sanguinis.* Two different solutions (0.85 % NaCl-BHI broth + 2 % sucrose medium, and physiological saline-BHI broth + 2 % sucrose) were used to test the antibacterial effects of the nanomaterials. The bacterial growth was determined by two different assays; the MIC and lactate production assays. The main findings were that silver nitrate was the most effective antibacterial material against *S. sanguinis*, and among the tested nanomaterials, only AgNPs showed antibacterial activity against the bacteria. The MIC of silver nanoparticles is 50 mg/l in 0.85 % NaCl and 400 mg/l in physiological saline. Furthermore, the growth of the bacteria in milliQ water (with no added NaCl) was higher compared to its growth in 0.85 % NaCl. In terms of antibacterial assays, lactate production assay could be a good alternative to routine measurements of growth inhibition with the MIC method, because the latter relies on turbidity measurements which can be problematic for the nanomaterials.

2.4.1 Characterization of the nanomaterials and their equivalent bulk powder or salt solutions

The need to characterize the nanomaterials prior to any *in vitro* study is highly important, especially for those nanoparticles where their toxicity depends mainly on the particle size (Murdock *et al*., 2008). The nanoparticles and their bulk or metal salts were characterized in the physiological saline using NTA (Figure 2.4). The main finding of this study was that the physiological saline (with no added particles) showed a hydrodynamic diameter of aggregates (147 ± 12 nm). It seems possible that this high background noise is due to the presence of salt crystals in

physiological saline. Hence, it was difficult to get reliable values for the particles distribution in physiological saline, particularly for $AgNO_3$ and AgNPs (Figure 2.4B and C). This is mainly because of rapid precipitation of the silver in a solution containing NaCl. It is well known that silver has a high ability to bind to the halide groups and will produce insoluble particles of silver chloride. The results of dialysis experiment also support this idea, as the dissolution of both silver nitrate and AgNPs were drastically decreased in physiological saline (Figure 5.2B). This is probably mainly due to AgCl formation. This finding is in accordance with a study done by Loza *et al*. (2014), who found that the dissolution of AgNPs is very low in the presence of NaCl in the biological solutions.

The titanium dioxide nanoparticles and microparticles were also characterized using NTA (Figure 2.4D and E); they did show a negligible difference in the particle size distribution compared to its distribution in milliQ water as reports in Besinis *et al*. (2014). This means that the nano form has aggregated to make aggregates of a similar size to that of the bulk material. In contrast, dialysis experiment showed that the dissolution of titanium dioxide nanoparticles was higher in physiological saline compared to milliQ water. Hence, this should be considered when titanium dioxide will be used in the medical field; as the titanium dioxide can accumulate in the tissues (Fabian *et al*., 2008).

Furthermore, the results of dialysis experiment showed that hydroxyapatite nanoparticles and microparticles almost completely dissolved in water (Figure 2.7A and B). Hydroxyapatite, upon dissolution, will release calcium and phosphorus which are the main component of hydroxyapatite. This finding is in agreement with Clark *et al*. (1955) who showed that hydroxyapatite has ability to dissolve in the water. It was difficult to investigate the dissolution of hydroxyapatite in the physiological saline,

because this media contains a high concentration of calcium and phosphorus. However, cumulative increase was noticed in the beaker over time for both hydroxyapatite nanoparticles and microparticles (Figure 2.7C and D), which can be related to their dissolution. This finding seems to be consistent with the research done by Tsui *et al*. (1998) who found that hydroxyapatite can dissolve in ringer solution, but at a low rate. Nevertheless, in term of comparing the change in the dissolution of hydroxyapatite in water and in biological fluid, it is difficult to use these results.

2.4.2 MIC assay

The MIC assay was used to determine the antibacterial effect of the nanomaterials and their equivalent bulk or metal salts. Overall, the results showed that the growth of bacteria was higher in physiological saline than in 0.85 % NaCl media. This is because physiological saline is a more nutrient-rich media for the bacterial growth than a simple salt solution. Moreover, the results showed that most of the tested materials had a concentration-dependent antibacterial effect in both media (0.85 % NaCl and physiological saline, Figure 2.2 and 2.3). Previous research done by Besinis *et al*. (2014), using bulk TiO_2, showed antibacterial effect upto 12.5 mg/l. This is because different microbe was used for the study. The MIC of nHA and mHA was 200 mg/l in 0.85 % NaCl, whereas the antibacterial effect of nHA was upto 50 mg/l in physiological saline. Hydroxyapatite nanoparticles and microparticles did not show any antibacterial effects. Overall, these data must be interpreted with caution because the MIC assay has some limitations for testing nanoparticles, especially at high concentrations (> 12.5 mg/l, Besinis *et al*., 2014). The MIC assay depends on measuring the absorbance of the samples, and the nanoparticles used in this study added some turbidity to the media. Hence, the natural turbidity of the particles may

potentially mask any absorbance caused by the bacteria. The protocol of Besinis *et al*. (2014) was followed to improve the validity of the turbidity measurements in the MIC assay, by subtracting the natural turbidity of the particles. This correction led to negative values for most of the materials at high concentrations in both media (physiological saline and 0.85 % NaCl, Figure 2.2 and 2.3). This could be due the effect of the bacteria on aggregation of the particles (Otsuka *et al*., 2003). The aggregated particles allow the light of spectrophotometry to pass through the sample faster, so the absorbance values become lower. Hence the absorbance values of the particles alone was higher than the absorbance value of particles and bacteria.

Interestingly, the turbidity of $AgNO_3$ (nominal concentrations, 400, 200, and 100 mg/l) in the 0.85% NaCl was significantly higher than the control (0.85 % NaCl alone). This finding was unexpected and there are two explanations for this observation, either (i) the silver was not bioavailable to inhibit the bacterial growth, or (ii) the high absorbance values is due to rapid precipitation of silver as silver chloride, in the presence of high concentration of silver in 0.85 % NaCl solution. The latter seems more likely, as the $AgNO_3$ showed high antibacterial activity even at lower concentration (50 down to 3.125 mg/l of $AgNO_3$). While in physiological saline, $AgNO_3$ showed high antibacterial activity against *S. sanguinis* in all concentrations, and did not show high absorbance values in nominal concentrations 400, 200, and 100 mg/l. This finding is somewhat surprising, an explanation for this could be the presence of other chemicals in physiological saline that impede the precipitation of silver as AgCl formation. Another possible explanation could be due to the difference in chloride concentration in these two solution. The concentration of chloride in physiological saline was 123 mM and 145.5 mM in 0.85 % NaCl solution; the higher concentration of chloride in the latter might have an effect on the silver precipitation.

Another observation was that the antibacterial activity of AgNPs in 0.85 % NaCl media was better than its activity in physiological saline. AgNPs showed bacterial growth inhibition down to 25 mg/l in 0.85 % NaCl. This finding accords with the earlier observations by Besinis *et al*, (2014), which showed that AgNPs also had antibacterial effect against *Streptococcus mutans* down to 25 mg/l in 0.85 % NaCl. AgNPs have less antibacterial activity in physiological saline compared to the 0.85 % NaCl, this could be due to the fact that AgNPs lose its bioavailability in more complex media. For example, Stebounova *et al*. (2011) stated that the bioavailability of the AgNPs will decrease in a solution with high ionic strength, due to their settling in such media.

2.4.3 Lactate production assay

The lactate assay was used to investigate the antibacterial activity of different nanomaterials. This assay relies on the metabolic activity of the bacteria; apparently it is more sensitive than the MIC assay (Besinis *et al*., 2014). A high lactate concentration in the media would indicate metabolic lactate production from live cells. Consequently, an increase in lactate concentration might infer a higher percentage of surviving bacteria. The results indicated that the bacteria was growing better in physiological saline compared to their growth in 0.85 % saline (Figure 2.3A and B). That was not unexpected, because it is well known that bacteria can not grow well in high concentration of sodium chloride alone. The high concentration of NaCl solutions are traditionally used for food preservation (Doyle *et al*., 2010). Silver nitrate showed a higher antibacterial activity against *S. sanguinis* in both physiological saline and NaCl solution compared to the most common disinfectant in

use in dentistry (chlorheixidine), this results are consistent with those found by Besinis et al. (2014). Moreover, the antibacterial activity of $AgNO_3$ in physiological saline was higher compared to its activity in 0.85 % NaCl (Figure 2.3). It is supposed that the antibacterial activity of silver will differ, depending on the composition of the media that is used for bacterial growth. This could be due to the higher concentration of chloride in 0.85% NaCl compared to chloride concentration in physiological saline as described previously. This may result in the rapid precipitation of $AgNO_3$ and slow its action against the bacteria. Hence, the bacteria were produce some lactate before their death, but this lactate subsequently remained in the media.

Contrary to $AgNO_3$, the AgNPs showed higher antibacterial effect on *S. sanguinis* in 0.85% NaCl compared to its effect in physiological saline (Figure 2.3). This probably mainly due to the effect of high electrolyte content of physiological saline on the AgNPs, by which led to its aggregation and loss of the bioavailability (Lok *et al*., 2007). Furthermore, the presence of glucose in the media could also slow down the dissolution of AgNPs and inhibits their action against bacteria consequently (Loza *et al*., 2014).

The TiO_2 nanoparticles and bulk did not show any antibacterial activity against *S. sanguinis* in physiological saline, and showed a negligible effect in the 0.85% NaCl. This may be because NaCl solution in broth is not a complete media for the bacteria to grow as mentioned earlier, hence the bacteria will become more sensitive to unfavorable condition and their metabolic activity will decrease. No growth inhibition was noticed in all hydroxyapatite nanoparticles/ microparticles solution. Interestingly, the high concentrations of hydroxyapatite microparticles increase the growth of bacteria in NaCl, since the hydroxyapatite contributes to the favorable conditions for the bacterial growth (Rameshbabu *et al*., 2007). Another possible explanation

could be due to the fact that the dissolution of the hydroxyapatite will lead to calcium and phosphorus release in the media; this resulted in a nutreint-rich media that can increase the growth of the bacteria.

2.5 Conclusion

The purpose of this study was to characterize different nanomaterials and investigate their antibacterial activity against *S. sanguinis*. The following conclusion can be drawn from the present study:

1- Only Ag NPs had antibacterial activity among the tested nanomaterials. Moreover, antibacterial effect of Ag NPs in 0.85 % NaCl was better than in physiological saline.

2- $AgNO_3$ was showed antibacterial activity against the tested microbe in all concentration and in both tested media.

3- Another significant finding to emerge from this study is that, the lactate production was more reliable than MIC assay for investigating the antibacterial effects of nanoparticles.

4- Finally, the dissolution of both $AgNO_3$ and AgNPs was very low in the physiological saline compared to milliQ water, this is mainly due to the presence of chloride.

Taken together, these findings suggests an important role for the composition of the media in the antibacterial activity of silver nanoparticles and salts.

Chapter 3

Investigating the antibacterial activity of different coatings on titanium discs against *Streptococcus sanguinis*

3.1 Introduction

Peri-implantitis due to biofilm formation is one of the leading causes of medical and dental implants failure (Norowski *et al*., 2009). Several studies have focused on improving the surface of the implants for better anti-biofilm properties (Huang *et al*., 2010; Vogel *et al*., 2014; and Mei *et al*., 2014). To date, various methods have been developed to provide coatings with novel properties for the implants that can also prevent biofilm formation on their surfaces. Recently, a number of different researchers have sought to develop a multi-layered coating for the implant composed of silver and a bioactive material such as hydroxyapatite (Ciobanu *et al*., 2012; Akiyama *et al*., 2013). Moreover, it was proposed that electrically prepared silver coatings could show a broad spectrum antibacterial activity (Scales *et al*., 1984).

The stability of the coating is one of the essential criteria that is difficult to obtain, because most of the biomaterials will act differently when they come in contact with the body fluid (Williams, 1987). For example, metals such as silver can release free ions in the biological fluid which might circulate in the blood. The exact mechanism by which silver ion circulate in blood is unknown, but might be related to strong binding of silver ions with proteins (Walker *et al*., 2012). Hence, it is important to ensure a controlled or negligible ion release from the implant surface over the long term. Furthermore, detachment of the coating from the surface of implant might also compromise the mechanical stability of the implant; leading to its failure (Yang *et al*., 2003).

The aim of this study was to prepare a stable coating for the titanium that has a good anti-bacterial property; using simple inexpensive techniques. The main objectives were to: (i) prepare and characterize different coatings on titanium surfaces, (ii) investigate the antibacterial activity of different coatings against one of the early colonizers of the biomaterial surfaces, *S. sanguinis*. Qualitative and quantitative methods were used for this purpose, and (iii) evaluate the stability or the degradation of the coatings in the physiological conditions.

3.2 Methodology

3.2.1 Preparation of titanium discs

Titanium discs, 15 mm in diameter and 1 to 1.5 mm thickness, were cut by a laser from medical grade 5 titanium alloy (Ti6Al4V). To standardize surface characteristics, the titanium discs has been polished by sand paper (#800-1200) using a rotary instrument (Grinder-Polisher, Buehler, UK Ltd, Coventry, England) for 10 minutes. The final polishing was performed using 0.1 µm diamond solution (Diamond solution, Kemet International Ltd, Parkwood Trading Estate, Maidstone, Kent ME15 9NJ UK). Then, the discs were cleaned with 20 g/l of NaOH + Na_2CO_3 solution in an ultrasonic bath (Metason 129T, Struers). To remove the oxide layer on the surface of the discs, further cleaning was carried out by immersing the discs in 5% HCl solution for 3-5 minutes.

3.2.2 Coating techniques

Three techniques were used to coat the titanium discs: (i) solution deposition and heating for hydroxyapatite micro and nanoparticles, (ii) electroplating to coat the discs with silver, and (iii) anodization to coat the discs with titanium dioxide.

Ultimately, nine types of titanium discs were prepared which were: uncoated Ti alloy used as a control group, silver plated (Ag), anodized (TiO_2), hydroxyapatite nanoparticles coated (nHA), hydroxyapatite microparticles coated (mHA), silver plated then coated with hydroxyapatite nanoparticles (Ag + nHA), silver plated then coated with hydroxyapatite microparticles (Ag + mHA), anodized and then coated with hydroxyapatite nanoparticles (TiO_2 + nHA), anodized and then coated with hydroxyapatite microparticles (TiO_2 + mHA).

3.2.3. Electroplating

Electroplating is a process of coating a metal with a thin layer of another metal by putting it in a chemical solution (the electrolyte) through which an electric current flows. The discs were cleaned (section 3.2.2), then the silver solution (electrolyte) was heated to 40°C which increase the adhesion of silver to the titanium. The silver solution was made of 0.2 M Ag, 0.4M succinimide and 0.5 M KOH with pH 8.5. Discs were hung on silver wire which was connected to the cathode (negative side) of the DC power and another silver wire was connected to the anode (positive side), and both sides (cathode and anode) were dipped in an electrolyte and the voltage was adjusted to 1 V and left for 3 minutes. Finally the discs were washed with distilled water and dried with a hair dryer. Figure 3.1 illustrates the silver plating method.

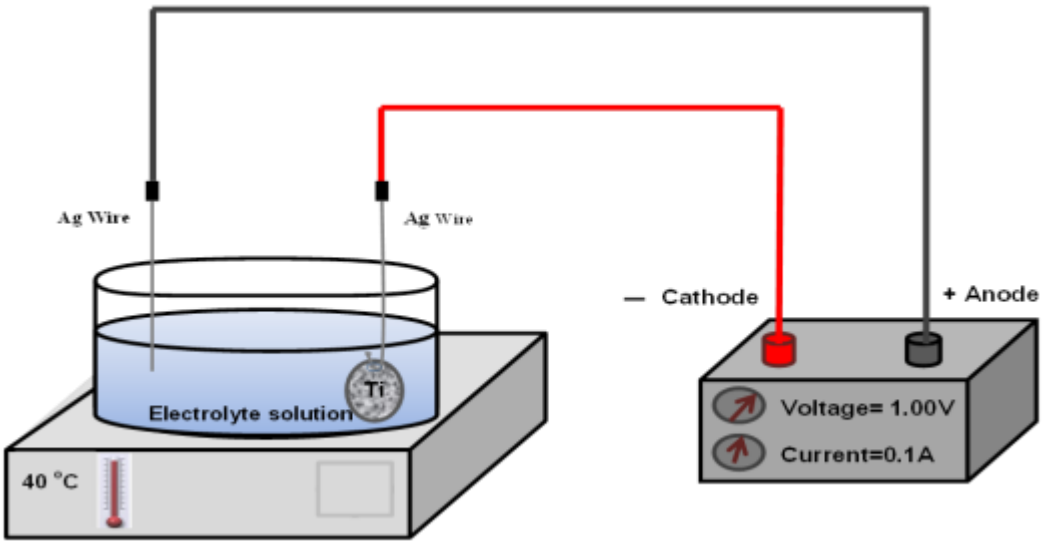

Figure 3.1 Silver-plating technique

3.2.4 Anodization to coat the alloy surface with titanium dioxide

This technique was used to produce a dense, compact and thin oxide layer on the titanium surface. First of all, discs were ultrasonically cleaned as described previously, then the disc was held on platinum wire and connected to the anode; the copper plate was connected to the cathode. Then both sides were dipped in the electrolyte; 5 g/l sodium acetate (NaAc) was used as an electrolyte solution. DC power was used to apply the anodization voltage. The voltage was adjusted to 30 V for 5 minutes in order to get a thin layer of titanium oxide. Finally the discs were removed and washed with distilled water and dried with a hair dryer.

3.2.5 Deposition and heating technique

This technique was used to coat the titanium discs with hydroxyapatite nanoparticles or microparticles. This technique includes deposition of hydroxyapatite nanoparticles or microparticles solutions on the titanium discs, then heating the coated discs upto

500 °C. Heating the hydroxyapatite coating has an important role in increasing the bonding strength between the hydroxyapatite and the titanium surface (Kim *et al*., 2004). Briefly, 15 % wt/v of hydroxyapatite nanoparticles and microparticles solutions were used for this technique. The hydroxyapatite nanoparticles solution was purchased from Fluidinova (Rua Eng. Frederico Ulrich 2650, 4470-605 Maia, Portugal); whereas 15 % wt/v hydroxyapatite microparticles solution was prepared by adding 15 g of hydroxyapatite microparticles powder (Fluidinova, Rua Eng. Frederico Ulrich 2650, 4470-605 Maia, Portugal) to 100 ml of water. Firstly, discs were sterilized with 70 % ethanol and were put in 24 well microplates (flat-bottom sterile, tissue culture treated polystyrene microplate, code: Greiner 662160, Bio-One Ltd., UK), Then 20 µl of hydroxyapatite (nanoparticles/microparticles) solution was added to the top of the discs and distributed evenly by pipette. The samples were left at room temperature to dry for 2 days. Afterwards the discs were put in a porcelain dish and put in the furnace (Carbolite, ELF 11/14, UK). The setting of the furnace was adjusted by which the temperature increased gradually (10 °C each min) until it reached 500 °C. Then the furnace was kept at this temperature for 10 min. Finally, the samples were left to cool down to room temperature. The reason for adjusting the temperature to 500 °C was to prevent the damage of the silver plated discs, as this temperature is lower than the melting point of silver. The time of heating the samples was adjusted to only 10 min at 500 °C to preserve the crystallinity of the hydroxyapatite.

Prior to using the technique above, a pilot study was carried out to investigate the effect of heating on the adhesion of hydroxyapatite microparticles and nanoparticles coatings to titanium discs. The concentration of the calcium and phosphorus released into the NaCl solution was measured, as it is an indicator of

coating degradation. The approach to the experiment was that hydroxyapatite (micro and nanoparticles) solution was applied on titanium surface as described above. After this the discs were divided into two groups (n = 3), the first group was heated up to 500 $^{\circ}$C and the second group were not. Then the discs of each group were placed in a glass bottle contained 70 ml of 0.85 % NaCl. Then the glass bottles were placed in a sonic bath up to 10 minutes. Samples (0.7 ml) were taken from the glass bottles in different times (0, 1, 2, 3, 4, 5, and 10 minutes). Then 0.7 ml of 2% nitric acid was added to each sample and measured by ICP-MS for metal concentrations (Table 3.1). Based on the results of this pilot study, heated discs showed less hydroxyapatite degradation (i.e. better adhesion of the coating). Hence, heating technique was used to coat the discs with hydroxyapatite. Furthermore, the Hydroxyapatite nanoparticles showed better adhesion to the titanium discs compared to hydroxyapatite microparticles.

Table 3.1 Total phosphorus and calcium concentration in µg/l released from hydroxyapatite coated discs after sonication up to 10 min to check degradation.

Time/ min	Total phosphorus (µg/l)			
	Non heated nHA	Heated nHA	Non heated mHA	Heated mHA
0	1.1 ± 1.4 a	0.07 ± 0.02 a	0.2 ± 0.03 *a	0.00 ± 0.01 *a
1	2.3 ± 1.4 ab	0.5 ± 0.2 a	4.0 ± 0.6 * b	1.4 ± 1.4 *bc
2	5.08 ± 0.6 bc	2.29 ± 1.7 a	5.22 ± 0.08 *c	1.54 ± 0.2 *bc
3	5.50 ± 0.4 *bc	1.86 ± 0.3 *b	5.05 ± 0.5 *c	1.8± 3.3 *bc
4	7.397 ± 0.5 *#cd	1.26 ± 0.15 *ab	5.437 ± 0.3 *#c	1.28 ± 0.5 *ab
5	6.84 ± 0.6 *#c	2.64 ± 0.2 *#ab	5.28 ± 0.2 #c	3.05 ± 1.06 #d
10	10.40 ± 1.8 d	4.59 ± 1.1 b	5.66 ± 0.2 *c	3.2 ± 0.6 *c
Time/ min	**Total calcium (µg/l)**			
	Non heated nHA	**Heated nHA**	**Non heated mHA**	**Heated mHA**
0	4.7 ± 6.6 a	0.4 ± 0.08 a	0.6 ± 0.1 a	0.2 ± 0.02 a
1	5.8 ± 3.6 #a	1.9 ± 0.4 a	9.6 ± 1.4 #b	3.9 ± 3.5 b
2	12.66 ± 1.7#b	6.08 ± 4.1 ab	12.5 ± 0.1 *#c	4.25 ± 0.4 *bc
3	13.71 ± 0.8 *b	5.17 ± 0.8 *c	12.3 ± 1.3 *c	5.0 ± 1.7 *bc
4	17.583 ± 1.5 *#b	4.361 ± 0.5 *abc	12.87 ± 1 *#c	4.5 ± 1.85 *ab
5	16.57 ± 1.5 *#b	7.38 ± 0.7 *#bc	12.99 ± 0.5 #c	7.92 ± 2.4 #c
10	24.68 ± 3.9 c	11.74 ± 2.4 c	13.62 ± 0.6 *c	8.7 ± 1.4 *d

The total concentration of the phosphorus and calcium (in µg/l) that released from the hydroxyapatite coatings, data are presented as mean ± S.E.M (n = 3), Different letters are statistically different from each other within the column (one way ANOVA, $p<0.05$). * means statistic significant difference between the heated and non-heated nHA or mHA in each time point (one way ANOVA, $p< 0.05$). # indicates a statistic significant difference between the nHA and mHA samples at each time point for heated and non-heated groups (one way ANOVA, $p<0.05$).

3.2.6 Characterization of the titanium discs

3.2.6.1 Surface roughness

The surface roughness, Ra, was quantified by using an Olympus LEXT Confocal Microscope OLS 3000, with a total magnification of 50× and an optical zoom of 1×. Ra is an arithmetical mean of surface roughness of every measurement within the total measured distance (Lou et al., 1998). Surface roughness was measured at three different locations in each of 3 replicates from each treatment. The topography was also investigated by taking 3D images using an Olympus LEXT Confocal Microscope OLS 3000.

3.2.6.2 Investigating the surface topography and chemical composition of titanium discs

Scanning electron microscopy (SEM, JEOL / JSM-7001F, Oxford instruments INCA X-ray analysis system) was also used to qualitatively investigate the surface topography of prepared titanium discs. At least one replicate from each type were coated with chromium cobalt and examined by SEM. The detective energy was 15 Kev at a working distance of 10 mm. In addition, Qualitative element analysis using Energy Dispersive Spectroscopy (EDS) was performed (spot size: 10 µm; accelerating voltage: 15 kV; working distance 10 mm), data and spectra analysis were achieved using Aztec 2.2 software.

3.2.7 Antibacterial properties of the different coated discs

3.2.7.1 Experimental design

The experiment involved exposing *S. sanguinis* in 24-well microplates (flat-bottom sterile, tissue culture treated polystyrene microplate, code: Greiner 662160, Bio-One Ltd., UK) for 24 h to different coated titanium discs. Titanium discs were placed in 24-well microplates using sterile forceps, then sterile physiological saline and bacterial suspension were added to each well in a 1:10 ratio (*S. sanguinis* culture was prepared as described in chapter 2 section 2.2.1). Then the 24-well microplates were incubated at 37 °C under 5% CO_2 and 95 % air for 24 h. The 24-well microplates was used as the unit of replication in the experiment (n = 6 plates/treatment); one of each coated discs above was added to each plate including two control groups (uncoated control disc and blank well with no disc as a reference). At the end of the exposure time (24 h), the external media were assessed for bacterial growth measuring the turbidity, the proportion of lactate production, and cell viability using a live/dead kit. The integrity of the different coatings was also tested by measuring the metal concentration in the external media using ICP-MS. Furthermore the biofilm formation on the discs also investigated (section 3.2.7.2).

3.2.7.2 Assessing the adherence of the bacteria to the discs

To investigate the the adherence of bacteria to the coated discs comparing to the control uncoated disc, two methods have been used, scanning electron microscopy (section 3.2.7.3) and the protocol used by Besinis et al. (2014) with some modification. In brief, the titanium discs were carefully removed from the 24-well

microplates by sterile forceps. Each disc was washed three times with sterile saline (0.85 % NaCl) to remove the unattached cells. Then each disc was placed in a separate sterile glass bottle contained 2 ml of sterile 0.85 % NaCl and sonicated in the ultrasonic bath (35 kHz frequency, Fisherbrand FB 11010, Germany) for 60 seconds to remove the attached cells. Then the discs were removed and the solutions vortexed for a few seconds to homogenize it. Then, 500 µl of the media from the sonicated discs was aliquoted into 5 ml of BHI + 2 % sucrose and incubated for 16 h at 37 °C under 5% CO_2 and 95 % air. The media from the blank well with no disc from the experiment was mixed well with a pipette, and then centrifuged for 10 min at 2000 rpm (2040 Rotors microplate centrifuge, Centurion Scientific Ltd, Ford, UK). Then the media were removed and the pellet containing the microbes was washed with saline twice and re-suspended in 2 ml of 0.85 % saline. Then 0.5 ml of the resulting solution was diluted in 5 ml of BHI + 2 % sucrose broth and incubated for 16 h. The bacterial growth was assessed using lactate production, the live/dead kit, and turbidity assays.

3.2.7.3 Bacterial adhesion and electron microscopy

The bacterial growth on the different coated discs was also investigated qualitatively using SEM. Briefly; titanium discs were exposed to *S. sanguinis* for 24 h exactly as described previously (n = 2). At the end of the exposure time the discs were washed with 0.85 % NaCl to remove the detached bacteria and were subsequently fixed with 2.5 % glutaraldehyde solution for 2 h. The specimens were dehydrated in a series of ethanol steps (50, 75, 95, 100 %) for 30 minutes in each concentration, then the discs were immersed in 50/50 ethanol / hexamethyldisilazine (HDMS) for 30 min, the specimens were then dipped in 100 % HDMS for 20 min. Finally, the discs were left

in the fume cupboard to dry. The resultant specimens were then coated with chromium in a sputter coater and visualised for remaining bacterial cells with SEM. The detective energy was 20 Kev and working distance was 10 mm.

3.2.7.4 Bacterial growth measurement

The bacterial growth of both suspended (external media) and the attached cells (media from the sonicated discs) were assessed by measuring the turbidity, by transferring 275 µl of the external media (after 24 h) and sonicated media (after 16 h) to 96-well plates (flat-bottom sterile polystyrene microplates, dis-210-070j, Fisher Scientific, UK). The turbidity was measured at 595 nm absorbance using a VersaMax plate reader (VersaMax microplate reader with SoftMax Pro 4.0 software, Molecular Devices, Sunnyvale, CA).

3.2.7.5 Lactate production assay

The amount of the lactate that was produced by *S. sanguinis* was measured using the lactate production assay. For the suspended bacteria, after 24 h incubation, 100 µl from each well were transferred to V-shaped bottom 96-well plates (code: 3896, corning, UK). Then the 96-well plate was centrifuged for 20 minutes at 2000 rpm. Then the amount of lactate in the supernatant was measured as described in chapter 2 (section 2.2.3). Similar to suspended bacteria, the same technique was used to measure lactate production in the supernatant of attached bacteria after 16 h.

3.2.7.6 Assessing cell viability (live/dead assay)

The viability of suspended cell after 24 h exposure, as well as the attached cells after 16 h incubation, was examined using L7012 Live/Dead® Backlight™ Kit (Invitrogen Ltd, Paisley, UK). The manufacturer's protocol with an optimized emission

wavelength was used as described by Besinis *et al* (2014). The kit consists of two stains, SYTO 9 which is a green fluorescent DNA stain for all kinds of cells, and propidium iodide, a red fluorescent stains for cells with a compromised membrane. The ratio of 1:1 of these two stains was mixed into sterile milliQ water to bring the final concentration of the stains (red and green fluorescent stain) to 0.6 %. Afterwards, 100 µl of the sample was transferred into a 96-well plate (flat-bottom sterile polystyrene Microplates, dis-210-070j, Fisher Scientific, UK) and mixed with the same volume of the staining solution. The 96-well plates were then incubated for 15 min at room temperature. The 96-well plates were covered with tin foil during the incubation time, because the stains are sensitive to light. A Cytofluor II, fluorescence plate reader (perspective Biosystems, Framingham, MA) was used to assess the samples. Two different emissions were used to assess the samples, 530 nm for SYTO 9 dye and 645 nm for the propidium iodide. The excitation wavelength was 480 nm for both dyes and the gain was 70.

3.2.7.7 Calibration of live dead assay

In order to convert the fluorescence data of the live/dead assay to equivalent live cells percentage values (Appendix C), the protocol of Besinis *et al*, (2014) was followed with some modification. Two sets of calibration curves were prepared, one for the 24 h exposure (external media) and the other for 16 h exposure (media of the sonicated discs). This is because of the difference in the type of the media used to grow the attached and suspended bacteria. In brief, S*. sanguinis* culture was prepared as described in chapter 2 (section 2.2.1). For the 24 h calibration curve, the resuspension of the cell pellet and washing was performed in physiological saline-BHI. While for the 16 h calibration the resuspension and washing of cell pellet was

performed in 0.85 % NaCl-BHI. Calibration used 100% live (no treatment) and 100 % dead (in 70% formaldehyde for 3 h at room temperature) cells. Then the calibration curve was plotted as reported in Besinis *et al*. (2014). A typical calibration for 24 h gave a linear response (e.g., r^2 = 0.998; y = 0.1311x+6.6267), and for the 16 h gave a linear response (e.g., r^2 = 0.994; y = 0.1402x + 5.9573).

3.2.7.8 Re-investigating the antibacterial activity of anodized groups and silver plated

The above experiment was repeated again, due to concerns about the results of anodized groups (TiO_2, TiO_2+nHA, and TiO_2+mHA discs); the solution that was used for anodization was likely contaminated with some silver. Hence new anodized discs were prepared in uncontaminated solution and the experiment repeated exactly as described above, except for the concentration of calcium in physiological saline had also been corrected, since an incorrect concentration was used in the previous experiment; 1.55 mM of $CaCl_2$ was used in the first run instead of 2 mM. Moreover, Ag discs were also used in this experiment, to check whether using a silver plate source rather than silver wire in the silver plating process had an effect on antibacterial activity of the Ag discs. Similar to the first run, Ti discs were used as control groups in this experiment.

3.2.9 Statistical analysis

All data were presented as mean ± S.E.M, and were analysed using STATGRAPHICS Centurion XVI.I. The differences between the tested samples and the control were evaluated using one-way ANOVA or Kruskal-Wallis. All statistical analysis used a 95 % confidence limit.

3.3 Result

3.3.1 Characterization of the titanium discs

The titanium discs were successfully polished and coated with silver, titanium dioxide and hydroxyapatite. There was a difference in roughness between the different coatings. Table 2 illustrates that Ag or TiO_2 discs showed no significant difference with the Ti (control) discs in roughness (one way ANOVA, $p>0.05$). In contrast the discs that were coated with hydroxyapatite (microparticles or nanoparticles) from all groups were significantly rougher than control disc (one way ANOVA, $p<0.01$); 3D images (Figure 9) confirmed this. In addition, there were some cracks on those discs coated with hydroxyapatite nanoparticles (Figure 3.2D, E and F). While Ag, TiO_2, and Ti showed surfaces without cracking (Figure 3.2A, B, and C).

EDS analysis (Figure 3.3A) showed an elemental composition of 80.5 % titanium, 11.4 % vanadium, and 3.8 % aluminium for the uncoated discs. The discrepancy from manufacturer's data (Al 5.5-6.75 %, V 3.5-4.5 %) is due to the non-uniform distribution of elements in the material. While for the silver plated discs showed 97 % of silver, traces of other elements were also detected from the surface (Figure 10B). On the other hand, the surface of the anodized titanium discs consisted of 11.7 % oxygen, 79.5 % titanium, and traces of aluminium and vanadium (Figure 10C). For the discs that coated with hydroxyapatite nanoparticles and microparticles (Figure 3.4 and 3.5), calcium and phosphorus can be easily detected on the surface of all the discs that coated with hydroxyapatite.

Table 3.2: surface roughness measurements of different coated titanium discs

Surface	**Roughness (R_a)**
Polished uncoated (control)	0.212 ± 0.02 a
Hydroxyapatite microparticles (mHA) coated disc	1.149 ± 0.20 bc
Hydroxyapatite nanoparticles (nHA) coated disc	2.501 ± 0.25 d
Anodized (TiO_2)	0.217 ± 0.02 a
Anodized and coated with nHA	0.755 ± 0.009 e
Anodized and coated with mHA	1.183 ± 0.12 c
Silver plated	0.267 ± 0.06 a
Silver plated and coated with nHA	0.783 ± 0.01 be
Silver plated and coated with mHA	0.948 ± 0.12 bce

* data are expressed as (Mean ± S.E.M, in µm), different letters are statistically different from each other (Kruskal-Wallis, p = 0.003).

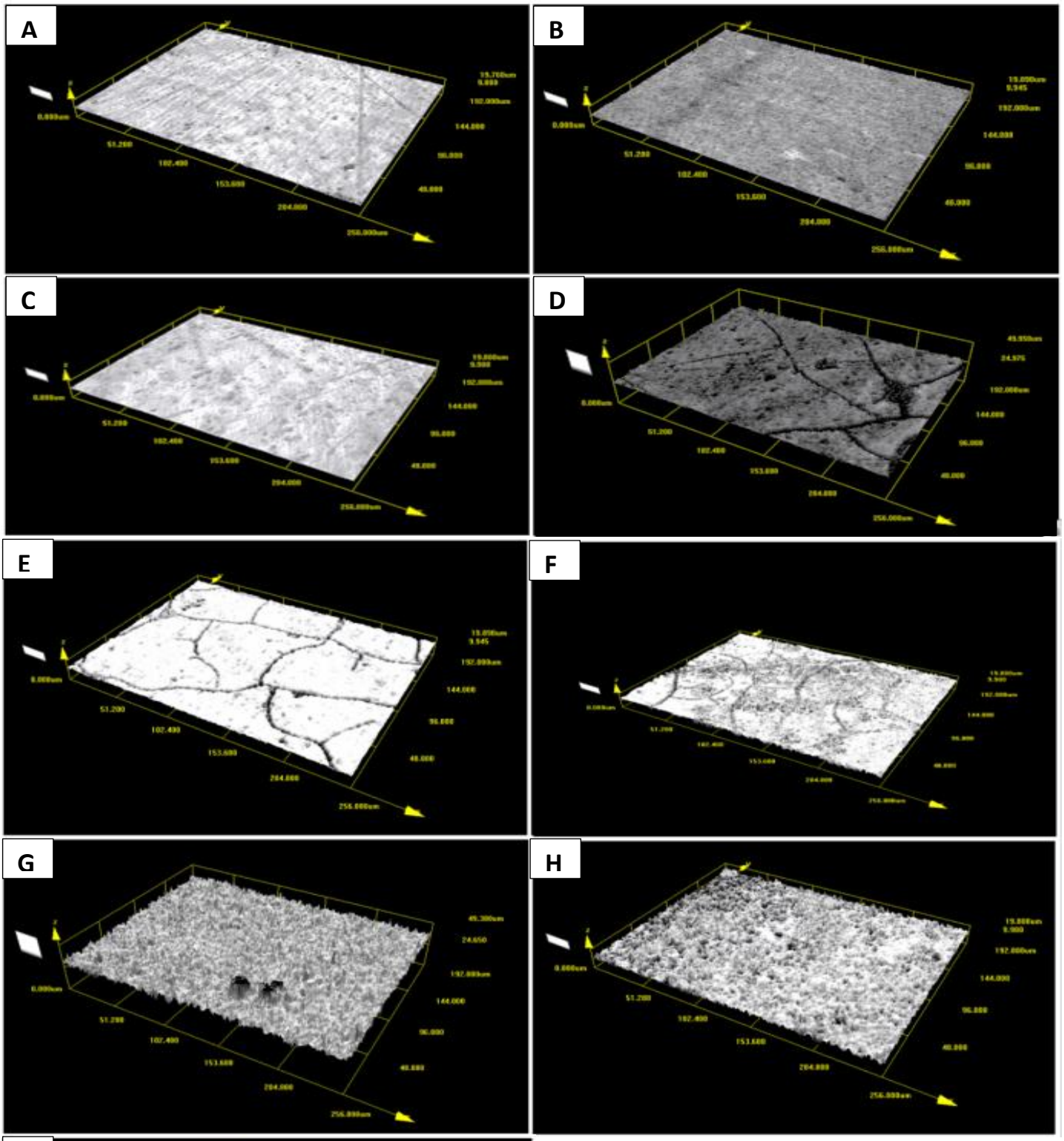

Figure 3.2 3D images obtained from a confocal microscopy (Olympus LEXT Confocal Microscope OLS 3000) A,B,C show the uncoated, silver plated, and anodized discs respectively before coating with hydroxyapatite there is no any irregularities. D, E, F show the three groups after coating with hydroxyapatite nanoparticles, cracks can be observed on their surfaces. G, H, I show the three groups after coating with hydroxyapatite microparticles, they showed rough surfaces.

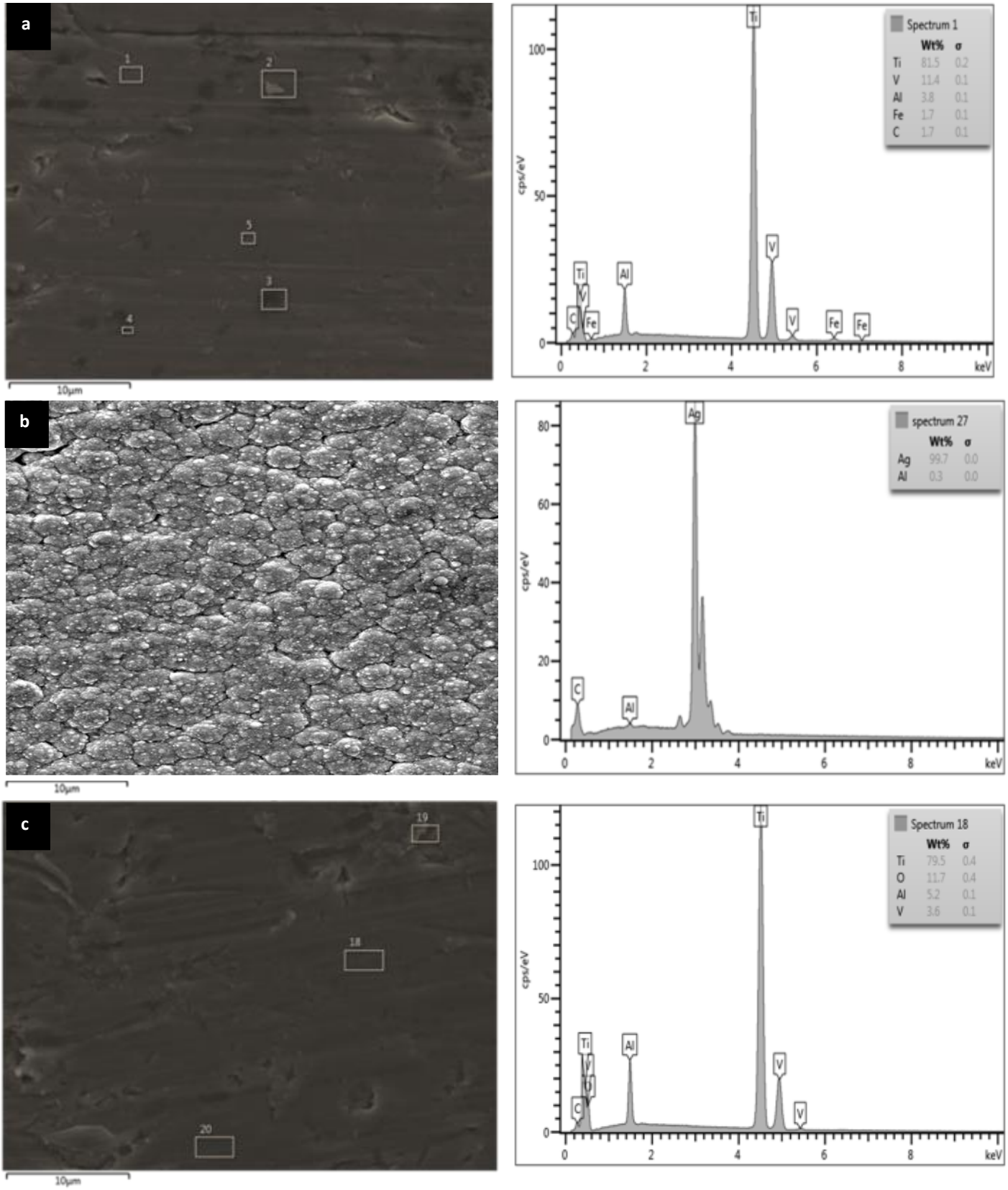

Figure 3.3 Scanning electron micrographs (SEM) and EDS analysis of titanium discs a) uncoated titanium alloy disc, 80 % of the surface is titanium and 11 % vanadium; b) silver plated disc, 97 % of the surface content is silver; c) anodized discs show 14 % oxygen and 80 % titanium. The image in the left is the SEM graph and the right side indicate the EDS analysis. The image in the left is the SEM graph and the right side indicate the EDS analysis,scale bar 10 µm

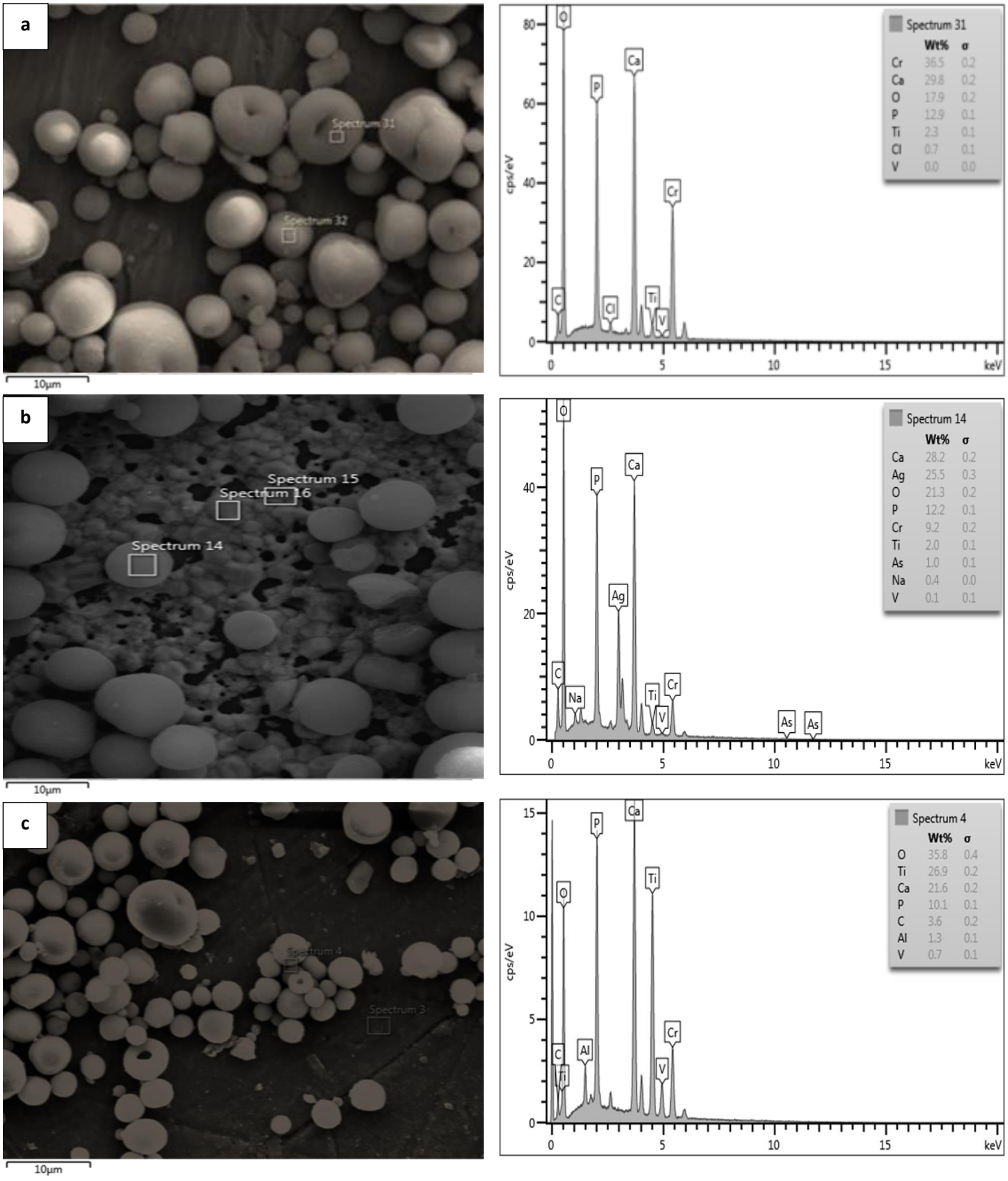

Figure 3.4 Scanning electron micrographs (SEM) and EDS analysis of hydroxyapatite microparticles a) uncoated titanium coated with hydroxyapatite microparticles, b) silver plated coated with hydroxyapatite microparticles; b) anodized coated with hydroxyapatite microparticles. The image in the left is the SEM graph and the right side indicate the EDS analysis, scale bar 10 µm.

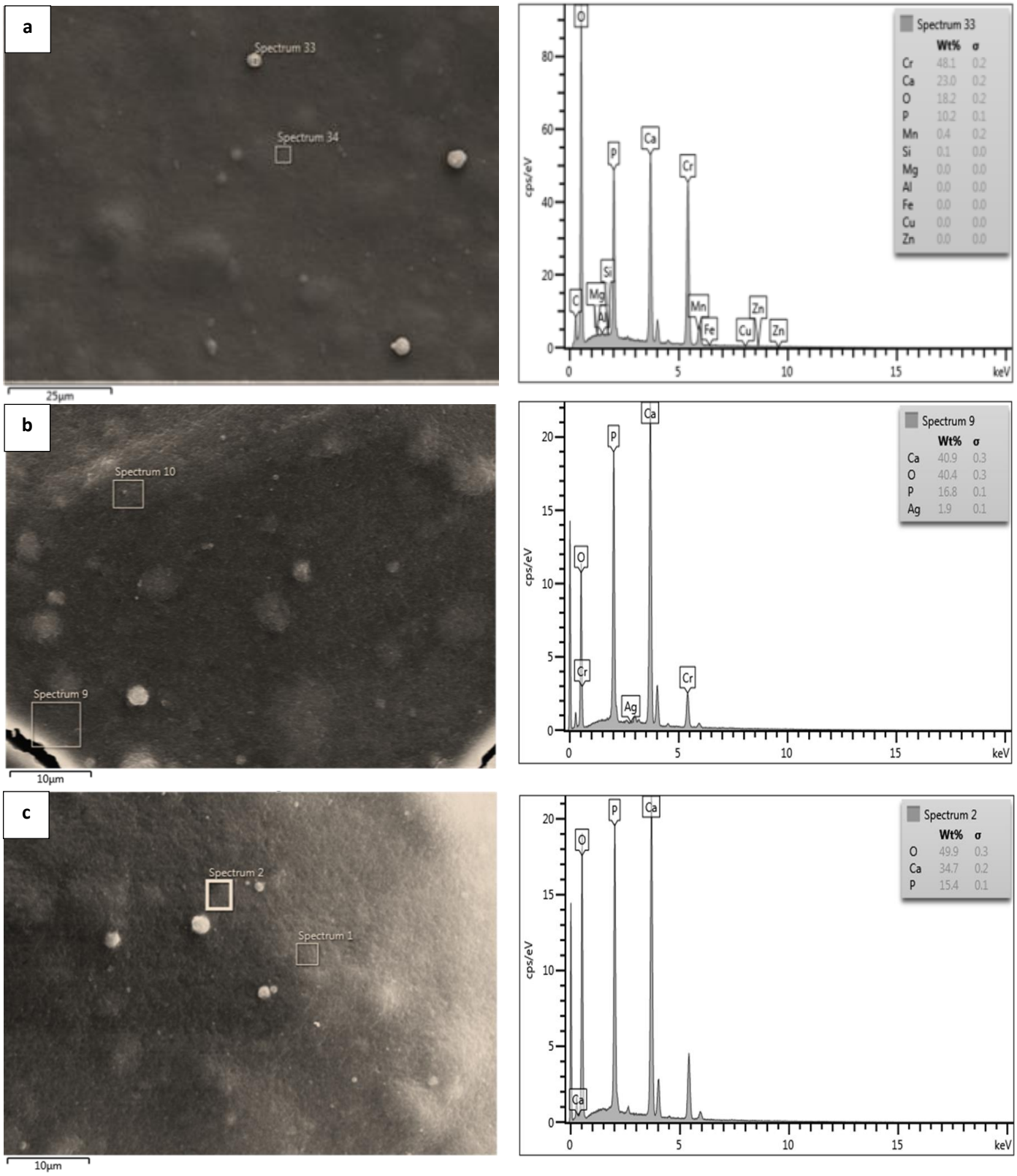

Figure 3.5 Scanning electron micrographs (SEM) and EDS analysis of hydroxyapatite nanoparticles. a) Polished titanium coated with hydroxyapatite nanoparticles, b) silver plated coated with hydroxyapatite nanoparticles; b) anodized coated with hydroxyapatite nanoparticles. The image in the left is the SEM graph and the right side indicate the EDS analysis, scale bar 10 µm.

3.3.2 Investigation of the bacterial growth suspended in the external media

The growth inhibition of *S. sanguinis* was investigated by measuring the turbidity of the media at 595 nm using a Versa Max plate reader. Statistical analysis showed a significant difference between the treatment groups (Kruskal-Wallis, $p<0.005$); Figure 3.6A shows that there was growth inhibition on all silver plated and anodized groups in the external media. The media of nHA, and mHA discs showed negligible decreases in bacterial growth compared to the control groups.

The amount of lactate produced by the bacteria was measured (Figure 3.6C), as an indicator of metabolism from living cells. There was no lactate in the external media of all anodized and silver plated groups. In contrast, there was lactate in the external media of nHA and mHA discs, but it was still significantly lower than the control groups (blank and uncoated disc, Kruskal Wallis, $p<0.005$).

The proportion of viable cells in the external media was also measured using the live/dead assay (Figure 3.6E). The data were normalized to the control (uncoated titanium discs); assuming that the bacterial growth was 100 % in the control. Similar to the lactate and turbidity results, there was a significant decrease in cell viability in the external media of all anodized and silver plated discs; as the bacterial viability was lower than the control (uncoated Ti disc) by approximately 90 %. While the cell viability in the external media of the nHA and mHA discs was 20 % lower than the control (uncoated Ti disc).

3.3.3 investigating of the bacterial adherence to the titanium discs

The turbidity of media obtained from sonicated discs was measured as it indicates the growth of bacteria on the discs. Similar to the external media there was a significant difference in the turbidity between the groups (Kruskal-Wallis, $p<0.001$). There was a growth inhibition on all silver plated and anodized groups (Figure 3.6B). While, there was bacterial growth on the uncoated discs, interestingly the bacterial growth on the nHA and mHA groups was higher than the uncoated discs.

The results of the lactate production assay also showed a significant difference between the different titanium discs (Kruskal-Wallis, $p<0.005$). There was a significant reduction in lactate production on all silver plated and anodized groups compared to the control (uncoated Ti discs, Figure 3.6D). In contrast, nHA and mHA discs showed high lactate production compared to the control (uncoated Ti discs).

Figure 3.6F shows the results of the live/dead assay for attached bacteria; the data was normalized to control group (uncoated Ti discs) as for the external media. The viability of the bacterial cells was significantly reduced on all anodized and silver plated discs compared to control Ti discs (Kruskal-Walis, $p< 0.05$). while the viability of the bacteria on nHA and mHA discs was higher than control Ti discs.

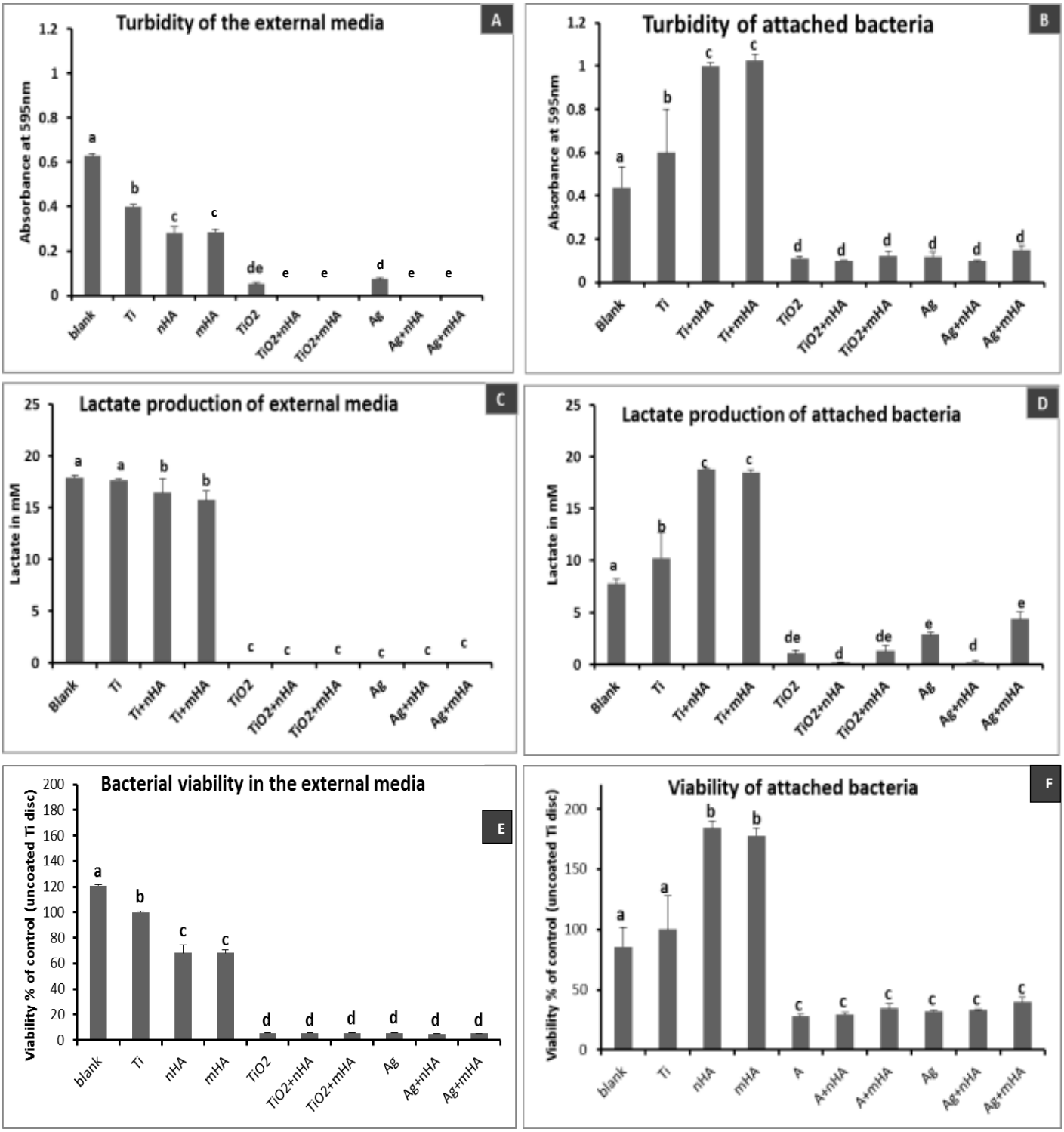

Figure 3.6 Growth inhibition of *S. sanguinuis* A) the turbidity of external media, B) the turbidity of attached bacteria to different titanium coated discs, C) lactate production in external media, D) lactate production of attached bacteria to different titanium coated discs.(Kruskal-Wallis, $p<0.001$), E) proportion of live bacterial cells in external media after normalization with control discs (Ti), F) proportion of live bacterial cells attached to the discs after normalization with control discs (Ti). Different letters indicate significant difference between the groups.

3.3.4 Assessing the bacterial attachment to titanium discs by SEM

The bacterial growth on the coated titanium discs was qualitatively analysed using SEM. Control uncoated discs showed a full growth of bacteria on the surfaces; *S. sanguinis* did not show any sign of stress and grew in multiple layers (Figure 3.7A). Likewise, nHA and mHA discs and all anodized groups were showed full bacterial growth (Figure 3.7B, C, D, E, and F). In contrast, the silver plated group (Figure 3.8G, H, and I) did not display any bacterial growth on their surfaces. Surprisingly, one of the Ag plated replicate (Figure 3.8B) showed bacterial growth; there were fewer numbers of bacterial cells compared to the control disc (Figure 3.7A) and *S. sanguinis* culture of filter paper (Figure 3.8 A) with a large amount of extracellular matrix, possibly mucopolysaccharide.

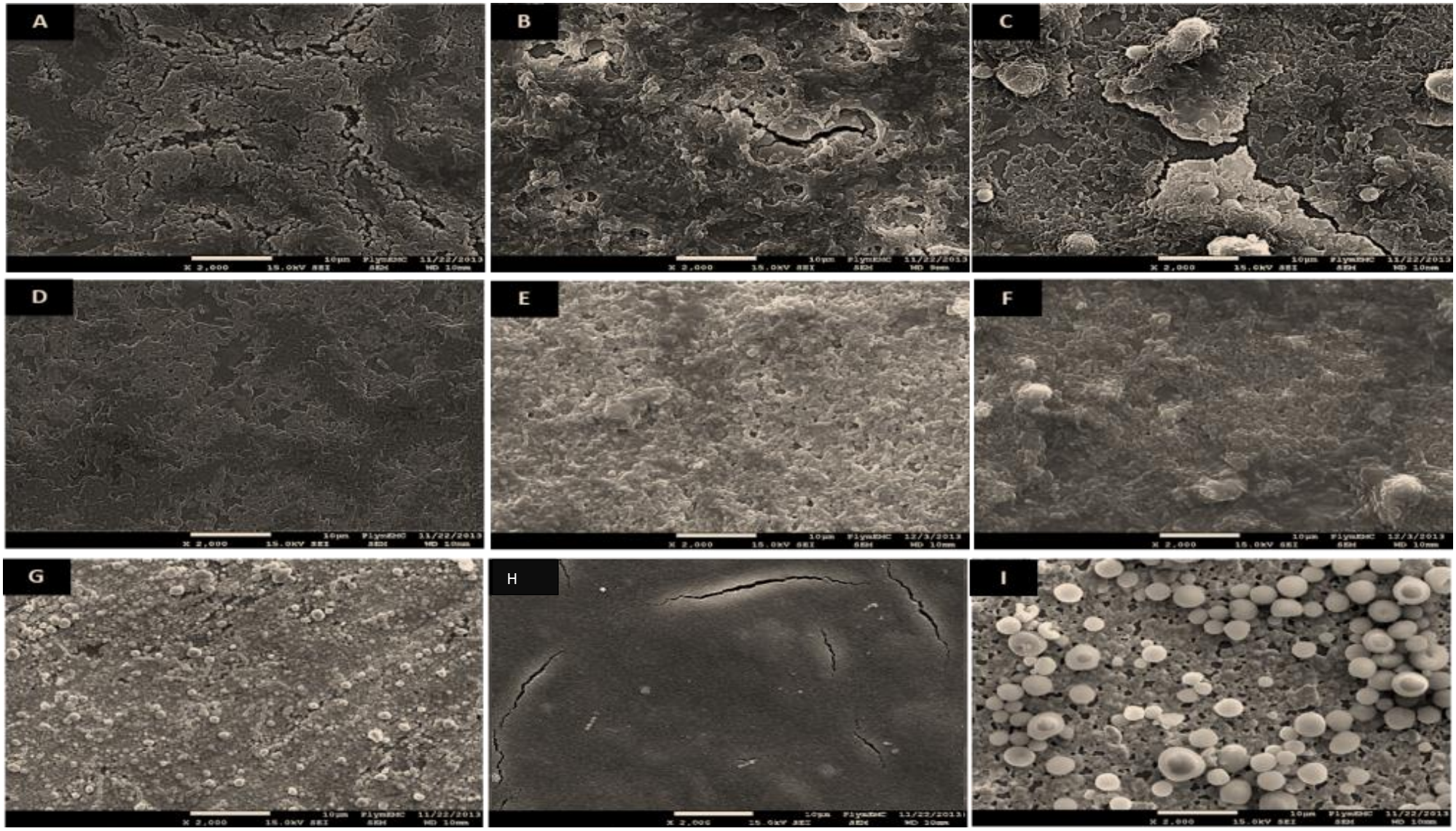

Figure 3.7. Scanning electron micrographs of different coated titanium discs exposed to *S. sanguinuis* for 24 h, A) Ti disc, B) nHA disc, C) mHA disc, D) TiO2 disc, E) TiO2+nHA disc, F) TiO2+mHA disc, All the discs showed full bacterial growth G) Ag disc, H) Ag+nHA disc, I) Ag+mHA disc, showed no growth on their surfaces. Scale bar, 10 µm

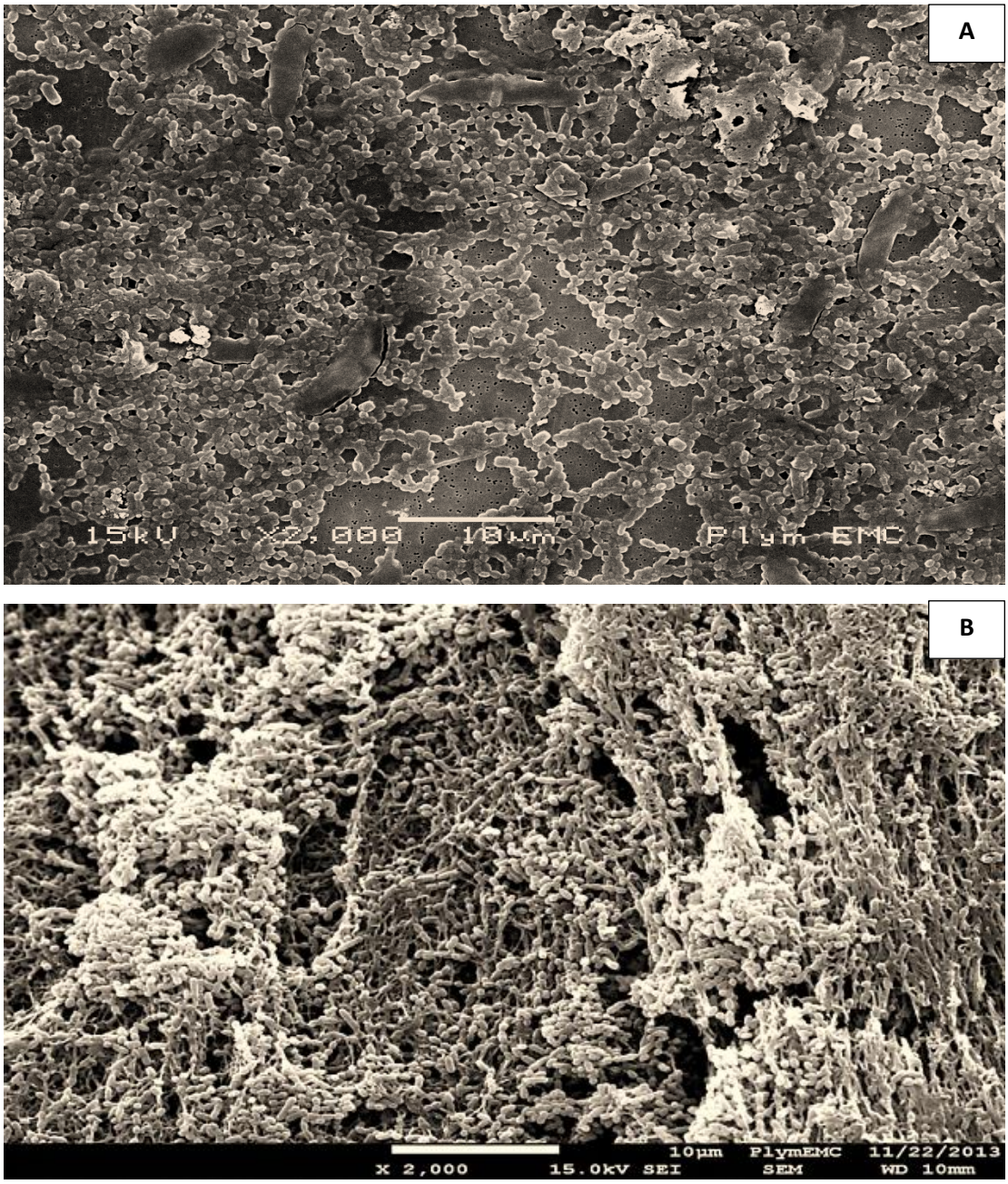

Figure 3.8 Scanning electron micrograph of A) *S. sanguinis* culture, B) silver plated disc after exposing to *S. sanguinuis*. A huge amount of extracellular matrix covered the surface of silver plated disc. Scale bar= 10 µm, magnification 2000x.

3.3.4 Investigating the stability of the coatings

In order to check the stability of the silver coatings on the titanium discs, the concentration of the silver was measured in both the external and sonicated media. In the external media (Table 3.3), silver release from silver plated discs coated with hydroxyapatite (Ag+nHA and Ag+mHA) is higher than the release of silver from silver

plated disc (Ag without HA). The concentration of silver was 0.163 ± 0.013 and 0.342 ± 0.013, 0.32 ± 0.011 mg/l for Ag, Ag+nHA and Ag+mHA respectively (mean ± S.E.M., n = 6). The external media of anodized groups was contained silver, which was more than the detection limit (< 0.04 mg/l). It was 0.075 ± 0.01, 0.056 ± 0.009, and 0.052 ± 0.01 mg/l for TiO_2, TiO_2+nHA, and TiO_2+mHA respectively (mean ± S.E.M). Silver concentrations in the media of sonicated discs were also measured. Overall, higher silver concentration observed in the media of sonicated discs compared to the external media, as the total silver concentration was 0.704 ± 0.039, 0.825 ± 0.084, and 0.632 ± 0.036 mg/l for Ag, Ag+nHA and Ag+mHA discs respectively (mean ± S.E.M). Furthermore, the anodized group also showed high silver concentration in the media after sonication (Table 3.3).

The concentration of calcium and phosphorus in both media were also measured as an indicator of hydroxyapatite coating degradation. In external media, there was a significant difference between the groups in calcium concentration (Kruskal Wallis, $p<0.005$). The concentration of calcium for silver plated and anodized groups was lower compared to the control groups (Table 3.3). In the sonicated media, it was observed that the concentration of calcium was high for all the groups that were coated with hydroxyapatite compared to those discs that were not coated with hydroxyapatite (Table 3.3). Phosphorus concentration in the external media showed no significant difference for all groups. In contrast, the media obtained from sonicated discs showed high concentrations of phosphorus compared to control (Kruskal-Wallis, $p > 0.05$).

Table 3.3 Total Ag, Ti, P, and Ca concentrations (mg/l) released from the discs to the external media after 24 h, and to the media of sonicated discs after 1 min.

	Treatment	Materials in mg/l			
		Ag	Ti	P	Ca
External media	blank	0.00 ± 0.00 a	0.01 ±0.00 a	112.43 ±1.61 a	56.00 ± 0.80 ab
	Ti	0.00 ± 0.00 a	0.07 ± 0.01 b	101.9 ± 9.77 ab	56.10 ± 4.15 ab
	Ti+nHA	0.01 ± 0.00 a	0.02 ± 0.00 a	96.14 ± 16.0 ab	73.28 ± 20.10 b
	Ti+mHA	0.01 ± 0.00 a	0.02 ± 0.00 a	109.9 ± 7.49 ab	78.28 ± 13.30 b
	TiO_2	0.07 ± 0.01 b	0.02 ± 0.00 a	97.24 ± 1.94 ab	34.27 ± 0.61 ac
	TiO_2+nHA	0.05 ± 0.00 b	0.01 ± 0.00 a	109.7 ± 6.26 ab	46.95 ± 18.64 ac
	TiO_2+mHA	0.05 ± 0.01 b	0.01 ± 0.00 a	100.8 ± 4.22 ab	28.08 ± 2.69 c
	Ag	0.16 ± 0.01 c	0.02 ± 0.00 a	93.7 ± 12.87 ab	32.09 ± 6.14 ac
	Ag+nHA	0.34 ± 0.01 d	0.01 ± 0.00 a	89.95 ± 1.45 b	17.51 ± 0.65 c
	Ag+mHA	0.32 ± 0.01 d	0.01 ± 0.00 a	94.84 ±1.53 ab	27.05 ± 2.91 ac
Sonicated media	Ti	0.04 ± 0.01 ab	0.01 ± 0.01 a	3.47 ± 1.91 a	2.36 ± 1.38 ab
	Ti+nHA	0.03 ± 0.01 ab	0.31 ± 0.09 b	39.46 ± 14.12 b	20.4±6.70 cd
	Ti+mHA	0.01 ± 0.04 a	0.28 ± 0.09 b	42.10 ± 11.44 b	21.2 ± 5.05 cd
	TiO_2	0.14 ± 0.01 b	0.00 ± 0.02 a	0.59 ± 0.08 a	0.21 ± 0.02 a
	TiO_2+nHA	0.13 ± 0.03 ab	0.04 ± 0.01 a	5.75 ± 0.42 a	3.62 ± 0.22 abc
	TiO_2+mHA	0.15 ± 0.05 b	0.22 ± 0.09 b	25.26 ± 10.34 b	14.04 ± 5.26 cd
	Ag	0.70 ± 0.03 c	-0.008 a	1.15 ± 0.24 a	0.42 ± 0.08 ab
	Ag+nHA	0.82 ± 0.08 c	0.12 ± 0.04 b	21.89 ± 5.07 ab	14.37 ± 3.73 bcd
	Ag+mHA	0.63 ± 0.03 d	0.09 ± 0.02 a	22.23 ± 3.91 ab	11.88 ± 1.90 bcd

External media: the concentration of the coating materials in the external media after 24 h., data expressed as means ± S.E.M (n = 6 for each treatment). Different letters are statistically different from each other within the column (Kruskal- Wallis test, $p< 0.05$. Sonicated media: the concentration of the coating materials in the media after sonication for 1 min. data expressed as means ± S.E.M (n = 6 for each treatment). Different letters are statistically different from each other within the column (Kruskal- Wallis test, $p< 0.05$).

3.3.5 Re-investigating the antibacterial activity of anodized groups and silver plated discs

The turbidity measurement for the external media from the Ag and TiO_2+nHA discs were significantly lower than the control, indicative of growth inhibition (Kruskal-Wallis, $p = 0.02$). While absorbance in media from TiO_2 and TiO_2+mHA discs did not show any difference with the control group (Figure 3.9A). Likewise, the results of lactate production showed a significant decrease in bacterial growth in the external media of Ag and TiO_2+nHA compared to control Ti discs (Figure 3.9C and E). The data of the live/dead assay normalized to the control; Ag and TiO_2+nHA showed almost 50 % decrease in bacterial growth compared to control uncoated discs (Ti).

The results of turbidity and lactate production showed a significant decrease in bacterial attachment to Ag discs compared to the control Ti disc (Kruskal-Wallis, $p<0.001$). In contrast the anodized groups showed no significant difference with the control (Figure 3.9B and D). There was full bacterial growth on the three groups of anodized discs. Likewise, the live/dead showed bacterial growth inhibition on silver plated discs, whereas the anodized groups did not show any growth inhibition of the attached bacteria (Figure 3.9F).

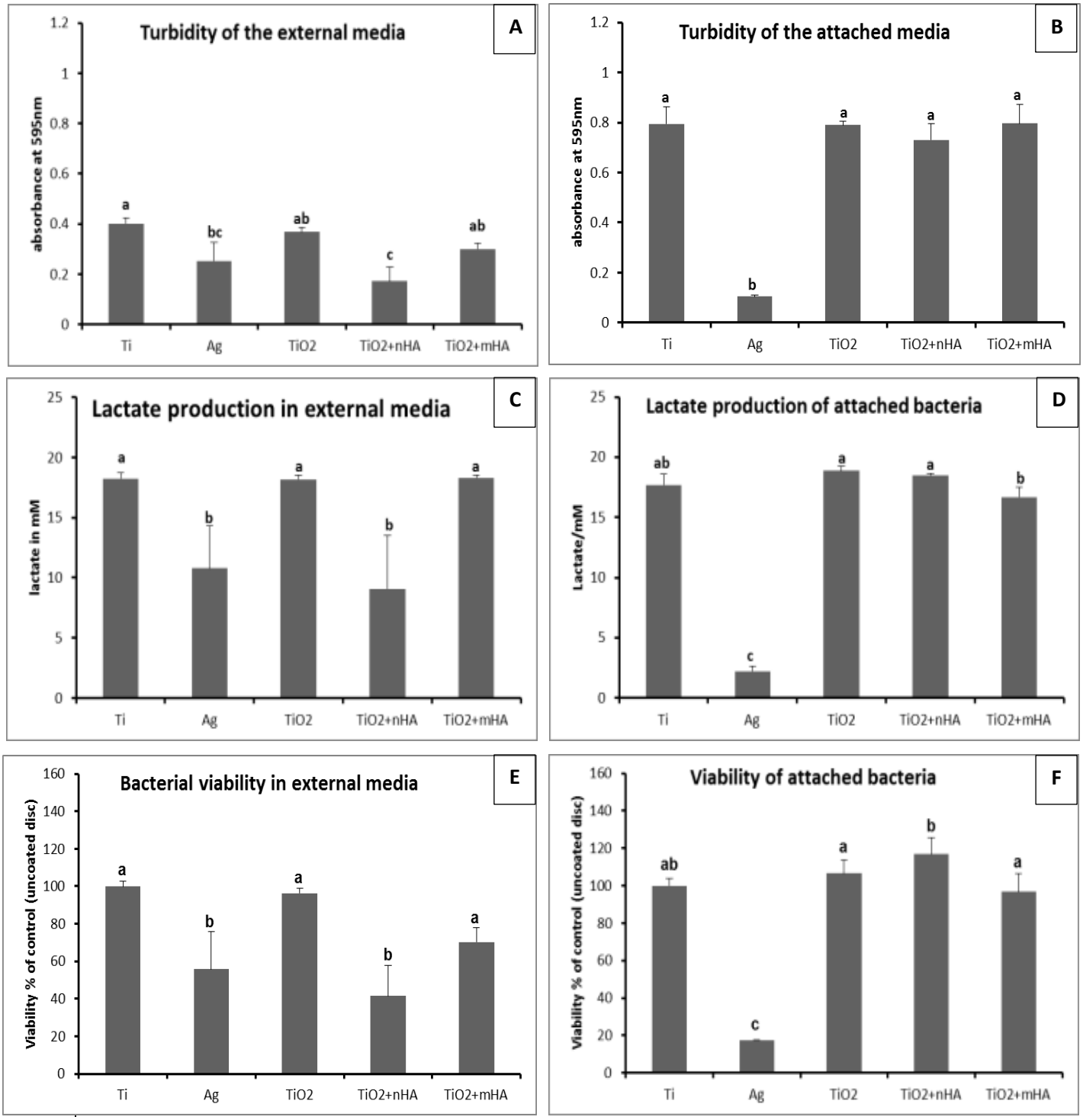

Figure 3.9 the Growth of *S. sanguinis* in the external media and on the discs. A) Bacterial growth of *S. sanguiuis* in external media of different coated titanium discs, measured as absorbance values (one way ANOVA, p = 0.01) B) the turbidity measurement of the attached bacteria to different coated titanium discs after 16 h incubation (Kruskal-Wallis, p = 0.001), C) the lactate production in the external media (Kruskal-Wallis, p = 0.03), D) lactate production of the attached bacteria (Kruskal-Wallis, p = 0.0005), E) the percentage of live S. sanguinis normalized to control uncoated disc in the external media (Kruskal-Wallis, p = 0.03), F) the percentage of live *S. sanguinis* normalized to control (uncoated disc) attached to the different coated discs (Kruskal-Wallis, p = 0.009), different letters indicate a significant difference between the groups.

3.3.6 Investigation of the coating stability for the repeated experiment

Inductively coupled plasma optical emission spectrometry (ICP-OES) was used to measure the concentration of silver in the media (Table 3.4). Total silver concentration (in mg/l) for the silver coated discs was 0.112 ± 0.044 in the external media. The silver concentration for Ti discs was below the detection limits (< 4 µg/l). A low concentration of silver was also noticed in the anodized groups. Silver concentration was 0.067 ± 0.023, 0.038 ± 0.004, and 0.015 ± 0.005 mg/l in TiO_2, TiO_2+nHA and TiO_2 ± mHA respectively (mean ± S.E.M). Sonicated media on the other hand showed a higher silver release for silver plated discs compared to the external media, as the silver concentration in sonicated media for silver plated discs was 1.07 ± 0.482 mg/l. The concentration of silver for the remaining groups, including control uncoated discs, was below the detection limit (< 9 µg/l). Table 3.4 also shows the concentration of calcium in external media, there was a significant difference in the concentration of calcium between the groups (Kruskal-Wallis, $p < 0.005$). It is apparent from Table 3.4 that the concentration of calcium for TiO_2+nHA and TiO_2+mHA in sonicated media is higher than the other groups (Kruskal-Wallis, $p<0.005$). The concentration of phosphorus in external media showed negligible variation between the groups, and sonicated media showed a significant difference between those discs coated with hydroxyapatite micro/nanoparticles and the other groups (ANOVA, $p<0.001$), as the concentration of phosphorus was higher in hydroxyapatite coated discs.

Table 3.4 Total Ag, Ti, P, and Ca (mg/l) released from the discs to the external media after 24 h and to the sonicated media after 1 min. sonication.

	Treatment	**Materials in mg/l**			
		Ag	Ti	P	Ca
External media	Blank	0.00 ± 0.00 a	0.01 ± 0.00 a	104.00 ± 1.9 a	61.73 ± 0.24 a
	Ti	0.00 ± 0.00 a	0.14 ± 0.01 b	100.04 ± 2.2 ab	64.30 ± 0.80 ab
	TiO_2	0.06 ± 0.02 bc	0.08 ± 0.01 c	96.11 ± 2.15 bc	59.20 ± 0.91 a
	TiO_2+nHA	0.03 ± 0.00 ab	0.01 ± 0.00 ad	86.17 ± 2.98 d	35.37 ± 8.25 c
	TiO_2+mHA	0.01 ± 0.00 ab	0.07 ± 0.01 c	101.47 ± 4.47 ab	74.64 ± 5.56 b
	Ag	0.11 ± 0.04 c	0.03 ± 0.00 d	91.55 ± 0.55 cd	45.71 ± 4.26 c
Sonicated media	Ti	0.009 ± 0.00 a	0.00 ± 0.00	0.91 ± 0.29 a	1.54 ± 0.13 a
	TiO2	0.005 ± 0.00 a	0.00 ± 0.00	1.32 ± 0.28 a	2.01 ± 0.30 a
	TiO_2+nHA	0.01 ± 0.00 a	0.02 ± 0.01	3.30 ± 0.46 b	5.58 ± 0.54 b
	TiO_2+mHA	0.01 ± 0.00 a	0.19 ± 0.14	3.85 ± 0.55 b	7.20 ± 1.08 b
	Ag	1.07 ± 0.48 b	0.02 ± 0.02	0.45 ± 0.15 a	1.32 ± 0.10 a

External media: the concentration of the coating materials in the external media after 24 h, data expressed as means ± S.E.M (n = 6 for each treatment). Different letters are statistically different from each other within the column (Kruskal Wallis test, $p < 0.001$). **Sonicated media**: the concentration of the coating materials in the media after sonication for 1 min. data expressed as means ± S.E.M (n = 6 for each treatment). Different letters are statistically different from each other within the column (Kruskal- Wallis test, $P < 0.05$).

3.4 Discussion

This study was designed to prepare a novel coating for dental implants to prevent peri-implantitis; titanium discs were coated with different material by various techniques and their antibacterial activity examined against *S. sanguinis*. The main findings were that some of the coating techniques were successful with some draw backs. The metal composition of the surface was confirmed by SEM/EDS. Furthermore, the silver plated groups showed good antibacterial activity. Among them, silver plated discs coated with hydroxyapatite nanoparticles (Ag+nHA) were the best, as they show antibacterial activity against suspended bacteria as well as the attached bacteria. However there was some silver release into the media. The uncoated and anodized groups did not show any antibacterial activity against *S. sanguinis.* In contrast, hydroxyapatite coated discs (nHA and mHA) provided a favourable condition for bacteria to attach to the titanium discs. Table 3.5 Shows the antibacterial activity of the coatings according to the assays that used in the study.

Table 3.5 The antibacterial activity of the different coated discs against *S. sanguinis* according to the assays used in the study

Treatments	Turbidity assay	Lactate production assay	Live dead assay	Scanning electron microscopy images
uncoated disc (Ti)	X	X	X	X
Hydroxyapatite nanoparticle coated (nHA)	X	X	X	X
Hydroxyapatite microparticle coated (mHA)	X	X	X	X
Anodized disc (TiO_2)	X	X	X	X
Anodized disc coated with hydroxyapatite nanoparticle (TiO_2+nHA)	X	X	X	X
Anodized disc coated with hydroxyapatite microparticle (TiO_2+mHA)	X	X	X	X
Silver plated disc (Ag)	✓	✓	✓	✓
Silver plated disc coated with hydroxyapatite nanoparticle (Ag+nHA)	✓	✓	✓	✓
Silver plated disc coated with hydroxyapatite microparticle (Ag+mHA)	✓	✓	✓	✓

✓ refers to the coatings that showed bacterial growth inhibition, X refers to the coatings that did not show any bacterial growth inhibition.

3.4.1 Surface characterization

The roughness of the coated discs was investigated, because roughness might have an effect on the ability of bacteria to colonize on titanium discs. The roughness more than 10 µm increase the risk of peri-implantitis (Le Guéhennec *et al*., 2007).The results revealed that silver plating and anodization retained the roughness of the titanium discs at the nanometer scale (Table 3.2). While the hydroxyapatite microparticle coatings increased disc roughness. This result could be explained by the fact that hydroxyapatite microparticles tend to produce clusters (Onuma *et al*., 1998) with different sizes on titanium surfaces; which make the surfaces irregular comparing to the control uncoated discs. Nonetheless, the roughness of the discs was still in the 1- 2 µm range, which will not enhance bacterial growth. It has been stated by Le Guéhennec *et al*. (2007) that roughness below 2 µm will limit peri-implantitis.

Scanning electron microscopy was used to investigate the morphology of the coatings. It showed that the silver plating method formed an evenly distributed silver layer in a nanocrystalline form (Figure 3.3B); with their diameter estimated to be between 25-50 nm. It is encouraging to compare this figure with that found by Lin *et al*. (2011), who found that silver plating will lead to formation of particles with a grain size of less than 25 nm. Moreover, the deposition and heating method for both hydroxyapatite microparticles and nanoparticles was also successful with some shortcomings. It led to the formation of a thick layer of hydroxyapatite microparticles or nanoparticles on the surface. However this method has some drawbacks, as some cracks were noticed on those discs coated with hydroxyapatite nanoparticles (Figure 3.2). This may perhaps be due to the thermal expansion mismatch between the coating and the metal substrate, which generates an internal stress at the

coating-metal interface to cause micro cracking (Li *et al*,. 2009). Jarernboon *et al*. (2009) assumed that the difference in the thermal expansion coefficients between the substrate and the deposited particle will cause cracking on the surface. The cracks only happened in discs coated with hydroxyapatite nanoparticles rather than hydroxyapatite microparticles (Figure 3.2), because hydroxyapatite in the nanophase has a higher surface energy and produces a continuous coating on the titanium surface rather than clusters. Subsequently, during the drying step of the coating process, the shrinkage of the coating causes some cracking. This explanation corroborates the ideas of Mahé *et al*. (2008), who suggested that the drying step is responsible for cracking. In the case of hydroxyapatite microparticles, the cohesion between the particles and substrate is weaker, hence the particles can migrate and form clusters while the water molecules escape. For that reason the hydroxyapatite coated discs of all groups showed uneven distributions of the hydroxpatite microparticles.

3.4.2 Antibacterial activity of the different coatings

The results of the turbidity and lactate production assay confirmed antibacterial activity of silver plated groups against *S. sanguinis* in suspension (Figure 13). There are two possible explanation for this; either it is due to silver ion release or the direct contact of the microbe with the silver nanoparticles (Liao *et al*., 2010). The former is more likely, because the ICP-MS results showed silver ion release from the discs to the external media (Table 7). It is assumed that the potency of silver is related to its active form (soluble silver ion). Schreurs *et al*. (1982) found that the silver ion interfere with the integrity of bacterial membrane. Damm *et al*., (2008) stated that silver ions can bind to the electron donor groups in biological molecules containing

sulphur, oxygen or nitrogen, which cause defects in cell membrane and bacterial death.

It was also found that the silver plated groups had anti-biofilm activity and can decrease the colonisation and attachment of the bacteria to the discs (Figure 3.6 B and D). There are two possible mechanisms to explain the anti-biofilm activity of silver plated groups, the bacteria have been killed in the suspension before settling down due to the effect of the silver that have been released to the media (Table 3.3), which support the above hypothesis. Another explanation for the anti-biofilm effect could be due to the direct bacterial contact with the silver nanoparticles, because silver nanoparticles have a large specific surface area to interact with bacteria (Feng *el al*., 2000). It was confirmed by SEM that the silver coating produced by silver plating seems like silver nanoparticles (Figure 3.3B). The direct contact of silver nanoparticles with bacteria may result in bacterial membrane rupture as suggested by Lok *et al*. (2006). Furthermore, Sondi *et al*., (2004) revealed that AgNPs can accumulate in the bacterial membrane and increase the permeability of the cell wall; this will lead to loss of cell content and bacterial death. Furthermore, it was found that the Ag+nHA discs showed the highest anti-biofilm activity among all the tested groups (Figure 3.6B and D). This is probably due to the silver release for those discs as shown in (Table 3.3). this finding is in accordance with the previous study done by Chen *et al*. (2007), who found that the low silver release from silver containing hydroxyapatite reduce the bacterial growth. Another explanation could be due to the effect of heating step in coating process, which led to activation of silver through reacting with hydroxyl group of hydroxyapatite to form silver oxide. Scales *et al*. (1984) stated that heating of silver to above 180 °C can activate bioerodible silver components.

It was noticed that all the anodized groups showed antibacterial and anti-biofilm activity (Figure 3.6C and D). It seems possible that this finding is due to the contamination of anodization solution with silver (Table 3.3), because anodization technique will thicken the oxide layer of the titanium that has no antibacterial activity. In order to check whether this antibacterial activity is because of anodization or the silver contamination, the experiment was repeated again by using new anodized discs that were prepared in fresh uncontaminated solution (section 3.4.3).

The results of lactate production assay (Figure 3.6C and D) showed a full growth on nHA and mHA discs in the external media and in the media obtained from sonicated discs. This suggests that hydroxyapatite has no antibacterial activity against *S. sanguinis,* but enhances their growth instead. This finding further supports the idea of Rameshbabu *et al*. (2007), who assumed that hydroxyapatite can absorb many proteins, amino acids and other organic materials which favour the attachment and colonization of bacteria. Contrary to the lactate production assay result, the turbidity and live/dead results showed less bacterial growth in external media of nHA and mHA compared to the control (uncoated disc, Figure 3.3A). This is possibly because most of the bacteria were removed from the media of hydroxyapatite coated discs during their collection. Nevertheless, this effect was not reflected in the results of the lactate production assay, because the lactate released early on and remained in the media.

The results of the lactate assay and turbidity measurements for the control discs showed a limited growth in the media after sonication of the discs (Figure 3.3B and D). There are two possible explanations for this: either due to the sonication step as it was not possible to remove all the bacteria from the discs, or it could be due to the smooth surface of the uncoated titanium discs which may decrease the bacterial

attachment (Bürgers, 2010). The former seems more likely, because all the replicates of control uncoated discs showed full growth in the repeated experiment as well as the SEM experiment (Figure 3.6a). Hence an optimization for this step is recommended for future work.

Although the live/dead assay results (Figure 3.3E and F) were in agreement with the other two assays (lactate production and turbidity assays), the data values must be interpreted with caution, since it was not possible to follow the protocol that is recommended by the manufacturer exactly. The calibration curves were not performed on the same day as the measurements of fluorescence from the biofilms in the experiment, and with differences in the performance of the dyes each day, it became clear that calibrations should be done with each use of the dyes in the kit. The source of error may be small differences in dye concentration or quenching effects each day, which when converted from a calibration curve led to difference in the apparent live and dead ratios in the samples. Hence, using the calibration curve to the experiment data resulted in negative values. For that reason, the data were normalized to control, assuming that the growth of bacteria in the control uncoated discs was 100 %.

The concentration of calcium was measured to investigate the degradation of hydroxyapatite; it was difficult to identify whether the calcium and phosphorus are from the hydroxyapatite or from the culture media (Table 3.3), as the concentration of calcium and phosphorus in the coating were very small compared to their concentration in the physiological saline. Furthermore, the concentration of the calcium in the external media for those discs that have been silver plated and anodized had lower than the expected concentration. This could be as a result of the effect of these coating on adsorption of the calcium (Ca^{2+}) from the media (Horie *et*

al., 2009), which led to decrease the concentration of calcium in the media. Moreover, coating titanium with hydroxyapatite nanoparticles and microparticles led to precipitation of the calcium and phosphorus from the media. This suggestion is supported by the results of ICP-MS, which showed higher concentration of calcium and phosphorus compared to control discs in the media of sonicated discs (Table 3.3). Tsui *et al* (1998) also found that immersion of hydroxyapatite in ringer solution (almost the same solution as used in the present study) lead to formation of precipitates.

3.4.3 Repeat experiment for anodized group using uncontaminated anodization solution

The results of the repeated experiment showed that anodized discs have neither antibacterial nor anti-biofilm against *S. sanguinis;* suggesting that the reason for killing bacteria at the first run of the experiment was due to silver contamination. On the other hand, the external media for Ag discs showed different results from the first run of this experiment; they displayed higher bacterial growth compared to silver plated discs in the first run of experiment. This may be due to the use of a silver plate as the source of silver instead of the silver wire plating process. The surface area of silver wire is larger than silver plate; which might have effect on the quality of resulted coating on titanium discs. According to the results of the turbidity measurements and lactate production assay some of the discs showed full growth similar to the control groups, whereas the others showed a reduction or no growth (Figure 3.7). This may be related to the amount of silver ion release in the media, as silver release was low for those discs that showed high growth of bacteria, while the discs with limited growth of bacteria showed high silver release. However this was

not the case for the sonicated media. Despite the variation in the silver concentration between the discs, all the discs showed antibacterial activity against the bacteria (Figure 3.7B and D). The inconsistency in silver dissolution may be because the direct application of silver to titanium. Gosheger *et al*. (2004) assumed that if silver was applied directly on titanium, this would cause inconsistency in the silver ion dissolution. Hence the sustained release of silver ion cannot be accomplished. Nevertheless, the amount of silver that was measured in the media may have had no antibacterial effect, as it was lower than the minimum inhibitory concentration of silver. This interpretation was confirmed by running a separate experiment to assess the MIC of silver nitrate (representing the concentration of silver released from the discs to the media) against *S. sanguinuis* (Appendix D).

The growth on some of the silver plated discs may be due to resistance to the silver ion in the media by some population of these bacteria, through producing a kind of mucopolysaccharide by the bacteria (Figure 3.8B). This layer of mucopolysaccharide will prevent silver ion reaching the bacteria in the media. It is well known that bacteria use matrix polysaccharides as a protection mechanism in biofilms (Van Acker *et al*., 2014). Kang *et al*. (2014) stated that the extracellular polymeric substance (EPS) produced by bacteria impede intracellular penetration of the silver ion, because reducing of sugar content of EPS lead to converting silver ion to AgNPs. Stewart *et al*. (2001) found that there was a subpopulation of bacteria in biofilm called persisters, which are responsible for broad resistance including to chemicals such as disinfectant.

3.5 Conclusion

In the present study, a protocol was developed to produce a coating from silver plate and hydroxyapatite nanoparticles, which is suitable to provide a good antibacterial and anti-biofilm activity to the surface of dental implants. The evidence from this study supports the idea that the antibacterial activity of the silver is not just due to ion release, but the direct contact of particles with bacteria also plays an important role in its action. However, there is concern about the biological safety of silver releasing implantable materials, as there was silver release from the coating. Therefore, further *in vitro* and *in vivo* studies are needed to investigate the biosafety of this coating prior its clinical use.

Chapter 4

Investigating the biocompatibility of silver coating

4.1 Introduction

Biocompatibility is one of the prerequisite for the safety and efficacy of biomaterials that are used to coat the dental implants, as the materials will be in long term intimate contact with bone and connective tissues. There is growing interest on using metal nanoparticulate such as titanium dioxide, titanium nanotube, and silver, to improve the clinical outcome of dental implants. In particular, many studies focused on using silver as a coating for dental implants, since it has a good antibacterial activity and reduce perioperative infection (Albers *et al*., 2013). However, there is a concern about the toxic effect of silver against human cells (Cortizo *et al*., 2004), which is mainly due to ion release (Ahamed *et al*., 2010; Foldbjerg *et al*., 2009; and Greulich *et al*., 2009). In general, most of the material that used as a coating for dental implants will undergo degradation, this is mainly due to the shear force during implant insertion, and this will lead to release of metal ion in case of using metal as a coating. To determine the biocompatibility of a material, attention should be paid to its effect on specific human cells, because the toxicity of the material differs from one cell type to other (Cortizo *et al*., 2004). Hence most of the studies that investigate the biocompatibility of the dental implant they used bone or bone like cells such as primary human osteoblast, osteoclast, and osteosarcoma cells (Anselme *et al*., 2000; Cortizo *et al*., 2004; and Albres *et al*., 2013).

The aim of this study was to investigate the toxicity of the silver nanoparticle coatings that were prepared by electroplating (chapter 3, section 3.2.3) and coated with hydroxyapatite nanoparticles, or microparticles, on human cells. For this purpose, primary human osteoblast cells were used, since these cells will be in direct contact with the coated implants. The objectives were to: (i) investigating the dissolution of

the silver by measuring the concentration of the silver in the external media and cell homogenate using ICP-OES. Furthermore, to investigate the concentration of the electrolytes (K^+ and Na^+), to check whether there is any change in cell uptake of these two electrolytes in the presence of silver; (ii) investigate the cell viability qualitatively using light microscopy (Olympus SZ X7 microscope); (iii) evaluate the toxicity effect of the silver nanoparticles coatings on osteoblast. The toxicity assays such as lactate dehydrogenase activity and protein assays were used, and (iv) to investigate the effect of silver on the osteoblast cell functions using the alkaline phosphatase (ALP) activity assay. ALP is commonly used as a biomarker to evaluate the metabolic activity of bone. This is because it plays an important role in the mineral formation by bone cell, due to its effect on both the increase of the local concentration of inorganic phosphate (mineralization promoter) and decrease of the extracellular pyro phosphatase which is mineralization inhibitor (Golub *et al*., 2007).

4.2 Methodology

4.2.1 Cell culture

Primary human osteoblast cells (Hob) obtained from ECACC (European Collection of Cell cultures) were cultured at a density 1 x 10^6 in 75 cm^2 flasks (Sterilin, Newport, UK) containing 15 mL of DMEM (Dulbecco's Modified Eagle's medium) with L-glutamine, 10 % foetal bovine serum (FBS), and 1 % penicillin-streptomycin (100 IU Penicillin- 100 µg/ml Streptomycin) purchased from Invitrogen. The media were routinely changed every 3 days and the cells sub-cultured when confluence reached 80-85 %. For sub-culturing, the cells were washed twice with phosphate buffer saline, D-PBS, (Fischer scientific, without added calcium and magnesium), then tryptinized (2 ml of 0.25% trypsin and EDTA) and resuspended in fresh media and counted with haemocytometer.

The cell viability was checked with trypan blue. All cells were kept in 37 °C in 5 % CO_2 and 95 % air; passage 5 was used for the experiment below.

4.2.2 Experimental design

The biosafety of the silver plated discs coated with hydroxyapatite nanoparticles or microparticles (Ag+nHA, and Ag+ mHA) were investigated. Briefly, sterile coated titanium discs were placed in 24 well microplates and 20000 cells/ml media were added (*n*= 9 per treatment each 3 replicates in one plate) and incubated for 72 h. Two control groups were used in this experiment; uncoated titanium discs (Ti), and a reference control (media + cells without titanium discs which are referred as the “blank” hereafter). The media were replaced with fresh media every 24 h; and the removed media was used to determine the lactate dehydrogenase activity (LDH), alkaline phosatase activity (ALP), and measuring the total silver and electrolytes (K^+, Na^+) concentration by ICP-OES.

At the end of incubation period (72 h), the external media was removed from each well and the cells were washed twice with sucrose buffer (300 mmol/l sucrose, 0.1 mmol/l EDTA, 20 mmol/l HEPES buffered to 7.4 with few drops of trizma base), then 1 ml of lysis buffer was added to the well (as the washing buffer above except the concentration of sucrose was 30 mmol/l (hypotonic) and 0.01 % of Triton-X was also added to facilitate the detachment of cells from the well). The cell homogenate were further diluted in milliQ water, to minimize the effect of Triton-X on the enzyme activity measurements. After that, the cell homogenate was sonicated for a few seconds. The cell homogenate were used to measure cellular LDH activity, ALP activity, protein content using BCA, and metal analysis (*n* = 6 per treatment).

Photographs were also taken for the cells after 72 h exposure (*n* = 3 plates). For this, the media were removed and the cells were washed with sucrose buffer. The cells were then fixed with 100 % ethanol for 3 min and stained with Harris's Haematoxylin and Eosin (H & E). The cells were examined using a dissection microscopy (Olympus SZ X7).

4.2.3 Lactate dehydrogenase assay

In order to measure the toxicity or cell injury caused by silver, the LDH activity in the media was measured at 24, 48, and 72 h. In addition LDH was also determined in the cell homogenate after the cells were lysed with lysis buffer to measure the leakage of LDH from inside the cells. The assay was performed following the protocol of Plummer (1971). For the assay, 1 ml of reagent assay (0.6 mM of pyruvate in 50 mM phosphate buffer at pH 7.5) was added to a 1 ml cuvette, and then 0.035 µl of 0.6 mM of NADH was added to the mixture, and 0.035 µl of the test sample (cell culture media/ cell homogenate) was added at the end and mixed quickly with a paddle. The oxidation of NADH was followed at 340 nm (Helios β Spectrophotometer, manufacturer, England) for 2 minutes. The LDH activity (µmol/min/ml) was calculated using extinction coefficient of 6.3 mM for a path length of 1 cm. The intracellular LDH was normalized with intracellular protein content (µmol/min /mg protein).

4.2.4 Protein assay

The Bicinchoninic acid (BCA) method was used to measure the protein concentration of homogenates (MC155208, Pierce, Rockford, USA). After the cells had been lysed, 10 µl of the cell homogenate was added to 190 µl of BCA reagent in 96 well plates. The plate was incubated in a 37 °C incubator for 30 min, and then the absorbance was read at 562 nm (VersaMax, molecular devices, Berkshire, UK). A series of bovine

serum albumin standards (1.25, 0.625, 0.312, 0.156 and 0 mg/l) were used for calibration (Appendix E).

4.2.5 Alkaline phosphatase activity

The activity of alkaline phosphatase (ALP) enzyme was measured in the external media and the cell homogenate, in order to check the effect of the silver coatings on osteoblast function. In brief, 0.065 µl of the sample (external media or cell homogenate) was added to 0.665 of the reagent assay (0.265 ml of 0.1 M glycine buffer + 0.330 ml of 0.5 mM p-Nitrophenylphosphatase (pNPP) in glycine buffer). The appearance of p-Nitrophenol was measured spectrophotometrically at 405 nm (Helios β Spectrophotometer, manufacturer, England). ALP activity was calculated using an extinction coefficient of 18.3 mM for a path length of 1 cm. The intracellular ALP activity was expressed as mmol/min/ml for the external media and mmol/min/mg cell protein for cell homogenate.

4.2.6 Statistical analysis

All data are expressed as mean ± S.E.M and analysed using Stat Graphic version 5.1. The differences between the treatments and controls within a day were evaluated using one way ANOVA. Parametric data were tested by one way ANOVA, and non-parametric data analysed by Kruskal-Wallis. Two way ANOVA was used to assess the time and treatments effects. p values equal or less than 0.05 was considered to be significant.

4.3 Results

4.3.1 Investigating the silver exposure of the osteoblast cells

Total silver concentrations were measured in the external media on days 1, 2, and 3 (Table 4.1). There was a significant difference in silver concentration between the groups (Kruskal- Wallis, $p < 0.05$). The highest concentration of silver was observed after one day in the external media of the Ag+nHA and Ag+mHA treatments; the concentration of silver (in mg/l) was 10.99 ± 1.32 and 7 ± 1.53 in Ag+nHA and Ag+mHA respectively. At day 2 and day 3, the total silver concentration was lower compared to day 1 (Table 4.1). The concentration of silver in the control (blank) was below the detection limit (detection limit < 0.04 mg/l). Media from the uncoated Ti discs showed a low concentration of silver (0.06 mg/l) on the first day, while in second and third days it was below the detection limit. In the cell homogenate (Table 4.2), the concentration of silver in the control groups was below detection limit. The concentration of silver in the Ag+mHA and Ag+nHA discs was statistically higher than the blank (Kruskal-Wallis, $p = 0.0005$). The electrolytes, Na^+ and K^+, were also measured in the external media and cell homogenate (Tables 4.1 and 4.2); there was no significant difference between the treatment and control in the electrolytes concentrations except in the day 1, where the concentration of Na^+ in the treatments was higher than the blank (Table 4.1).

Table 4.1 The total concentration of Ag (mg/l) and electrolytes, Na^+, and K^+ (in mmol/l) in the media after exposing osteoblast to silver coatings over 72 h.

	Treatment	Day 1	Day 2	Day 3
Silver	blank	0.04 ± 0.00 a	0.01 ± 0.00 a *	0.01 ± 0.00 a *
	Ti	0.06 ± 0.01 a	0.01 ± 0.00 a *	0.00 ± 0.00 a *
	Ag+nHA	10.99 ± 1.32 b	10.34 ± 1.60 b	2.31 ± 0.60 b *#
	Ag+mHA	7.83 ± 1.53 c	5.02 ± 1.07 c	3.47 ± 0.50 c *
Sodium	blank	128.00 ± 15.00 a	162 ± 0.9 *	156 ± 14 *
	Ti	163.00 ± 11.00 b	161 ± 4.7	161 ± 16
	Ag+nHA	166.00 ± 7.70 b	160 ± 3.2	152 ± 8.2
	Ag+mHA	179.00 ± 6.30 b	170 ± 4.5	157 ± 3.6
Potassium	blank	10.50 ± 0.66	10.30 ± 0.11 ab *	9.90 ± 0.96 *
	Ti	10.30 ± 0.97	10.20 ± 0.28 a	10.30 ± 1.20
	Ag+nHA	10.60 ± 0.59	10.30 ± 0.30 ab	9.90 ± 0.62
	Ag+mHA	11.30 ± 0.46	11.00 ± 0.28 b	10.00 ± 0.28

Data expressed as means ± S.E.M (n = 9 for each treatment). Different letters are statistically different from each other within the column. * Significant different from day 1 within row, # significantly different from previous end point within row (one way ANOVA or Kruskal- Wallis test, $P < 0.05$).

4.3.2 Investigation of cell morphology

Table 4.2 The total concentration of Ag in mg/l, Na^+, and K^+ in mmol/l the cell homogenate after 72 h

Concentration on mg/l for silver and mmol/l for Na^+ and K^+			
	Ag	**Na**	**K**
blank	0.02 ± 0.01 a	0.98 ± 0.10	0.39 ± 0.02 ab
Ti	0.02 ± 0.00 a	1.00 ± 0.28	0.30 ± 0.05 a
Ag+nHA	0.34 ± 0.07 b	1.16 ± 0.16	0.61 ± 0.03 b
Ag+mHA	0.42 ± 0.23 b	1.40 ± 0.30	0.25 ± 0.02 a

Data expressed as means ± S.E.M (n = 6 for each treatment). Different letters are statistically different from each other within the column (Kruskal- Wallis test, $P < 0.05$)

The morphology of the Hob cells were investigated after incubating with the titanium discs over 72 h (Figure 4.1). The blank showed a high density of osteoblast cells, with a normal nucleus and elongated cytoplasm. While a lower density of cells was observed in the uncoated control discs. Furthermore, the cells showed shrinkage in cytoplasm on uncoated control discs (Figure 4.1 B). The Ag+nHA and Ag+mHA discs did not show any cells on their surfaces (Figure 4.1 C and D). Moreover, Ag+nHA discs showed a precipitation of discs which is either the aggregates of nanomaterials (Ag and HA) or cell debris.

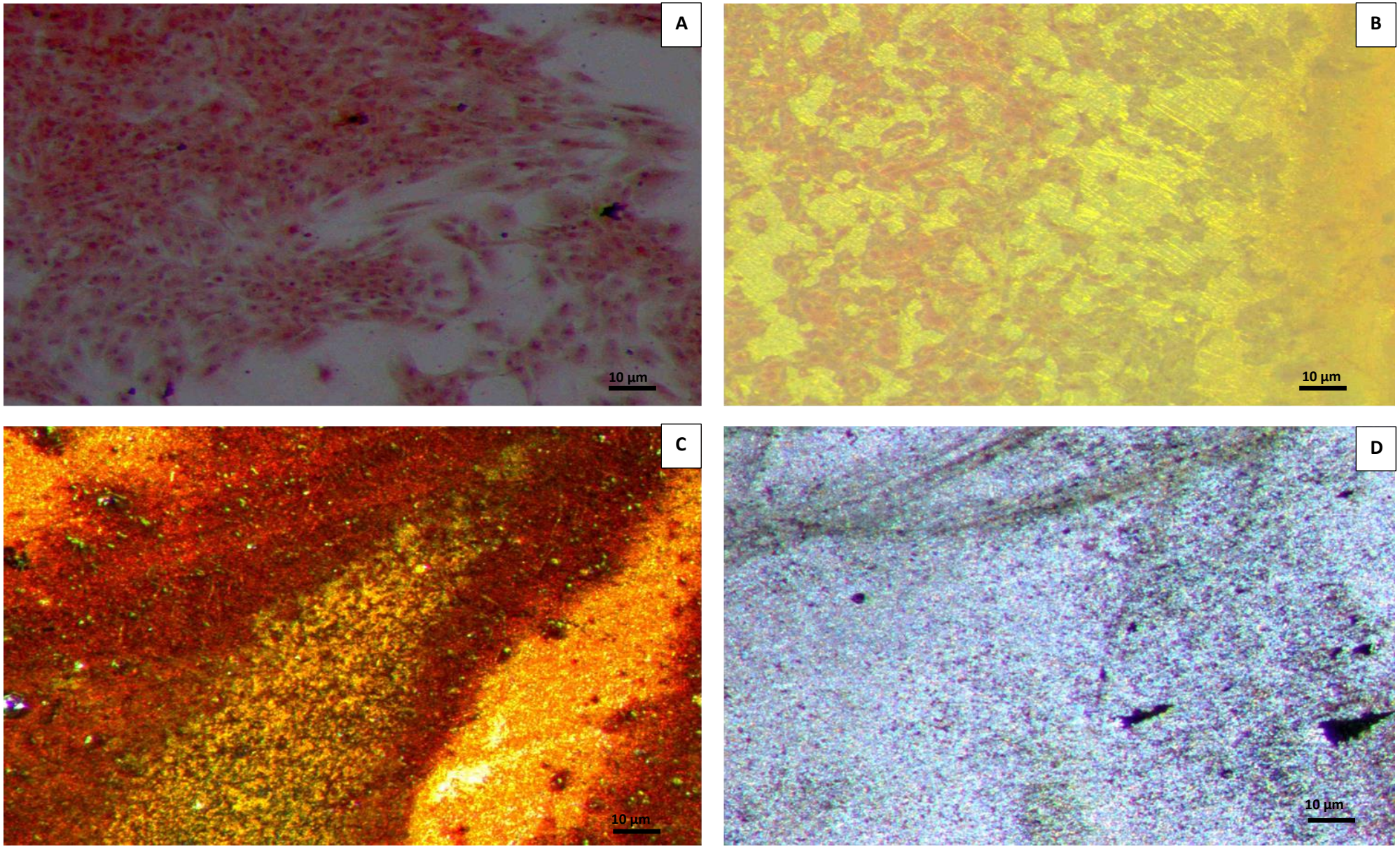

Figure 4.1 Morphology of osteoblast cells after 72 h exposure to silver. Dissection microscopy (Olympus SZ X7) (n = 3) scale bar = 10 µm. Osteoblast cells stained with Haematoxylin and Eosin grown on (A) 24 well microplate (reference control) (B) uncoated titanium disc, (C) silver plated disc coated with hydroxyapatite nanoparticles (Ag+nHA), (D) silver plated disc coated with hydroxyapatite microparticles (Ag+mHA).

4.3.3 Lactate dehydrogenase

Lactate dehydrogenase release to the media is one of the parameter that indicates cell injury. Table 4.3 shows the concentration of LDH (µmol/min/ml) in the external media after 24, 48, and 72 h. At 24 and 48 h, the data were not significantly different between any tested groups compared to both control groups (Ti and blank), whereas, at 72 h the LDH activity in Ag+mHA was significantly lower than the control groups (Ti and blank, one way ANOVA, p = 0.03). Furthermore, both the time and treatments had effect on the LDH activity in the media (two way ANOVA, p = 0.006). The activity of the LDH was also measured in the cell homogenate, to investigate the cell viability after 72 h incubation (Figure 4.2). Uncoated control discs (Ti) did not show a statistical difference with the reference control (blank). There was a significant decrease in LDH activity on Ag+nHA, and Ag+mHA compared to blank (one way ANOVA, p = 0.008). However, the silver coated groups (Ag+nHA and Ag+mHA) were not statistically different from the uncoated control group.

Table 4.3 Lactate dehydrogenase activity in the external media (µmole/min/ml) during exposure of osteoblast cells to silver coated discs (Ag+nHA and Ag+mHA) over 72 h.

Treatment	Day 1	Day 2	Day 3
Blank	0.012 ± 0.00	0.014 ± 0.00	0.078 ± 0.01 a *#
Ti	0.019 ± 0.00	0.032 ± 0.00	0.093 ± 0.01 a *#
Ag+nHA	0.015 ± 0.00	0.019 ± 0.00	0.065 ± 0.01 ab*#
Ag+mHA	0.024 ± 0.01	0.015 ± 0.00	0.034 ± 0.00 b

The data are presented as mean ± S.E.M (*n* = 9); different letters within column indicate significa difference, and absence of the letters means there is no significant difference. * Statistical significant difference from day 1 within row. # Statistically different from previous time point with row (one way ANOVA, p <0.05).

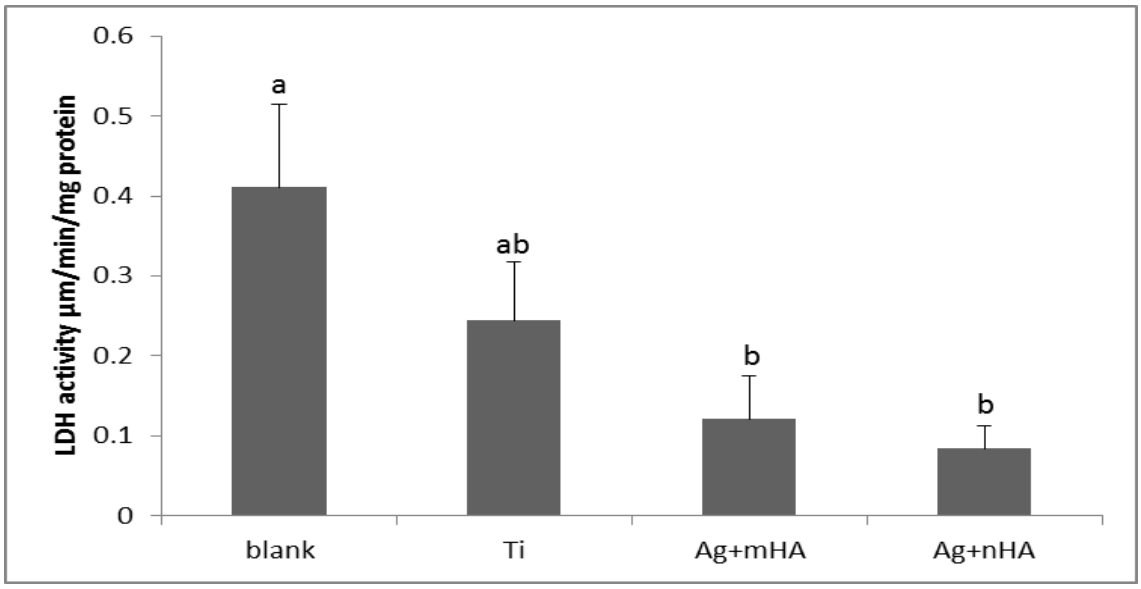

Figure 4.2 LDH activity from cell homogenate after 72 h. Data are mean ± S.E.M (*n* = 6), bars with different letters are statistically different from each other (p< 0.05).

4.3.4 Protein assay

The concentration of the protein in the cell homogenate was measured after 72 h incubation (Figure 4.3). The data did not show any significant differences between the control groups (blank and Ti discs) and the silver coated discs (Ag+nHA and Ag+mHA) (one way ANOVA, p>0.05). These data were used to normalize the LDH and ALP activity of cell homogenate.

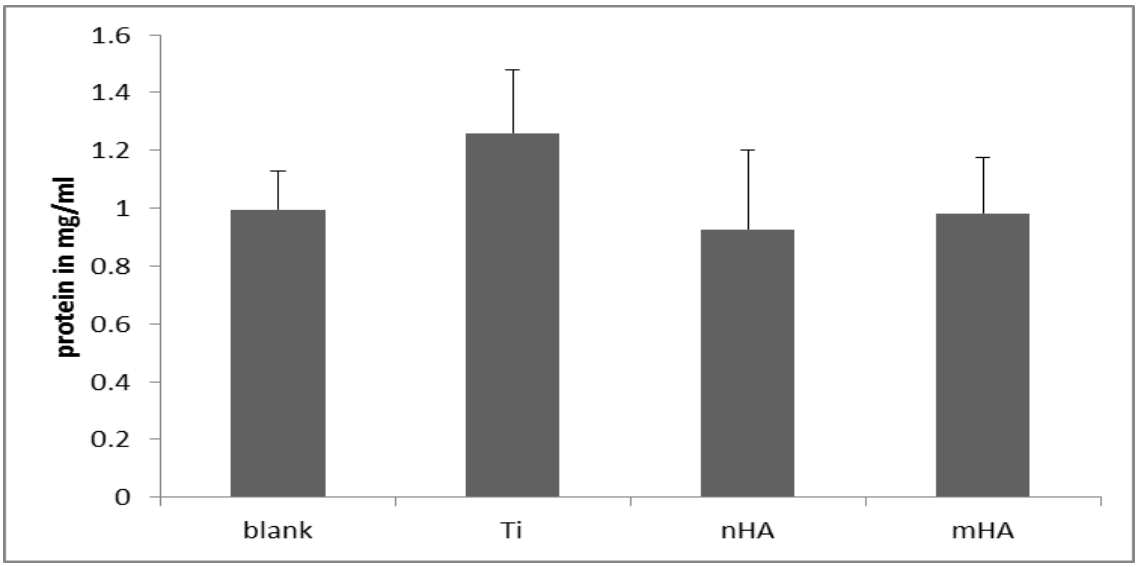

Figure 4.3 the concentration of protein in the cell homogenate after 72 h incubation. Data are mean ± S.E.M (*n* = 6), one way ANOVA, p>0.05 (no treatment effects).

4.3.5 Alkaline phosphatase activity

The presence of alkaline phosphatase in the media indicates the presence of metabolically active osteoblast cells. Table 4.4 shows the ALP activity (U/ml) in the external media at days 1, 2, and 3. The data did not show any significant differences between the groups at day 1, whereas at day 2 uncoated Ti and Ag+mHA discs showed decreases in ALP activity compared to the blank (one way ANOVA, p = 0.046). At day 3, the ALP activity in Ag+nHA and Ag+mHA discs was lower than the controls blank and uncoated Ti disc (one way ANOVA, p = 0.045). After 3 days incubation the ALP activity for the cell homogenate was also measured (Figure 4.4). There was a significant difference between the treatments and the blank; the ALP activity in the treatments (Ag+nHA and Ag+mHA) and uncoated control discs was lower than reference control (blank).

Table 4.4 Alkaline phosphatase activity of the external media in U/ml after exposing the osteoblast cells to silver coatings over 72 h

Treatment	**Day 1**	**Day 2**	**Day 3**
blank	0.009 ± 0.001	0.017 ± 0.004 a	0.016 ± 0.002 a *
Ti	0.009 ± 0.001	0.011 ± 0.008 b	0.016 ± 0.001 a *
Ag+nHA	0.010 ± 0.001	0.012 ± 0.005 ab	0.010 ± 0.002 b
Ag+mHA	0.007 ± 0.001	0.010 ± 0.005 b	0.010 ± 0.002 b

The data are presented as mean ± S.E.M (*n* = 9); different letters within column indicate significant difference, and absence of the letters means there is no significant difference, * statistically significant difference from day 1 within column. # are statistically different from previous time point within row (one way ANOVA, p <0.05).

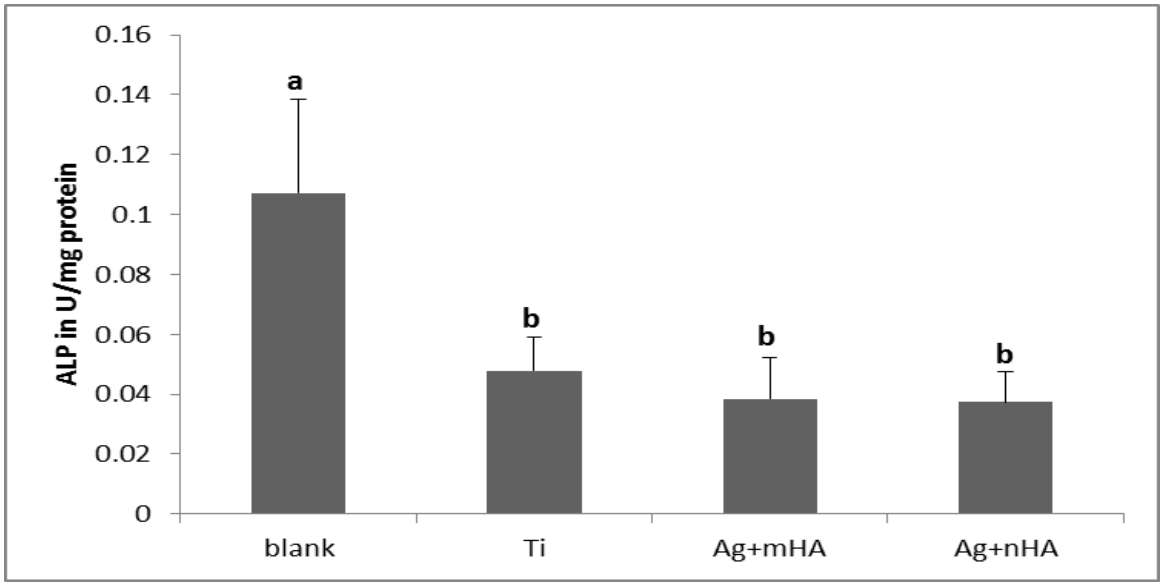

Figure 4.4 alkaline phosphatase activity (ALP) from cell homogenate after 72 h. Data are mean ± S.E.M (*n* = 6), bars with different letters are statistically different from each other (one way ANOVA, p=0.04).

4.4 Discussion

This study set out with the aim of evaluating the biosafety of the silver coatings (Ag+nHA and Ag+mHA). Primary human osteoblast cells were chosen for this study, representing human bone. The main finding was that the presence of the silver in the media affected the cell growth, as the osteoblast growth on the silver coated discs was lower than in the control (blank). Moreover, it was difficult to detect any cells on the surface of the silver coated discs by microscopy. Another main finding was the effect of the media on the silver coating stability, because there was high release of silver for those discs that coated with silver; in particular in Ag+nHA coating.

4.4.1 The exposure of the cell and silver accumulation

Silver concentrations were measured in the external media and cell homogenates (Table 4.1 and 4.2) in order to confirm the silver exposure to human osteoblast cells. High concentrations of silver were observed in the external media of silver coated

discs (Ag+nHA and Ag+mHA), specifically after 24 h incubation and then start to diminish in day 2 and 3. Since the dissolution of the metallic materials depends on the composition of the biological fluid (Cortizo *et al*., 2004); it can be argued that the high concentration of the silver closely related to the DMEM composition. Possible explanation might be the presence of amino acids such as L-Cysteine (63 mg/l) enhanced the silver dissolution. This finding can be further supported by the previous study by Tsipouras *et al*. (1995), who found that the presence of cysteine, methionine, or glutathione resulted in dissociation of silver sulfadiazine and release of free silver. He also mentioned that the serum protein increase the solubility of the silver. Furthermore, silver was also observed in the cell homogenate for the treatment and controls, the silver accumulation in the cells was observed for the silver coatings. This result seems to be consistent with previous research by Arora *et al*. (2009), who found that silver can accumulate in the mammalian cells such as fibroblast cells.

4.4.2 The effect of silver coatings on human osteoblast cells

The LDH assay was used to measure the cytotoxicity of silver against osteoblast cells. The leakage of this enzyme refers to irreversible cell death due to cell membrane damage (Fotakis *et al*., 2006). The results of the LDH in the external media showed that the silver has no toxic effect on the cells, because the concentration of LDH in the media from the silver coated discs (Ag+nHA and Ag+mHA) was not statistically different from the reference control (blank) over 72 h (Table 4.3). This could be due to the presence of protein in the media (10 % FBS) that might bind any free silver. Hence, the silver is no longer bioavailable to cause toxicity to the cell. Another possible explanation could be the interference of the metal ion with the LDH assay, because the high concentration of silver in the media. Han et al. (2012) assumed that with

increase the concentration of metal nanoparticles in the media the LDH activity will decrease; by providing more surface area for LDH adsorption.

In contrast, the cell homogenate showed a low level of LDH activity in the silver coated disc treatments compared to the reference control (blank, Figure 4.2), which apparently infer less number of viable cells on the surface of silver coatings. It seems possible that the concentration of the silver in the media was at a sublethal dose; as the silver did not kill the cells but prevents the proliferation of the cells. This result is in accordance with a research done by Pauksch *et al.* (2014), who showed that 10 mg/l of silver will impair the proliferation of osteoblast cells. Albres *et al*. (2013) also confirmed the toxicity of the free silver ions to human osteoblast cells in concentration of > 5 mg/l. The possibility of a reduction in LDH activity due to silver interference seems unlikely because the concentration of silver in cell homogenate was much lower than in the media.

The mechanisms underlying the toxic effect of silver to human cells is not fully understood, and whether the ions or the particles themselves will cause the toxicity. Hsin *et al*. (2008) assumed that silver nanoparticle enhance mitochondria-dependent apoptosis of the cells, through increasing the production of intracellular reactive oxygen species. While, Park *et al*. (2010) related the toxicity of the silver to the free ion release. Furthermore, Kone *et al*. (1988) stated that silver ions can exert toxic effect to human cell; through changing the permeability of the cell membrane to K^+ and Na^+. However, the results did not show any significant difference in the concentration of K^+ in the cell homogenate compared to control group.

The viability of the cells was also evaluated qualitatively using dissection microscopy; contrary to expectation, the microscope images did not show any cell on the silver

coated discs (Figure 4.1C and D). Since this finding is not in accordance with the results of the LDH, alkaline phosphatase, and protein assay, is it possible that the cells detached during staining steps. One explanation would be that the attachment of the cells to the surface of silver coated discs is very weak compared to uncoated control disc, and the cells could therefore easily detach from the surface. Another explanation for this could be the interference of the stain with coatings which lead to cell detachment. It is difficult to provide the exact answer for this, as this technique has not been used often for this type of experiments. Hence, more investigations are needed before using this technique in future.

Alkaline phosphatase enzyme was also measured, because it is considered as an important biomarker to evaluate the activity of the bone cells. The activity of this enzyme infers a healthy cell that has ability to form a new bone. The results showed that the activity of alkaline phosphatase was not affected by the presence of silver in the media (Table 4.4), which apparently means that silver has no adverse effect on the ability of the osteoblast to work properly. This finding is consistent with study done by Pauksch *et al*. (2014), who found that silver at sublethal dose (10 mg/l Ag) will not inhibit alkaline phosphatase activity in human osteoblast cells. In contrast the results for cell homogenate (Figure 4.4) showed a decrease in the activity of this enzyme compared to blank, which means that silver impaired the activity of osteoblast to form new bone. This result supports the previous research done by Chen *et al*. (2007), who found that silver containing hydroxyapatite (1.5 % silver) will decrease the alkaline phosphatase activity of osteoblast like cells. Nevertheless, any protein based assay should be interpreted with caution, due to the ability of silver to interact with proteins and enzymes in mammalian cells (Panyala *et al*., 2008).

4.5 Conclusion

The purpose of the current study was to determine the biocompatibility of the silver coatings (Ag+nHA and Ag+mHA) against human osteoblast cells. One of the more significant findings to emerge from this study is that the coatings caused toxicity to the human cells and decreased their viability. Contrary to the result of chapter 3 as the silver coatings showed low silver degradation in physiological saline media (section 3.3.3), the degradation of silver coatings was very high in the DMEM, which led to high silver ion release. Hence, these coatings are not yet ready to be used for clinical purposes; further studies are needed to investigate the cause of the silver release in this specific media, and the exact mechanism of how the silver cause the reduction in cell viability.

Chapter 5

General Discussion

There is an increase in the use of dental implants worldwide; but the infection associated with the implants is one the common causes of their failure; for which there is no ideal treatment so far. The current study mainly aimed to prepare a coating for the dental implant, which can prevent peri-implantitis without causing toxic effect to the human cells. This first goal was achieved, by preparing a coating consists of two layers, which composed of silver and hydroxyapatite nanoparticles or microparticles. It is confirmed that the coating had antibiofilm effect against *S. sanguinis*. Furthermore, the silver ion release was controlled and low. However, their effect on the osteoblast preservation poses a major problem, because the osteoblast viability decreased by 60 % compared to uncoated titanium discs. This possibly was due to the high silver ion release in cell media. Hence, this issue could be considered before going any further to use this kind of coating clinically on the patient.

5.1 The toxicity of the silver coating to the bacteria compared to human cells

In this study both antibacterial activity and biocompatibility was investigated for these coatings that consisted of, silver and hydroxyapatite nanoparticles or microparticles. The antibacterial investigation showed a promising outcome for better dental implant coatings. This is because the silver coatings were able to reduce the bacterial growth on the titanium discs, with very low silver ion release. This type of coating may therefore be developed for clinical applicationsin the future. However, to use this type of coating clinically, their toxicity to human cells should be investigated. Hence, the human osteoblast cells were used to evaluate the toxicity of these coatings *in vitro.* The outcome of this experiment showed that the silver coatings reduced the viability of the human osteoblast cells. This effect of the coating on the osteoblast was mainly related to the high concentration of the silver measured in the

media. In particular, the coating that composed of silver and hydroxyapatite nanoparticles. It is interesting to note that the silver release was almost 30 fold higher in the cell experiment compared to the bacterial test. This is likely due to the difference between the media that was used for growing the bacteria and the cells. The composition of the physiological saline was almost the same as the electrolyte contents of blood. While DMEM which was used to grow osteoblast cells is more complex and contains some surfactants that might have effect on the stability of the silver coating. Furthermore, the foetal bovine serum (FBS) might also affect the dissolution of the silver. Shi *et al*. (2012) reported that the presence of serum in the media decrease the aggregation of the nanoparticles. It can be suggested that the media used to grow the bacteria was more relevant to the condition that the coating will be expose to in the patient's mouth.

5.2 Clinical perspectives

In order to translate any medical products to the clinic, several regulatory steps should be followed. Several criteria should be met by any new medical products in order to be approved clinically, which are: (i) the efficacy of the medical product, to demonstrate whether it works and gives a benefit to the patient's health, (ii) to prove that the new product it more effective for its purpose than the already existing product, and (iii) finally and most important, is to ensure the biosafety of the product for its use with patients. These criteria have been placed by health agencies such as the European Medicines Agency (EMA) in Europe, and the Food and Drug Administration (FDA) in the United States (Juillerat-Jeanneret *et al*., 2013). The coating that developed reaches some of these criteria in term of its efficacy to eradicate the biofilm formation on the current implant surfaces; this will decrease the infection associated with dental implants and can replace the dental implants that are

in use nowadays. However, an issue that remains to be resolved, is the toxic effect of this coating to the human osteoblast cell. Nevertheless, approval might eventually be achieved by considering that the concentration of silver that kill the bacteria was much lower than that causing toxicity to the human cells. Improving the stability of the silver coating by decreasing its dissolution in different biological solutions may help achieve the desired outcome of biocompatibility. Regardless, hydroxyapatite in both forms (nanoparticles and microparticles) did not show any difference in biocompatibility, but the hydroxyapatite nanoparticles showed a better antibiofilm effect. Hence, it will be beneficial to develop the coating that composed of silver and hydroxyapatite nanoparticles.

5.3 Limitations of the study

This study has a number of limitations that should be considered in the future, some of these limitations are listed below:

1- Using dissection microscopy to investigate the cell viability has some limitation, because it was difficult to visualise any cells on silver plated discs. This could be due to the interaction of the coating materials and the stains.

2- Assessing the bacterial growth using a turbidity assay was problematic due to the natural turbidity of the nanoparticles. Hence it was difficult to measure the turbidity caused by the bacterial growth. Furthermore, this assay does not measure the absolute value of the bacterial cells.

3- It was not possible to use the calibration curve for the live/dead assay, because the calibration curve was performed on a different day.

4- Protein based assays should be used with caution to measure the cell viability in such an experiment, because of the interaction between the protein and silver.

5- It was difficult to investigate the degradation of the hydroxyapatite nanoparticles and microparticles in dialysis experiment, due to the high concentration of the calcium and phosphorus in the physiological saline.

5.4 Future work

A number of areas need further investigation and some of them are listed below:

1- Further studies are required to investigate the mechanism by which *S. sanguinis* produces mucopolysaccharide, and to what extent this mucopolysaccharide can protect the bacteria from silver ion exposure. Another question arising is why some populations of the microbe can produce the extracellular matrix, whereas the other population cannot.

2- Investigating the antibacterial of the coating against only one species is not enough to confirm their efficacy. Hence the next step would be investigating the antibacterial effect of the coating by culturing more than one bacterial species, which are known to cause peri-implantitis such as, *Porphyromonas gingivalis*, *Prevotella intermedia*, *Veillonella* species and *Treponema denticola*. This is because the bacteria will act differently together in the biofilm. Furthermore, it would be interesting to investigate the antibacterial activity of this coating; by using a biofilm that is taken from the real patients.

3- It would interesting to run the dialysis experiment for the silver in DMEM, for better understanding the dissolution of the silver in this particular media.

4- It would be interesting to investigate the chemistry of the media to determine which factors are critical to silver dissolution, and also evaluating the mechanical properties of the coating.

5- The biocompatibility test was just a preliminary study and need more investigation such as standardize the silver release from the coating to the media, and also using more specific assays to observe the effect of silver coatings on the osteoblast. Another alternative assays also should be used to evaluate the toxicity of the coatings. This because there is concern about the validity of protein based assays, due to interference of the nanoparticles and metal ions to these kind of assays.

6- It is encouraging to investigate the effect of the silver on the human cells rather than the cytotoxicity. For example, investigating the effect of silver on the expression of interlukins and genes in the human osteoblast cells.

References

Abron, A., Hopfensperger, M., Thompson, J. and Cooper, L. F. (2001) Evaluation of a predictive model for implant surface topography effects on early osseointegration in the rat tibia model. The Journal of prosthetic dentistry, 85 (1). pp 40-46.

Ahamed, M., AlSalhi, M. S. & Siddiqui, M. K. J. (2010) Silver nanoparticle applications and human health. Clinica Chimica Acta, 411 (23–24), 1841-1848.

Akiyama, T., Miyamoto, H., Yonekura, Y., Tsukamoto, M., Ando, Y., Noda, I., Sonohata, M. & Mawatari, M. (2013) Silver oxide‐containing hydroxyapatite coating has in vivo antibacterial activity in the rat tibia. Journal of Orthopaedic Research, 31 (8), 1195-1200.

Albrektsson, T. & Isidor, F. (1994) Consensus report of session IV. In: Lang, N.P. & Karring, T., eds. Proceedings of the 1st European Workshop on Periodontology, 365–369. London: Quintessence publishing Co. Ltd.

Albers, C. E., Hofstetter, W., Siebenrock, K. A., Landmann, R. & Klenke, F. M. (2013) *In vitro* cytotoxicity of silver nanoparticles on osteoblasts and osteoclasts at antibacterial concentrations. Nanotoxicology, 7 (1), 30-36.

Alt, V., Bitschnau, A., Österling, J., Sewing, A., Meyer, C., Kraus, R., Meissner, S. A., Wenisch, S., Domann, E. and Schnettler, R. (2006) The effects of combined gentamicin–hydroxyapatite coating for cementless joint prostheses on the reduction of infection rates in a rabbit infection prophylaxis model. Biomaterials, 27 (26), 4627-4634.

Andrews, J. M. (2001) Determination of minimum inhibitory concentrations. Journal of antimicrobial Chemotherapy, 48 (suppl 1),5-16.

Anselme, K., Bigerelle, M., Noël, B., Iost, A. and Hardouin, P. (2002) Effect of grooved titanium substratum on human osteoblastic cell growth. Journal of Biomedical Materials Research, 60 (4), 529-540.

Anusavice, K. J. (2003) Phillips science of dental materials. Saunders.

Aparicio, C., Javier Gil, F., Fonseca, C., Barbosa, M. and Planell, J. A. (2003) 'Corrosion behaviour of commercially pure titanium shot blasted with different materials and sizes of shot particles for dental implant applications'. Biomaterials, 24 (2),263-273.

Balasundaram, G., Sato, M. and Webster, T. J. (2006) Using hydroxyapatite nanoparticles and decreased crystallinity to promote osteoblast adhesion similar to functionalizing with RGD. Biomaterials, 27 (14), 2798-2805.

Berger, T. J., Spadaro, J. A., Chapin, S. E. and Becker, R. O. (1976) Electrically generated silver ions - Quantitative effects on bacterial and mammalian cells. Antimicrobial Agents and Chemotherapy, 9 (2), 357-358.

Besinis, A., De Peralta, T. & Handy, R. D. (2014) The antibacterial effects of silver, titanium dioxide and silica dioxide nanoparticles compared to the dental disinfectant chlorhexidine on Streptococcus mutans using a suite of bioassays. Nanotoxicology, 8 (1),1-16.

Besinis, A, De Peralta, T, and Handy, R. Inhibition of biofilm formation and antibacterial properties of a silver nano-coating on human dentine. Nanotoxicology 8.7 (2014): 745-754.

Bosetti, M., Masse, A., Tobin, E. & Cannas, M. (2002) Silver coated materials for external fixation devices: in vitro biocompatibility and genotoxicity. Biomaterials, 23 (3), 887-892.

Brånemark, P.-I., Breine, U., Adell, R., Hansson, B., Lindström, J. & Ohlsson, Å. (1969) Intra-osseous anchorage of dental prostheses: I. experimental studies. Scandinavian Journal of Plastic and Reconstructive Surgery and Hand Surgery, 3 (2), 81-100.

Brånemark, P. I. (1971) Jaw reconstruction and intraosseous anchorage of dental prosthesis. Läkartidningen, 68 (27),3105-3116.

Bürgers, R., Gerlach, T., Hahnel, S., Schwarz, F., Handel, G. & Gosau, M. (2010) In vivo and in vitro biofilm formation on two different titanium implant surfaces. Clinical Oral Implants Research, 21 (2), 156-164.

Buser, D., Broggini, N., Wieland, M., Schenk, R. K., Denzer, A. J., Cochran, D. L., Hoffmann, B., Lussi, A. and Steinemann, S. G. (2004) Enhanced Bone Apposition to a Chemically Modified SLA Titanium Surface. Journal of Dental Research, 83 (7), 529-533.

Buser, D., Schenk, R. K., Steinemann, S., Fiorellini, J. P., Fox, C. H. and Stich, H. (1991) Influence of surface characteristic on bone integration of titanium implants – A histomorphometric study in miniature pigs. Journal of Biomedical Materials Research, 25 (7), 889-902.

Cabal, B., Cafini, F., Esteban-Tejeda, L., Alou, L., Bartolome, J. F., Sevillano, D., Lopez-Piriz, R., Torrecillas, R. and Moya, J. S. (2012) Inhibitory Effect on In Vitro Streptococcus oralis Biofilm of a Soda-Lime Glass Containing Silver Nanoparticles Coating on Titanium Alloy. Plos One, 7 (8). Chaturvedi, T. (2009) An overview of the corrosion aspect of dental implants (titanium and its alloys). Indian Journal of Dental Research, 20 (1), 91-98.

Chaturvedi, T. (2009) An overview of the corrosion aspect of dental implants (titanium and its alloys). Indian Journal of Dental Research, 20 (1).

Chen, W., Oh, S., Ong, A., Oh, N., Liu, Y., Courtney, H., Appleford, M. & Ong, J. (2007) Antibacterial and osteogenic properties of silver‐containing hydroxyapatite coatings produced using a sol gel process. Journal of Biomedical Materials Research Part A, 82 (4), 899-906.

Christenson, E. M., Anseth, K. S., van den Beucken, J. J. J. P., Chan, C. K., Ercan, B., Jansen, J. A., Laurencin, C. T., Li, W. J., Murugan, R. and Nair, L. S. (2006) Nanobiomaterial applications in orthopedics. Journal of orthopaedic research, 25 (1), 11-22.

Ciobanu, C. S., Iconaru, S. L., Chifiriuc, M. C., Costescu, A., Le Coustumer, P. & Predoi, D. (2012) Synthesis and antimicrobial activity of silver-doped hydroxyapatite nanoparticles. BioMed research international, 2013

Clark, J. (1955) Solubility criteria for the existence of hydroxyapatite. Canadian Journal of Chemistry, 33 (11), 1696-1700.

Cortizo, M., Mele, M. and Cortizo, A. (2004) Metallic dental material biocompatibility in osteoblastlike cells. Biological Trace Element Research, 100 (2), 151-168.

Damm, C., Münstedt, H. & Rösch, A. (2008) The antimicrobial efficacy of polyamide 6/silver-nano-and microcomposites. Materials Chemistry and Physics, 108 (1), 61-66.

De Giglio, E., Cafagna, D., Cometa, S., Allegretta, A., Pedico, A., Giannossa, L., Sabbatini, L., Mattioli-Belmonte, M. & Iatta, R. (2013) An innovative, easily fabricated, silver nanoparticle-based titanium implant coating: development and analytical characterization. Analytical and bioanalytical chemistry, 405 (2-3), 805-816.

De Paiva, A., Poulain, B., Lawrence, G., Shone, C., Tauc, L. & Dolly, J. (1993) A role for the interchain disulfide or its participating thiols in the internalization of botulinum neurotoxin A revealed by a toxin derivative that binds to ecto-acceptors and inhibits transmitter release intracellularly. Journal of Biological Chemistry, 268 (28), 20838-20844.

Donlan, R. M. & Costerton, J. W. (2002) Biofilms: survival mechanisms of clinically relevant microorganisms. Clinical microbiology reviews, 15 (2),167-193.

Doyle, M. E. & Glass, K. A. (2010) Sodium Reduction and Its Effect on Food Safety, Food Quality, and Human Health. Comprehensive Reviews in Food Science and Food Safety, 9 (1), 44-56.

Dunne, W. M. (2002) Bacterial adhesion: seen any good biofilms lately?. Clinical microbiology reviews, 15 (2), 155-166.

Esposito, M., Hirsch, J. M., Lekholm, U. and Thomsen, P. (1998) Biological factors contributing to failures of osseointegrated oral implants. (Maneerung, Tokura &

Rujiravanit). Etiopathogenesis. European Journal Of Oral Sciences, 106 (3), 721-764

Fabian, E., Landsiedel, R., Ma-Hock, L., Wiench, K., Wohlleben, W., & Van Ravenzwaay, B. (2008). Tissue distribution and toxicity of intravenously administered titanium dioxide nanoparticles in rats. Archives of toxicology,82(3), 151-157.

Feng, Q., Wu, J., Chen, G., Cui, F., Kim, T. & Kim, J. (2000) A mechanistic study of the antibacterial effect of silver ions on *Escherichia coli* and Staphylococcus aureus. Journal of biomedical materials research, 52 (4), 662-668.

Filipe, Vasco, Andrea Hawe, and Wim Jiskoot. "Critical evaluation of nanoparticle tracking analysis (NTA) by NanoSight for the measurement of nanoparticles and protein aggregates." Pharmaceutical research 27.5 (2010): 796-810.

Foldbjerg, R., Olesen, P., Hougaard, M., Dang, D. A., Hoffmann, H. J. & Autrup, H. (2009) PVP-coated silver nanoparticles and silver ions induce reactive oxygen species, apoptosis and necrosis in THP-1 monocytes. Toxicology letters, 190 (2), 156-162.

Fotakis, G. & Timbrell, J. A. (2006) In vitro cytotoxicity assays: Comparison of LDH, neutral red, MTT and protein assay in hepatoma cell lines following exposure to cadmium chloride. Toxicology letters, 160 (2), 171-177.

Jenner, G. A., Longerich, H. P., Jackson, S. E., & Fryer, B. J. (1990). ICP-MS—a powerful tool for high-precision trace-element analysis in earth sciences: evidence from analysis of selected USGS reference samples. Chemical Geology, 83(1), 133-148.

Gil, F. J., Rodriguez, A., Espinar, E., Llamas, J. M., Padullés, E. and Juárez, A. (2012) Effect of oral bacteria on the mechanical behavior of titanium dental implants. The International Journal Of Oral & Maxillofacial Implants, 27 (1), 64-68.

Gilbert, J. L., Mehta, M. and Pinder, B. (2009) Fretting Crevice Corrosion of Stainless Steel Stem-CoCr Femoral Head Connections: Comparisons of Materials, Initial Moisture, and Offset Length. Journal of Biomedical Materials Research Part B-Applied Biomaterials, 88B (1), 162-173.

Goenka, S., Sant, V. & Sant, S. (2014) Graphene-based nanomaterials for drug delivery and tissue engineering. Journal of Controlled Release, 173, 75-88.

Golub, E. E. & Boesze-Battaglia, K. (2007) The role of alkaline phosphatase in mineralization. Current Opinion in Orthopaedics, 18 (5), 444-448.

Gong, P., Li, H., He, X., Wang, K., Hu, J., Tan, W., ... & Yang, X. (2007). Preparation and antibacterial activity of Fe3O4@ Ag nanoparticles.Nanotechnology, 18(28), 285604.

Gosheger, Georg, et al. Silver-coated megaendoprostheses in a rabbit model—an analysis of the infection rate and toxicological side effects. Biomaterials 25.24 (2004): 5547-5556.

Goyal, N., Priyanka and Kaur, R. (2012) Effect Of Various Implant Surface Treatments On Osseointegration- A Literature Review. Indian Journal Of Dental Sciences, 4 (1), 154-157.

Greulich, C., Kittler, S., Epple, M., Muhr, G. and Köller, M. (2009) Studies on the biocompatibility and the interaction of silver nanoparticles with human mesenchymal stem cells (hMSCs). Langenbeck's Archives of Surgery, 394 (3), 495-502.

Größner-Schreiber, B., Griepentrog, M., Haustein, I., Müller, W.-D., Briedigkeit, H., Göbel, U. B. & Lange, K.-P. (2001) Plaque formation on surface modified dental implants. Clinical Oral Implants Research, 12 (6), 543-551.

Hamdi, M., Hakamata, S. and Ektessabi, A. M. (2000) Coating of hydroxyapatite thin film by simultaneous vapor deposition. Thin Solid Films, 377–378 (0), 484-489.

Han, Xianglu, et al. Validation of an LDH assay for assessing nanoparticle toxicity. Toxicology 287.1 (2011): 99-104.

Handy, R., Eddy, F. & Romain, G. (1989) In vitro evidence for the ionoregulatory role of rainbow trout mucus in acid, acid/aluminium and zinc toxicity. Journal of Fish Biology, 35 (5), 737-747.

Harris, L. G., Mead, L., Müller-Oberländer, E. and Richards, R. G. (2006) Bacteria and cell cytocompatibility studies on coated medical grade titanium surfaces. Journal of Biomedical Materials Research Part A, 78A (1), 50-58.

Heasman, P. A., Heasman, L., Stacey, F. and McCracken, G. I. (2001) Local delivery of chlorhexidine gluconate (PerioChipTM) in periodontal maintenance patients. Journal of Clinical Periodontology, 28 (1), 90-95.

Hernández-Sierra, Juan Francisco, et al. The antimicrobial sensitivity of< i> Streptococcus mutans</i> to nanoparticles of silver, zinc oxide, and gold.Nanomedicine: Nanotechnology, Biology and Medicine 4.3 (2008): 237-240.

Hsin, Y.-H., Chen, C.-F., Huang, S., Shih, T.-S., Lai, P.-S. & Chueh, P. J. 2008. The apoptotic effect of nanosilver is mediated by a ROS- and JNK-dependent mechanism involving the mitochondrial pathway in NIH3T3 cells. *Toxicology Letters,* 179**,** 130-139.

Horie, Masanori, et al. Protein adsorption of ultrafine metal oxide and its influence on cytotoxicity toward cultured cells. Chemical research in toxicology22.3 (2009): 543-553.

Howes, Philip D., Subinoy Rana, and Molly M. Stevens. Plasmonic nanomaterials for biodiagnostics. Chemical Society Reviews (2014).

Huang, H.-L., Chang, Y.-Y., Lai, M.-C., Lin, C.-R., Lai, C.-H. & Shieh, T.-M. (2010) Antibacterial TaN-Ag coatings on titanium dental implants. Surface and Coatings Technology, 205 (5), 1636-1641.

Jarernboon, W., Pimanpang, S., Maensiri, S., Swatsitang, E. & Amornkitbamrung, V. (2009) Effects of multiwall carbon nanotubes in reducing microcrack formation on electrophoretically deposited TiO< sub> 2</sub> film. Journal of Alloys and Compounds, 476 (1), 840-846.

Jimbo, R., Sotres, J., Johansson, C., Breding, K., Currie, F. and Wennerberg, A. (2012) The biological response to three different nanostructures applied on smooth implant surfaces. Clinical Oral Implants Research, 23 (6), 706-712.

Jovanovic, S. A. (1993) The management of peri-implant breakdown around functioning osseointegrated dental implants. Journal Of Periodontology, 64 (11 Suppl), 1176-1183.

Juan, L. A., Mo, A. C., Zhu, Z. M. and Quan, Y. A. (2010) Antibacterial titanium plate deposited by silver nanoparticles exhibits cell compatibility. International Journal of Nanomedicine, 5, 337-342.

Juillerat-Jeanneret, L., Dusinska, M., Fjellsbø, L. M., Collins, A. R., Handy, R. D. & Riediker, M. (2013) 'Biological impact assessment of nanomaterial used in nanomedicine. Introduction to the NanoTEST project'. Nanotoxicology, (0). pages 1-9.

Jung, W. K., Koo, H. C., Kim, K. W., Shin, S., Kim, S. H. and Park, Y. H. (2008) Antibacterial activity and mechanism of action of the silver ion in Staphylococcus aureus and Escherichia coli. Applied and Environmental Microbiology, 74 (7). pages 2171-2178.

Junker, R., Dimakis, A., Thoneick, M. and Jansen, J. A. (2009) Effects of implant surface coatings and composition on bone integration: a systematic review. Clinical Oral Implants Research, 20, 185-206.

Kanaparthy, R. and Kanaparthy, A. (2011) The changing face of dentistry: nanotechnology. Int J Nanomedicine, 6 pages 2799-2804.

Kang, F., Alvarez, P. J. & Zhu, D. (2014) 'Microbial Extracellular Polymeric Substances Reduce Ag+ to Silver Nanoparticles and Antagonize Bactericidal Activity'. Environmental science & technology,

Kazemzadeh-Narbat, M., Lai, B. F. L., Ding, C., Kizhakkedathu, J. N., Hancock, R. E. W. & Wang, R. (2013) Multilayered coating on titanium for controlled release of antimicrobial peptides for the prevention of implant-associated infections. Biomaterials, 34 (24). pp 5969-5977.

Kim, Hae-Won, et al. Hydroxyapatite coating on titanium substrate with titania buffer layer processed by sol–gel method. Biomaterials 25.13 (2004): 2533-2538.

Kim, K.-H. & Ramaswamy, N. (2009) 'Electrochemical surface modification of titanium in dentistry'. Dent Mater J, 28 (1). pages 20-36.

Klasen, H. (2000) A historical review of the use of silver in the treatment of burns. II. Renewed interest for silver. Burns, 26 (2). pages 131-138.

Koch, C. F., Johnson, S., Kumar, D., Jelinek, M., Chrisey, D. B., Doraiswamy, A., Jin, C., Narayan, R. J. & Mihailescu, I. N. (2007) 'Pulsed laser deposition of hydroxyapatite thin films'. Materials Science and Engineering: C, 27 (3). pages 484-494.

Kone, Bruce C., Melissa Kaleta, and Steven R. Gullans. "Silver ion (Ag+)-induced increases in cell membrane K+ and Na+ permeability in the renal proximal tubule: reversal by thiol reagents." *The Journal of membrane biology*102.1 (1988): 11-19.

Kozlovsky, A., Artzi, Z., Moses, O., Kamin-Belsky, N. and Greenstein, R. B. N. (2006) Interaction of chlorhexidine with smooth and rough types of titanium surfaces. Journal of Periodontology, 77 (7). pages 1194-1200.

Langer, Robert, and David A. Tirrell. "Designing materials for biology and medicine." Nature 428.6982 (2004): 487-492.

Lansdown, A. (2002) Silver 2: toxicity in mammals and how its products aid wound repair. Journal of wound care, 11 (5). pages 173-177.

Lansdown, Alan. "Silver in health care: antimicrobial effects and safety in use." (2006): 17-34.

Lu, Z., Rong, K., Li, J., Yang, H. & Chen, R. (2013) 'Size-dependent antibacterial activities of silver nanoparticles against oral anaerobic pathogenic bacteria'. Journal of Materials Science: Materials in Medicine, 24 (6), 1465-1471.

Lassus, J., Salo, J., Jiranek, W. A., Santavirta, S., Nevalainen, J., Matucci-Cerinic, M., Horák, P. and Konttinen, Y. (1998) Macrophage activation results in bone resorption. Clinical orthopaedics and related research, (352), 7-15.

Lavenus, S., Louarn, G. and Layrolle, P. (2010) Nanotechnology and Dental Implants. International Journal of Biomaterials, 2010

Le Guéhennec, L., Soueidan, A., Layrolle, P. and Amouriq, Y. (2007) Surface treatments of titanium dental implants for rapid osseointegration. Dental Materials, 23 (7), 844-854.

Leonhardt, A., Renvert, S. and Dahlen, G. (1999) Microbial findings at failing implants. Clinical Oral Implants Research, 10 (5), 339-345.

Liao, J., et al. (2010). Antibacterial titanium plate deposited by silver nanoparticles exhibits cell compatibility. International journal of nanomedicine 5: 337.

Li, Xiang. Electrohydrodynamic deposition and patterning of nano-hydroxyapatite for biomedical applications. Diss. UCL (University College London), 2009.

Liljensten, E., Adolfsson, E., Strid, K.-G. and Thomsen, P. (2003) Resorbable and Nonresorbable Hydroxyapatite Granules as Bone Graft Substitutes in Rabbit Cortical Defects. Clinical Implant Dentistry and Related Research, 5 (2). pp 95-102.

Lin, W. P., Wesolowski, D. E. & Lee, C. C. (2011) 'Barrier/bonding layers on bismuth telluride (Bi2Te3) for high temperature thermoelectric modules'. Journal of Materials Science: Materials in Electronics, 22 (9). pp 1313-1320.

Liu, H. & Webster, T. J. (2007) Nanomedicine for implants: a review of studies and necessary experimental tools. Biomaterials, 28 (2). pp 354-369.

Lok, C.-N., Ho, C.-M., Chen, R., He, Q.-Y., Yu, W.-Y., Sun, H., Tam, P. K.-H., Chiu, J.-F. & Che, C.-M. (2006) Proteomic analysis of the mode of antibacterial action of silver nanoparticles. Journal of Proteome research, 5 (4). pp 916-924.

Lok, C.-N., Ho, C.-M., Chen, R., He, Q.-Y., Yu, W.-Y., Sun, H., Tam, P. K.-H., Chiu, J.-F. & Che, C.-M. (2007) 'Silver nanoparticles: partial oxidation and antibacterial activities'. JBIC Journal of Biological Inorganic Chemistry, 12 (4). pp 527-534.

Lossdorfer, S., Schwartz, Z. & Boyan, B. D. (2003) Microrough implant surface topographies increase osteogenesis by reducing osteoclast formation and activity. Journal of Dental Research, 82 pp B45-B45.

Lövestam, G., Rauscher, H., Roebben, G., Klüttgen, B. S., Gibson, N., Putaud, J. P. & Stamm, H. (2010) Considerations on a definition of nanomaterial for regulatory purposes. Joint Research Centre (JRC) Reference Reports, 80004-80001.

Lou, M. S., et al. (1998). Surface roughness prediction technique for CNC end-milling. Journal of Industrial Technology 15(1): 1-6.

Loza, K., Diendorf, J., Greulich, C., Ruiz-Gonzales, L., Gonzalez-Calbet, J. M., Vallet-Regi, M., Koeller, M. & Epple, M. (2014) The dissolution and biological

effect of silver nanoparticles in biological media. Journal of Materials Chemistry B,

Mahé, M., Heintz, J.-M., Rödel, J. & Reynders, P. (2008) Cracking of titania nanocrystalline coatings. Journal of the European Ceramic Society, 28 (10), 2003-2010.

Martini, D., Fini, M., Franchi, M., Pasquale, V. D., Bacchelli, B., Gamberini, M., Tinti, A., Taddei, P., Giavaresi, G., Ottani, V., Raspanti, M., Guizzardi, SRuggeri, A. (2003) Detachment of titanium and fluorohydroxyapatite particles in unloaded endosseous implants. Biomaterials, 24 (7). pp 1309-1316.

Massaro, C., Rotolo, P., De Riccardis, F., Milella, E., Napoli, A., Wieland, M., Textor, M., Spencer, N. D. and Brunette, D. M. (2002) Comparative investigation of the surface properties of commercial titanium dental implants. Part I: chemical composition. Journal Of Materials Science. Materials In Medicine, 13 (6). pp 535-548.

Mehdikhani-Nahrkhalaji, M., Fathi, M. H., Mortazavi, V., Mousavi, S. B., Hashemi-Beni, B. and Razavi, S. M. (2012) Novel nanocomposite coating for dental implant applications in vitro and in vivo evaluation. Journal of Materials Science-Materials in Medicine, 23 (2). pp 485-495.

Meirelles, L., Currie, F., Jacobsson, M., Albrektsson, T. and Wennerberg, A. (2008) The effect of chemical and nanotopographical modifications on the early stages of osseointegration. International Journal of Oral & Maxillofacial Implants, 23 (4). pp 641-647.

Mei, S., Wang, H., Wang, W., Tong, L., Pan, H., Ruan, C., Ma, Q., Liu, M., Yang, H. & Zhang, L. (2014) Antibacterial effects and biocompatibility of titanium surfaces with graded silver incorporation in titania nanotubes. Biomaterials, 35 (14), 4255-4265.

Mombelli, A. & Lang, N. P. (1998) The diagnosis and treatment of peri‐implantitis. Periodontology 2000, 17 (1). pp 63-76.

Murdock, R. C., Braydich-Stolle, L., Schrand, A. M., Schlager, J. J. & Hussain, S. M. (2008) Characterization of nanomaterial dispersion in solution prior to in vitro exposure using dynamic light scattering technique. Toxicological Sciences, 101 (2), 239-253.

Norowski, P. A. & Bumgardner, J. D. (2009) Biomaterial and antibiotic strategies for peri‐implantitis: A review. Journal of Biomedical Materials Research Part B: Applied Biomaterials, 88 (2), 530-543.

Ogawa, T., Saruwatari, L., Takeuchi, K., Aita, H. and Ohno, N. (2008) Ti nano-nodular structuring for bone integration and regeneration. Journal of Dental Research, 87 (8), 751-756.

Onuma, K. & Ito, A. (1998) Cluster growth model for hydroxyapatite. Chemistry of materials, 10 (11), 3346-3351.

Oshida, Y., Tuna, E. B., Aktoren, O. and Gencay, K. (2010) Dental Implant Systems. International Journal of Molecular Sciences, 11 (4), 1580-1678.

Otsuka, H., Nagasaki, Y. & Kataoka, K. (2003) PEGylated nanoparticles for biological and pharmaceutical applications. Advanced drug delivery reviews, 55 (3), 403-419.

Panyala, N. R., Peña-Méndez, E. M. and Havel, J. (2008) Silver or silver nanoparticles: a hazardous threat to the environment and human healt. J. Appl. Biomed, 6 (3), 117-129.

Park, Eun-Jung, et al. Silver nanoparticles induce cytotoxicity by a Trojan-horse type mechanism. Toxicology in Vitro 24.3 (2010): 872-878.

Pauksch, L., Hartmann, S., Rohnke, M., Szalay, G., Alt, V., Schnettler, R. & Lips, K. S. (2014) Biocompatibility of silver nanoparticles and silver ions in primary human mesenchymal stem cells and osteoblasts. Acta biomaterialia, 10 (1), 439-449.

Pucher, J. J. & Daniel, C. (1992) 'The effects of chlorhexidine digluconate on human fibroblasts in vitro'. Journal of periodontology, 63 (6), 526-532.

Pye, A. D., Lockhart, D. E. A., Dawson, M. P., Murray, C. A. & Smith, A. J. (2009) A review of dental implants and infection. Journal of Hospital Infection, 72 (2), 104-110.

Rameshbabu, N., Sampath Kumar, T. S., Prabhakar, T. G., Sastry, V. S., Murty, K. V. G. K. & Prasad Rao, K. (2007) Antibacterial nanosized silver substituted hydroxyapatite: Synthesis and characterization. Journal of Biomedical Materials Research Part A, 80A (3), 581-591.

Radin, S., Campbell, J. T., Ducheyne, P. & Cuckler, J. M. (1997) Calcium phosphate ceramic coatings as carriers of vancomycin. Biomaterials, 18 (11), 777-782.

Rai, M., Yadav, A., & Gade, A. (2009). Silver nanoparticles as a new generation of antimicrobials. Biotechnology advances, 27(1), 76-83.

Romeo, E., Ghisolfi, M., Murgolo, N., Chiapasco, M., Lops, D. & Vogel, G. (2005) Therapy of peri‐implantitis with resective surgery. Clinical Oral Implants Research, 16 (1), 9-18.

Sadeghi, R., Owlia, P., Yaraee, R., Sharif, F. & Taleghani, F. (2013) An In vitro Assessment of Antimicrobial and Cytotoxic Effects of Nanosilver. Journal of Medical Bacteriology, 1 (3, 4).

Sahoo, S. K., Parveen, S. & Panda, J. J. (2007) The present and future of nanotechnology in human health care. Nanomedicine: Nanotechnology, Biology and Medicine, 3 (1), 20-31.

Scales, J. T. & Wilkinson, M. J. (1984) Antimicrobial surgical implants.[in Google Patents. (Accessed:Scales, J. T. & Wilkinson, M. J.).

Schreurs, W. & Rosenberg, H. (1982) Effect of silver ions on transport and retention of phosphate by Escherichia coli. Journal of bacteriology, 152 (1). pp 7-13.

Sharma, V. K., Yngard, R. A. & Lin, Y. (2009) Silver nanoparticles: green synthesis and their antimicrobial activities. Advances in Colloid and Interface Science, 145 (1-2). pp 83-96.

Shen, G. X., Du, R. G., Chen, Y. C., Lin, C. J. & Scantlebury, D. (2005) Study on hydrophobic nano-titanium dioxide coatings for improvement in corrosion resistance of Type 316L stainless steel. Corrosion, 61 (10). pp 943-950.

Shi, J., Karlsson, H. L., Johansson, K., Gogvadze, V., Xiao, L., Li, J., Burks, T., Garcia-Bennett, A., Uheida, A. & Muhammed, M. (2012) Microsomal glutathione transferase 1 protects against toxicity induced by silica nanoparticles but not by zinc oxide nanoparticles. ACS nano, 6 (3). pp 1925-1938.

Shrivastava, S., Bera, T., Roy, A., Singh, G., Ramachandrarao, P. & Dash, D. (2007) Characterization of enhanced antibacterial effects of novel silver nanoparticles. Nanotechnology, 18 (22).

Sivolella, S., Stellini, E., Brunello, G., Gardin, C., Ferroni, L., Bressan, E. & Zavan, B. (2012) Silver nanoparticles in alveolar bone surgery devices. Journal of Nanomaterials, 2012 , 15.

Sondi, I. & Salopek-Sondi, B. (2004) Silver nanoparticles as antimicrobial agent: a case study on< i> E. coli</i> as a model for Gram-negative bacteria. Journal of colloid and interface science, 275 (1), 177-182.

Steinemann, S. G. (1998) Titanium — the material of choice?. Periodontology 2000, 17 (1), 7-21.

Stebounova, L. V., Guio, E. & Grassian, V. H. (2011) Silver nanoparticles in simulated biological media: a study of aggregation, sedimentation, and dissolution. Journal of Nanoparticle Research, 13 (1), 233-244.

Stewart, P. S. & William Costerton, J. (2001) Antibiotic resistance of bacteria in biofilms. The Lancet, 358 (9276), 135-138.

Subbiahdoss, G., Kuijer, R., Grijpma, D. W., van der Mei, H. C. and Busscher, H. J. (2009) Microbial biofilm growth vs. tissue integration: The race for the surface experimentally studied. Acta Biomaterialia, 5 (5), 1399-1404.

Sul, Y.-T., Johansson, C. B., Jeong, Y., Wennerberg, A. and Albrektsson, T. (2002) Resonance frequency and removal torque analysis of implants with turned and anodized surface oxides. Clinical Oral Implants Research, 13 (3), 252-259.

Sul, Y. T., Johansson, C. B., Jeong, Y., Röser, K., Wennerberg, A. and Albrektsson, T. (2001) Oxidized implants and their influence on the bone response. Journal of Materials Science: Materials in Medicine, 12 (10), 1025-1031.

Svanborg, L. M., Hoffman, M., Andersson, M., Currie, F., Kjellin, P. and Wennerberg, A. (2011) The effect of hydroxyapatite nanocrystals on early bone formation surrounding dental implants. International Journal of Oral and Maxillofacial Surgery, 40 (3), 308-315.

Tomsia, A. P., Launey, M. E., Lee, J. S., Mankani, M. H., Wegst, U. G. K. and Saiz, E. (2011) Nanotechnology Approaches to Improve Dental Implants. International Journal of Oral & Maxillofacial Implants, 26, 25-44.

Tschernitschek, H., Borchers, L. and Geurtsen, W. (2005) Nonalloyed titanium as a bioinert metal - A review. Quintessence International, 36 (7-8), 523-530.

Tsipouras, N., Rix, C. J. & Brady, P. H. (1995) Solubility of silver sulfadiazine in physiological media and relevance to treatment of thermal burns with silver sulfadiazine cream. Clinical chemistry, 41 (1), 87-91.

Tsui, Y., Doyle, C. & Clyne, T. (1998) Plasma sprayed hydroxyapatite coatings on titanium substrates Part 2: optimisation of coating properties. Biomaterials, 19 (22), 2031-2043.

Van Acker, Heleen, Patrick Van Dijck, and Tom Coenye. Molecular mechanisms of antimicrobial tolerance and resistance in bacterial and fungal biofilms. Trends in microbiology (2014).

Vasilev, K., Cook, J. & Griesser, H. J. (2009) Antibacterial surfaces for biomedical devices. Expert Review of Medical Devices, 6 (5), 553-567.

Vargas-Reus, M. A., Memarzadeh, K., Huang, J., Ren, G. G. and Allaker, R. P. (2012) Antimicrobial activity of nanoparticulate metal oxides against peri-implantitis pathogens International Journal of Antimicrobial Agents, 40 (2), 135-139.

Venkateswarlu, Kotharu, et al. Fabrication of corrosion resistant, bioactive and antibacterial silver substituted hydroxyapatite/titania composite coating on Cp Ti. Ceramics International 38.1 (2012): 731-740.

Vogel, K., Westphal, N., Salz, D., Thiel, K., Wittig, L., Ciacchi, L. C., Grunwald, I., Vogel, K. & Grunwald, I. (2014) Dental implants coated with a durable and antibacterial film.

Walker, M., & Parsons, D. (2012). The biological fate of silver ions following the use of silver- containing wound care products–a review. International wound journal.

Wan, Y. Z., Raman, S., He, F. and Huang, Y. (2007) Surface modification of medical metals by ion implantation of silver and copper. Vacuum, 81 (9), 1114-1118.

Webster, T. J., Ergun, C., Doremus, R. H., Siegel, R. W. & Bizios, R. (2000) Specific proteins mediate enhanced osteoblast adhesion on nanophase ceramics. Journal of biomedical materials research, 51 (3), 475-483.

Webster, T. J., Schadler, L. S., Siegel, R. W. and Bizios, R. (2001) Mechanisms of enhanced osteoblast adhesion on nanophase alumina involve vitronectin. Tissue engineering, 7 (3), 291-301.

Williams, D. F. (1977) Titanium as a metal for implantation Part 2: biological properties and clinical applications. Journal of medical engineering & technology, 1 (5), 266-270.

Williams, D. F. (1987) Definitions in biomaterials: proceedings of a consensus conference of the European Society for Biomaterials, Chester, England, March 3-5, 1986. vol. 4. Elsevier Science Ltd.

Yang, Y. C., Chang, E. & Lee, S. Y. (2003) Mechanical properties and Young's modulus of plasma-sprayed hydroxyapatite coating on Ti substrate in simulated body fluid. Journal of Biomedical Materials Research Part A, 67A (3), 886-899.

Yokoyama, K. i., Ichikawa, T., Murakami, H., Miyamoto, Y. and Asaoka, K. (2002) Fracture mechanisms of retrieved titanium screw thread in dental implant. Biomaterials, 23 (12), 2459-2465.

Zhang, Z. T., Dunn, M. F., Xiao, T. D., Tomsia, A. P. and Saiz, E. (2002) Nanostructured hydroxyapatite coatings for improved adhesion and corrosion resistance for medical implants. in Komarneni, S., Parker, J.C., Vaia, R.A., Lu, G.Q. and Matsushita, J.I. (eds.) Nanophase and Nanocomposite Materials Iv. Warrendale: Materials Research Society, 291-296.

Zhao, L., Chu, P. K., Zhang, Y. and Wu, Z. (2009) Antibacterial coatings on titanium implants. Journal of Biomedical Materials Research Part B: Applied Biomaterials, 91B (1). pp 470-480.

Appendix

Appendix A: The growth curve

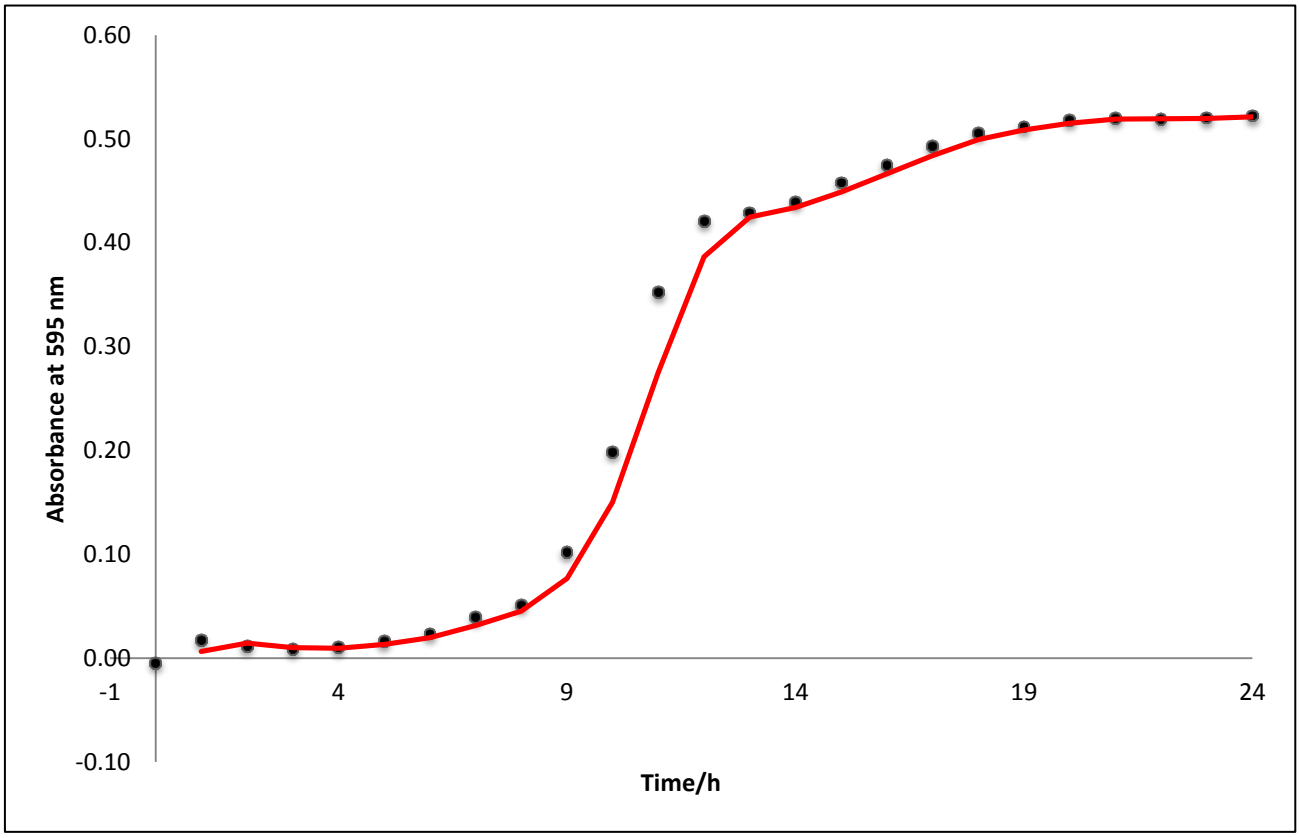

Figure: The growth curve of *Streptococcus sanguinis* over 24 h at 37 °C.

Appendix B: Lactic acid standards

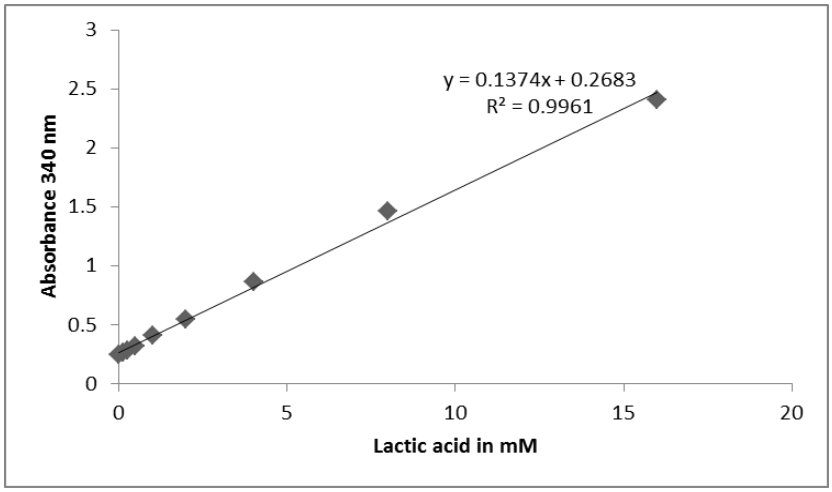

a

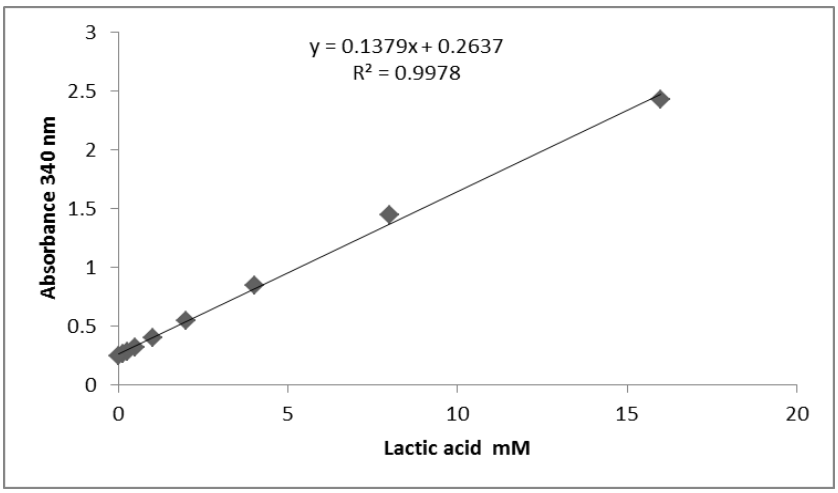

b

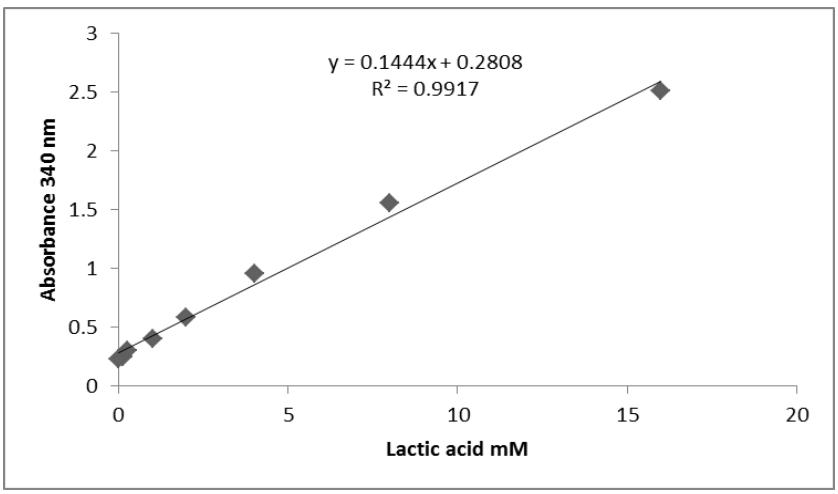

c

Figure: lactic acid standards for lactate production assay a) for the nanomaterial dispersions experiment (chapter 2) b) disc experiment c) repeated disc experiment (chapter 3).

Appendix C: Live/dead calibration curve

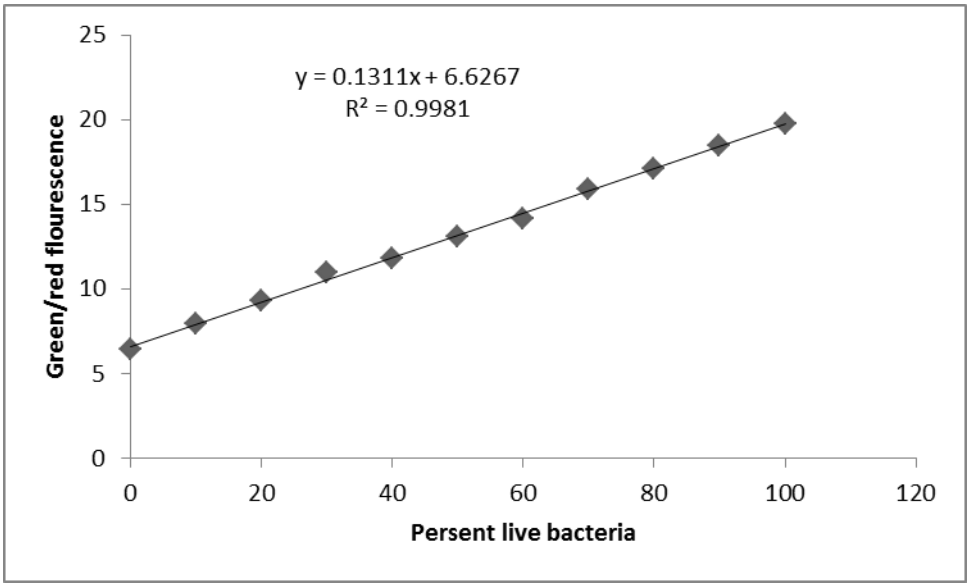

A

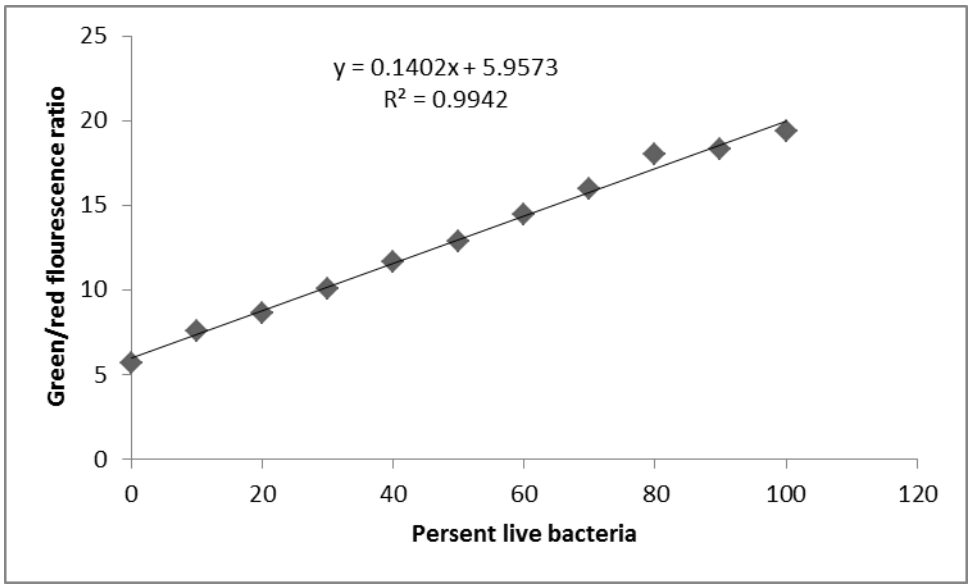

B

Figure: calibration curve for live/dead assay A) 24 h calibration curve, B) 16 h calibration curve.

Appendix D: MIC assay

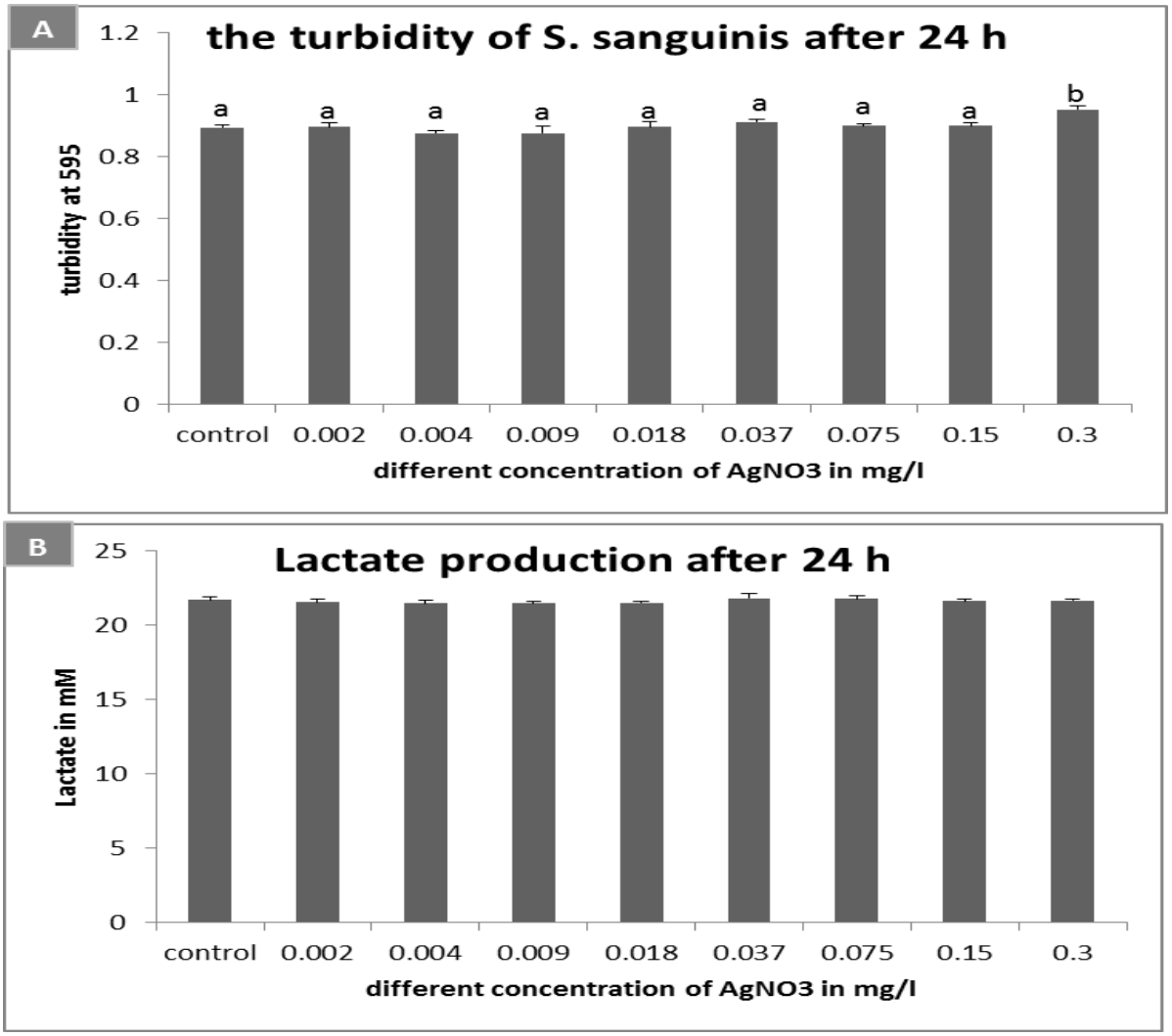

Figure: The antibacterial effect of low concentrations of silver nitrate against *S. sanguinuis*, A) the turbidity showed no difference with control, except for 0.3 mg/l was higher than control; this is due to the additional turbidity of particles. B) The lactate production assay, there is no growth inhibition in any of these concentration (One way ANOVA, $P > 0.86$*).*

Appendix E: Protein assay

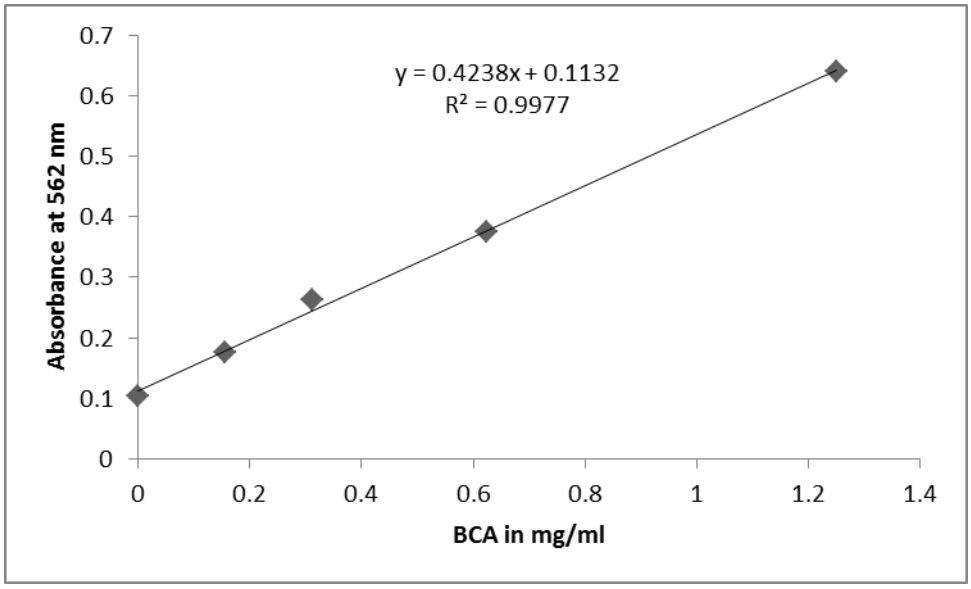

Figure: Standard curve for protein assay